VIRUSES AND THE INTERFERON (IFN) RESPONSE : METHODS TO IMPROVE PRODUCTION AND TO RAPIDLY SELECT IFN-SENSITIVE VIRUSES FOR VACCINE DEVELOPMENT

Claire Emma Stewart

A Thesis Submitted for the Degree of PhD
at the
University of St Andrews

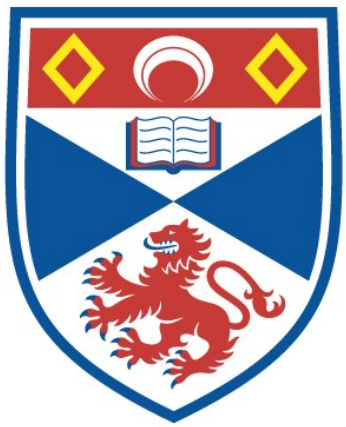

2017

Viruses and the Interferon (IFN) Response: Methods to Improve Production and to Rapidly Select IFN-sensitive Viruses for Vaccine Development

Claire Emma Stewart

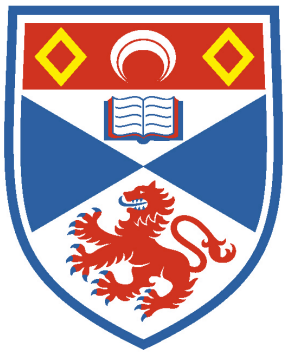

University of
St Andrews

A thesis submitted for the degree of PhD
at the
University of St Andrews

September 2016

Abstract

Manipulation of a virus's capacity to circumvent the interferon (IFN) response aids both fundamental studies as well as many practical applications including the design of live-attenuated vaccines. However, these IFN-sensitive viruses are often difficult to grow to high titer in cells that produce and respond to IFN. In the first part of this study we further characterised the use of the IFN inhibitor, Ruxolitinib (Rux) for its ability to block the IFN response and subsequently enhance replication of IFN-sensitive viruses. This study has shown that i) Rux could provide a more rapid and therefore more efficient alternative for the growth of IFN-sensitive viruses than the current default option, growth in Vero cells and ii) addition of Rux can increase growth of multiple viruses in numerous cell-lines. These results indicate that as well as aiding fundamental studies the addition of Rux could become a valuable technique in a number of virological applications including live attenuated vaccine production and techniques to isolate newly emerging viruses. In the second part of this study we developed a novel method to isolate IFN-sensitive viruses from Paramyxoviruses, using PIV5 (Parainfluenza virus 5) as an experimental model system to obtain selection parameters. We successfully isolated three mutant viruses (rPIV5mCh-α, rPIV5mCh-β and PIV5 W3-γ) that each contain mutations within the IFN antagonist V protein and the P protein which is essential for RNA replication. Subsequently, both rPIV5mCh-α and PIV5 W3-γ were shown to contain non-functional V proteins and exhibit IFN-sensitivity. Ultimately, this study is the first step towards creating a general method to isolate various types of IFN-sensitive viruses that as well as aiding fundamental studies, may be further developed as attenuated vaccines for clinically important viruses lacking vaccines.

Declarations

I, Claire Stewart, hereby certify that this thesis, which is approximately 50000 words in length, has been written by me, and that it is the record of work carried out by me, or principally by myself in collaboration with others as acknowledged, and that it has not been submitted in any previous application for a higher degree.

Date …… Signature of candidate ……

I was admitted as a research student in September, 2012 as a candidate for the degree of Doctor of Philosophy (PhD) in Molecular Virology; the higher study for which this is a record was carried out in the University of St Andrews between 2012 and 2016.

Date …… Signature of candidate ……

We hereby certify that the candidate has fulfilled the conditions of the Resolution and Regulations appropriate for the degree of Doctor of Philosophy at the University of St Andrews and that the candidate is qualified to submit this thesis in application for that degree.

Date…… Signature of supervisor ……..

Date…… Signature of supervisor ……..

In submitting this thesis to the University of St Andrews I understand that I am giving permission for it to be made available for use in accordance with the regulations of the University Library for the time being in force, subject to any copyright vested in the work not being affected thereby. I also understand that the title and the abstract will be published, and that a copy of the work may be made and supplied to any bona fide library or research worker, that my thesis will be electronically accessible for personal or research use unless exempt by award of an embargo as requested below, and that the library has the right to migrate my thesis into new electronic forms as required to ensure continued access to the thesis. I have obtained any third-party copyright permissions that may be required in order to allow such access and migration, or have requested the appropriate embargo below.

The following is an agreed request by candidate and supervisor regarding the publication of this thesis:

Access to printed copy and electronic publication of thesis through the University of St Andrews

Date …… Signature of candidate ……

Date …… Signature of supervisor ……..

Date …… Signature of supervisor ……..

Acknowledgements

I am extremely grateful to both of my supervisor's Dr Catherine Adamson and Prof Richard Randall for their continued advice, support and encouragement throughout my PhD studies. I would also like to express my warmest gratitude to the numerous colleagues in the Adamson and Randall labs, past and present, who I have met throughout my studies, with special thanks to Dr Lena Andrejeva and Mr Dan Young for your continued advice and support. I am also sincerely thankful to my fellow PhD student's and friend's Dr Stacey Bell, Dr Andri Vasou, Dr Lee Sherry, Dr Zoe Gage-Walker, Elizabeth Wignall-Fleming and Francisco Dominguez. We have been through so much together and I wish you all the best for whatever the future holds.

My final and biggest thanks goes to my family, with special thanks to my mum and dad, brother Gareth and my husband Fraser. You have always kept me grounded and pushed me to achieve goals which I never thought I could achieve. Without your continued support, encouragement and understanding I would never have made it to this point. It has been a long and emotional journey but we got there in the end!

I dedicate this thesis to my father-in-law Alexander Andrews who was always a pillar of great courage.

List of Figures

List of tables

Abbreviations

% [v/v]	Percentage concentration (volume per volume)
% [w/v]	Percentage concentration (weight per volume)
AKT1	RAC-alpha serine/threonine kinase
ANAV	Anopheles A virus
ATF-2	Activating Transcription Factor 2
BD	Becton-Dickinson Company
BRSV	Bovine Respiratory Syncytial Virus
BUN WT	Bunyamwera wild-type virus
BUNΔNSs	Bunyamwera with deleted NSs protein
BVDV	Bovine Viral Diarrhoea Virus
BWAV	Bwamba virus
CARDIF	CARD adaptor inducing interferon-β
CBP	CREB-binding protein
CD46	Cluster of Differentiation 46
cGAS	Cyclic guanosine monophosphate-adenosine monophosphate (GMP-AMP) cGAMP synthetase
CPE	Cytopathic effect
CPI+/-	Canine parainfluenza virus
cPPT	central Polypurine Tract
CV	Crystal Violet
CVV	Cache Valley virus
DAPI	4',6-diamindino-2-phenylindole
DDB1	Damage DNA binding protein 1
DMEM	Dulbecco's Modified Eagle Medium
DMSO	Dimethyl sulfoxide
dNTPs	deoxynucleotide
dsRNA	double stranded RNA
EDTA	Trypsin/ethylenediaminetetraacetic acid
F	Fusion protein
FACS	Fluorescence Activated Cell Sorting
FBS	Foetal bovine serum
G	Glycoprotein
GFP	Green fluorescent protein
H	Hemagglutinin
HCV	Hepatitis C
HeV	Hendra virus
HN	Hemagglutinin- Neuraminidase
HSV-1	Herpes Simplex Virus-1
IFN	Interferon
IFNAR1	Interferon-alpha/beta receptor alpha chain
IFNAR2	Interferon-alpha/beta receptor beta chain
IFNλR1	Interferon- gamma receptor 1
IKK-α	IκB kinase-α
IKK-β	IκB kinase-β
IPA	Isopropyl alcohol
IRAK4	Interleukin-1 receptor-associated kinase

IRF	Interferon regulatory factor
ISG	Interferon stimulated gene
ISGF3	IFN-stimulated gene factor 3
ISRE	IFN-stimulated response element
IκB	Inhibitor of κB
JAK	Janus Activated Kinases
KIRV	Kairi virus
L	Large protein
L Segment	Large Segment
LB	Luria-Bertani broth
LGP2	Laboratory of genetics and Physiology 2
LTRs	Long terminal repeat regions
M	Matrix protein
M Segment	Medium Segment
M-MLV RT	Moloney Murine Leukemia Virus Reverse Transcriptase
Mda-5	Melanoma Differentiation-Associated protein 5
MDV	Main Drain virus
MED8	Mediator complex subunit 8
MeV	Measles virus
MOI	Multiplicity of Infection
MuV	Mumps Virus
MyD88	myeloid differentiation factor 88
NEMO	NF-κB essential modulator
NF-κB	Nuclear factor-κB
NIBSC	The National Institute for Biological standards and controls
NiV	Nipah virus
NLR	Nucleotide oligomerization domain (NOD)-like receptors
NLRP3	NACHT, LRR and OYD domains-containing protein 3
NP	Nucleoprotein
NP^0	Soluble Nucleoprotein
NS1	Non-structural protein 1
NS2	Non-structural protein 2
NSm	Non-structural protein
NSs	Non-structural protein
OAS	2'-5'-oligoadenylate synthetase
ORF	Open reading frame
P	Phosphoprotein
PAC	puromycin-N-Acetyl-trasnferase
PAMPs	pathogen associated molecular patterns
PBS	Phosphate buffered Saline
PCR	Polymerase Chain reaction
PFU	Plaque forming units
PIV1-4	human parainfluenza virus 1-4
PIV5	Parainfluenza virus 5
PKR	Protein kinase R
PLK1	Polo-like kinase 1
PRR	Pattern recognition receptor
PVDF	Polyvinylidene difluoride
RIG-I	Retinoic acid-inducible gene 1

RIP1	Receptor-interacting protein 1
RLR	RIG-I like receptor
RNAP II	RNA polymerase II
rPIV5mCh	recombinant parainfluenza virus 5 mCherry
RRE	Rev response element
RSV	human Respiratory Syncytial Virus
RT	Room Temperature
Rux	Ruxolitinib
RVFV	Rift Valley Fever Virus
S Segment	Small Segment
SBV	Schmallenberg Virus
SDS-PAGE	Sodium Dodecyl Sulphate Polyacrylamide Gel Electrophoresis
SeV	Sendai virus
SFFV	Spleen focus-forming virus
SH	Small hydrophobic protein
SLAM	Signalling lymphocyte activation molecular (SLAM)
ssRNA	single stranded RNA
STAT	Signal Transducers and Activators of Transcription
SV5	Simian Virus 5
TAB2/3	TAK1-binding protein 2/3
TAK1	TGF-β activated kinase 1
TBE	Tris-Boric acid-EDTA buffer
TBK-1	TANK binding protein -1
TGS	Tris-Glycine-SDS buffer
TLR	Toll-like receptor
TRAF6	Tumour necrosis factor receptor-associated factor 6
TRIF	TIR domain-containing adaptor inducing interferon-β
TRIM25	Tripartite motif containing 25
Tyk2	Tyrosine kinase 2
USP3	Ubiquitin specific Protease 3
V	V protein
VSV	Vesicular Stomatis Virus
WHO	World Health Organization

1 Introduction

1.1 The Interferon (IFN) response

The Interferon (IFN) response is a vital defence against viral infection, without which we would not be able to survive. As an immediate response to infection, cells synthesize and release IFNs, a group of widely expressed cytokines, which can then communicate in an autocrine or paracrine manner to induce an antiviral response that limits the spread of infection. Despite the majority of viruses having known mechanisms to circumvent the IFN response, it remains critical to slow viral infection to allow the adaptive immune response to develop (reviewed in Iwasaki 2012, Randall and Goodbourn 2008, Schneider et al 2014)

1.1.1 Classes and subtypes of IFN

There are three classes of IFN, type I, II and III, grouped according to their similarity in amino acid sequence. The type I group consists of fourteen IFN-α subtypes, a single IFN-β subtype and the less well characterized IFN- ω, ε, τ, δ, κ subtypes, with IFN-α and -β playing the most well defined roles in the antiviral response (Schneider et al. 2014). It is known that IFN-α/β act through the same heterodimeric receptor, composed of interferon-alpha/beta receptor alpha chain (IFNAR1) and IFNAR2, to trigger what is termed the IFN signalling pathway (Kim et al 1997, Piehler et al 2000). This receptor is thought to be expressed ubiquitously throughout all tissues however hematopoietic cells are thought to be the main producers of IFN-α and fibroblasts of IFN-β (de Weerd et al 2007). Activation of this pathway then leads to the up-regulation of hundreds of IFN

stimulated genes (ISGs) and subsequently forms an antiviral state within the cell and its neighbours.

The type III IFNs comprise IFN- λ1, λ2, λ3, which again are released in response to viral infection in a similar manner to type I IFNs (Onoguchi et al. 2007). However, unlike the type I IFNs, they exhibit high tissue specificity due to the expression of their receptor, Interferon-lamda receptor 1 (IFNλR), on specific cell types such as epithelial cells (Lazear et al. 2015). Latterly, a 4th member of the type III IFNs has been discovered; namely λ4, however frameshift mutations render the gene inactive in a large proportion of the human population. Surprisingly, this inactivation has been shown to be associated with an increased chance of clearance of Hepatitis C virus (HCV) indicating that its suppression is somewhat beneficial despite it showing strong antiviral activity *in vitro* (Hamming et al. 2013). Type II IFN contains only one member, IFN-γ, and unlike the other types is secreted by natural killer cells and activated T cells as oppose to direct response to viral infection (Schroder et al. 2004; Billiau & Matthys 2009)

This study focuses mainly on the pathways associated in response to IFN-α/β. Predominately, IFN-β is used as an example as this pathway is better understood. The basic pathway is generally divided into two parts the IFN-β induction cascade and the IFN-β signalling cascade, both of which are outlined in the following sections.

1.2 IFN-β induction

The IFN-β induction cascade is mediated by the recognition of molecular pathogen-associated molecular patterns (PAMPS), these include single stranded RNA (ssRNA), double stranded RNA (dsRNA), genomic DNA, or viral proteins (reviewed in Iwasaki 2012). These PAMPS are recognised by pattern recognition receptors (PRRs) namely i) the Toll-like receptors (TLRs) such as TLR3, TLR7 and TLR9, ii) the RIG-I-like receptors (RLRs) Retinoic acid-inducible gene 1 (RIG-I) and Melanoma Differentiation-Associated protein 5 (Mda-5) iii) the nucleotide oligomerization domain (NOD)-like receptors (NLRs) such as NACHT, LRR and OYD domains-containing protein 3 (NLRP3) (Poeck et al. 2010), and the recently discovered range of cytosolic nucleic acid sensors such as cGAMP synthase (cGAS) (Sun et al. 2013; Cai et al. 2014). Each group recognises distinct PAMPs such as dsRNA in endosomes, recognised by TLR3, or ssRNA, recognised by TLR7 and TLR9, thereby allowing for recognition of many types of viral infection (reviewed in Broz and Monack 2013). For the purpose of this study we will focus on the pathways mediated by the cytoplasmic and endosomal recognition of RNA viruses, which is predominantly mediated by RLRs and the TLRs TLR3, TLR7 and TLR9. Aside from the recognition stage, the TLR3 and RLR dependent induction pathways are very similar, as demonstrated in Figure 1.1A. By contrast, the TLR7 and TLR9 dependent induction pathway exhibits greater differences and is represented in Figure 1.1B.

1.2.1.1 TLR3 and RLR (RIG-I and mda-5)-dependent induction cascade.

Both TLR3 and the RLRs recognise substrates at different stages during viral infection, therefore increasing the level of protection of the cell. In particular,

TLR3 can recognise dsRNA in endosomes or extracellular dsRNA at the cell surface (Randall & Goodbourn 2008). By contrast, the RLRs can only recognise infection once inside the cellular cytoplasm (Goubau et al 2013). Specifically, both RIG-I and Mda-5 are activated by dsRNA, however, RIG-I is also activated by short blunt ended dsRNA with a 5'triphosphate and is therefore indispensable for the recognition of many viruses such as Influenza A (Loo et al. 2008; Hornung et al. 2006). Interestingly, RIG-I but not Mda-5 activation has been shown to be dependent on ubiquitination and is regulated by the E3 ligases Tripartite motif containing 25 (TRIM25), TRIM4 and Riplet, and the Deubiquitylation enzymes Ubiquitin specific protease 3 (USP3) and ubiquitin C-terminal hydrolase (Heaton et al. 2016; Cui et al. 2014; Friedman et al. 2008; Yan et al. 2014; Gack et al. 2007). Irrespectively, once activated each receptor must then interact with an adaptor to confer activation of the induction pathway. In particular, TLR3 and the RLRs use the adaptors TIR domain-containing adapter inducing interferon-β (TRIF) and CARD adapter inducing interferon-β (CARDIF), respectively, both of which act as a scaffold for the recruitment of a number of other factors (Kawai et al. 2005; Meylan et al. 2005). Notably it appears that engagement of CARDIF by PRRs such as RIG-I results in a conformational change that recruits inactivated CARDIF and results in a large-scale amplification of the signalling cascades (Hou et al. 2011). This results in a highly sensitive mechanism to detect small amounts of viral RNA with evidence suggesting that less than 20 molecules of 5'triphosphate is sufficient to activate the RIG-I-CARDIF pathway (Zeng et al. 2010). From this point on, the signalling pathways are almost identical as the adaptors can activate both of the so-called 'arms' of the induction pathway, namely the nuclear factor-κB (NF-κB) 'arm' and the interferon regulatory factor

(IRF) 'arm' (Figure 1.1A). The NF-κB 'arm' initiates with the recruitment of tumour necrosis factor receptor-associated factor 6 (TRAF6) and receptor-interacting protein 1 (RIP1) to the adaptor (either TRIF or CARDIF depending on the initial receptor)(Sato et al. 2003). At this stage the TRAF6-RIP1-adaptor complex can then interact with a complex called TAK1 that consists of three subunits namely TAK1-binding protein 2/3 (TAB2/3), TAB1 and TGF-β activated kinase 1 (TAK1)(Jiang et al 2004, Meylan et al 2004, Sato et al 2003). This interaction then promotes the interaction with a second complex namely the IKK complex, which also consists of three subunits: NF-κB essential modulator (NEMO), IκB kinase-α (IKK-α) and IKK-β. Now that these two complexes (TAK1 and IKK) are in close proximity the TAK1 subunit of the TAK1 complex can then phosphorylate the IKK-β subunit of the IKK complex leading to its activation. Here it must be noted that NF-κB, one of the molecules that is required for the activation of the IFN-β promoter and thus IFN-β up-regulation, is held in an inactive state within the cytoplasm by the molecule inhibitor of κB (IκB)(Zandi et al. 1997; Alexopoulou et al. 2001). In view of this, the now active IKK-β subunit can phosphorylate the IκB subunit, subsequently leading to its ubiquitination and degradation (Jiang & Chen 2012). This then releases NF-κB from its inhibition and allows for its uptake into the nucleus where it assembles on the IFN-β promoter (Jiang & Chen 2012; Randall & Goodbourn 2008). This factor alone however does not result in IFN-β up-regulation, because the activation of both the NF-κB and IRF 'arms' of the pathway are required. In a similar manner to the NF-κB 'arm', a number of factors are recruited to the adaptor protein to begin activation of the 'IRF' arm. The process initiates with the recruitment of the E3 ligase TRAF3 to the adaptor (again either TRIF or CARDIF depending on

the initial receptor). TRAF3 can then also bind to a factor known as TANK, which in turn binds to TANK-binding protein 1 (TBK-1) and/or IKKε (Figure 1.1A)(Paz et al. 2011). Primarily TBK-1 and/or IKKε can then phosphorylate IRF3 directly, allowing it to migrate to the nucleus, however, in certain circumstances it is known that IRF7 is also activated in a similar manner (Trinchieri 2010). In this case, both IRFs can migrate to the nucleus to assemble on the IFN-β promoter. Ultimately, with both the NF-κB and IRF 'arms' of the pathway switched on, NF-κB and IRF3 (and IRF7) are now assembled on the IFN-β promoter. This in turn allows other factors to assemble on the promoter namely activating transcription factor 2 (ATF-2)/c-jun, CREB-binding protein (CBP)/p300 and RNA polymerase II which function collectively to up-regulate the production and secretion of IFN-β (Figure 1.1A) (Randall & Goodbourn 2008; Bhoj & Chen 2009; Takeuchi et al. 2010).

1.2.1.2 TLR7 and TLR9-dependent induction cascade

In addition to the TLR3 and RLR dependent pathway, TLR7 and TLR9 receptors can also trigger the induction of IFN-β. Notably, TLR7 and TLR9 recognise different PAMPs compared to the previous method such as ssRNA and CpG (unmethylated) DNA that has been engulfed by endosomes, respectively (Heil et al. 2004; Tabeta et al. 2004). This property thereby increases the number of ways in which viral infection can be recognised, allowing for greater protection of the cell. In a similar manner to the TLR3 and RLR-dependent pathway, the TLR7 and TLR9-dependent pathway uses an adaptor to recruit factors that subsequently activate the two NF-κB and IRF 'arms' of the induction pathway.

More specifically, once TLR7 and TLR9 are activated through recognition of viral PAMPs both can recruit the adaptor myeloid differentiation factor 88 (MyD88). This adaptor can then recruit two factors namely interleukin 1 receptor-associated kinase 4 (IRAK4) and IRAK1 (Kawagoe et al. 2008). Subsequently, IRAK4 and IRAK1 then lead to activation of the NF-κB and IRF 'arms' of the pathway, respectively. To initiate the activation of NF-κB, IRAK4 interacts with the factor TRAF6 (forming the MyD88-IRAK1-IRAK4-TRAF6 complex), which then interacts with a number of factors namely RIP1 and the TAK1 complex (Kim et al 2007). From this stage onwards, the activation cascade is exactly the same as in the TLR3/RLR-dependent pathway (Figure 1.1A and B). In brief, the TAK1 complex interacts with the IKK complex phosphorylating the IKK-β subunit. This active subunit can then phosphorylate the IκB subunit that inhibits NF-κB leading to its ubiquitylation and degradation, thus releasing NF-κB to relocate to the nucleus where it assembles on the IFN-β promoter (Figure 1.1B)(Zandi et al. 1997; Alexopoulou et al. 2001). Again, this alone does not result in IFN-β up-regulation, as it also requires the activation of the IRF 'arm' of the pathway. Unlike the previous method that contained an IRF 'arm' that activates IRF3 (and IRF7) this cascade offers another route to IFN-β induction using only IRF7. The MyD88-IRAK1-IRAK4-TRAF6 complex, described previously, has been shown to bind directly to IRF-7 (Kawai et al. 2004). IRF-7 is then polyubiquitinated by TRAF6 in the presence of polyubiquitinated RIP1 (Konno et al. 2009). IRF-7 is subsequently phosphorylated by IRAK-1 allowing the translocation of the whole complex into the nucleus, where it binds to the IFN-β promoter (Figure 1.1B)(Honda et al. 2004; Uematsu et al. 2005). Ultimately, activation of both the IRF and NF-κB 'arms' leads to the assembly of the IRF7-containing complex and

NF-κB on the IFN-β promoter, this along with a number of other co-factors such as ATF-2/c-jun, CBP/p300 and RNA polymerase II leads to increased transcription and secretion of IFN-β (Figure 1.1B)(Randall & Goodbourn 2008).

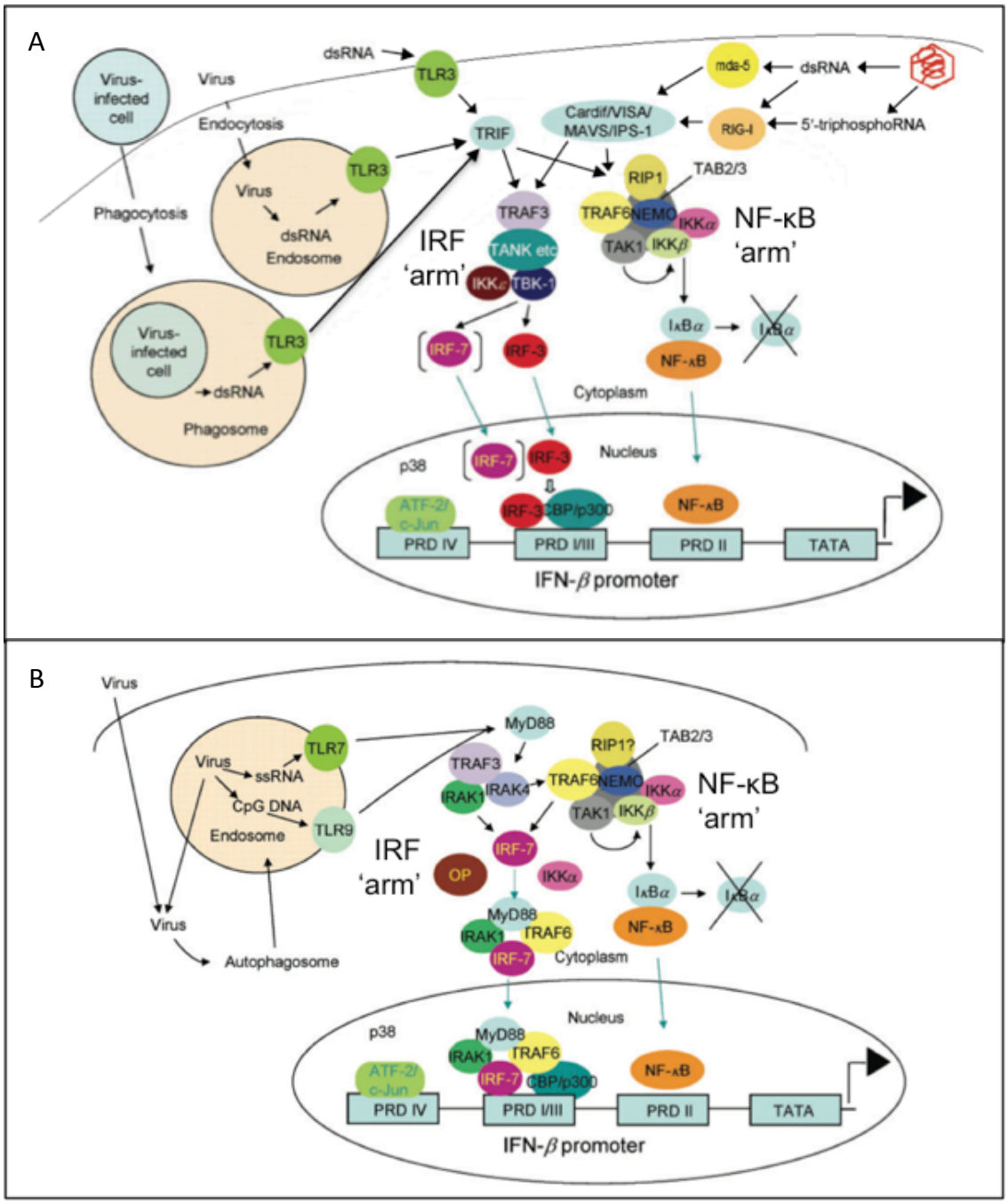

Figure 1.1: Overview of the IFN-β induction cascade. **A) TLR3 and the RLR (RIG-I and Mda5)-dependent induction cascade.** Both TLR3 and the RLRs recognise substrates at different stages during viral infection. In particular, TLR3 can recognise dsRNA in endosomes or extracellular dsRNA at the cell surface. By contrast, the RLRs can only recognise infection once inside the cell. Specifically, both RIG-I and Mda-5 are activated by dsRNA however RIG-I is also activated by 5'triphosphoRNA and is therefore indispensable for the recognition of many viruses such as Influenza A (Loo et al., 2008, Hornung et al., 2006). After recognition of the infection both TLR3 and the RLRs mediate the same induction cascade through the adaptors TRIF and CARDIF respectively, hence they are considered together in A. **B) TLR7 and TLR9-dependent induction cascade.** TLR7 and TLR9 recognise ssRNA and CpG (unmethylated) DNA that has been engulfed by endosomes, respectively. After recognition of the viral PAMPs both TLRs mediate the same induction cascade through interaction with the adaptor MyD88, hence they are considered together in B (Randall and Goodbourn, 2008).

1.3 IFN-β signalling

As outlined above there are a number of methods by which viral infection is recognised however ultimately they all lead to the up-regulation of production of IFN-β. Once produced, this cytokine is released by the cell into the surrounding area, this importantly signals to neighbouring cells that it has been infected and thus triggers them to up-regulate the production of many protective genes that are collectively known as interferon stimulated genes (ISGs). This so-called 'antiviral state' consequently reduces the spread of infection to surrounding cells allowing a greater chance of cell survival (reviewed in Ivashkiv and Donlin 2014). The process by which this 'antiviral state' is produced by IFN-β signalling is outlined in the following section.

1.3.1 IFN-β signalling cascade

The IFN-β signalling cascade initiates with the activation of the type I IFN receptor by IFN-β. This receptor is found at the cell surface and consists of two chains namely IFNAR1 and IFNAR2 (Kim et al 1997). The interaction with IFN-β results in autophosphorylation of the receptor itself and subsequently activation of two janus activated kinases (JAKs) namely tyrosine kinase 2 (Tyk2) and JAK1 which are found attached to the cytoplasmic domain of the receptor of IFNAR1 and IFNAR2, respectively (Figure 2)(Velazquez et al. 1994; Müller et al. 1993; Gauzzi et al. 1996). Once activated, these JAKs can then phosphorylate two signal transducers and activators of transcription (STAT), namely, STAT1 and STAT2 on tyrosine 701 and tyrosine 690, respectively (Stark et al. 1998). Phosphorylated STAT1 and STAT2 can then interact and translocate to the

nucleus where STAT1 is further phosphorylated by cyclin-dependent kinase 8 on Serine 727 (Wen et al. 1995; Uddin et al. 2002; Bancerek et al. 2013). This heterodimer subsequently forms a heterotrimer complex with interferon regulatory factor 9 (IRF-9) that is collectively termed IFN-stimulated gene factor 3 (ISGF3)(Fu et al. 1990; Ivashkiv & Donlin 2014). ISGF3 then translocates to the nucleus and binds to a specific sequence within target promoters, the IFN-stimulated response element (ISRE). This subsequently stimulates the transcription of hundreds of ISGs, thereby producing the 'antiviral state' (Figure 1.2)(Schoggins & Rice 2011; Stark & Darnell 2012). As well as regulation by post-translational modification such as phosphorylation, STAT- and ISGF3 mediated gene transcription is also regulated by cooperation with other transcription factors such as IRF1, IRF7, IRF8 and IRF9 (van Boxel-Dezaire et al. 2006), chromatin remodelling which is mediated by STAT1 and STAT2 and IRF-mediated recruitment of nucleosome-remodelling enzymes and histone acetyltransferases (HATs)(Tartey & Takeuchi 2015), and through the interaction of STATs with co-activators and co-repressors (Ivashkiv & Donlin 2014; Au-Yeung et al. 2013). Examples of ISGs upregulated by this pathway include protein kinase R (PKR) and 2'-5'-oligoadenylate synthetase (OAS), PKR prevents initiation of transcription in the presence of dsRNA and OAS degrades cellular and viral RNAs in the presence of dsRNA (Carlos et al. 2007). Another important example includes ISG56, which has been shown recently to specifically inhibit translation of mRNA from Rubulaviruses such as PIV5 but not other members of the *Paramyxoviridae* family due to the lack of methylation at a particular position in the 5' guanosine nucleoside cap of viral mRNA (Andrejeva et al. 2013; Young et al. 2016). As these examples show, the main aim of the up-regulation of ISGs is

to gain a 'head start' in producing the proteins that allow protection against viral infection. Understandably, this mechanism of defence has driven viruses to gain numerous ways in which to circumvent this response to tip the balance in favour of viral infection. Crucially, by studying these interactions we can gain an insight into how to weaken the virus to tip the favour back towards the host. This could ultimately aid in the production of attenuated viruses, which are the essential component of numerous vaccines.

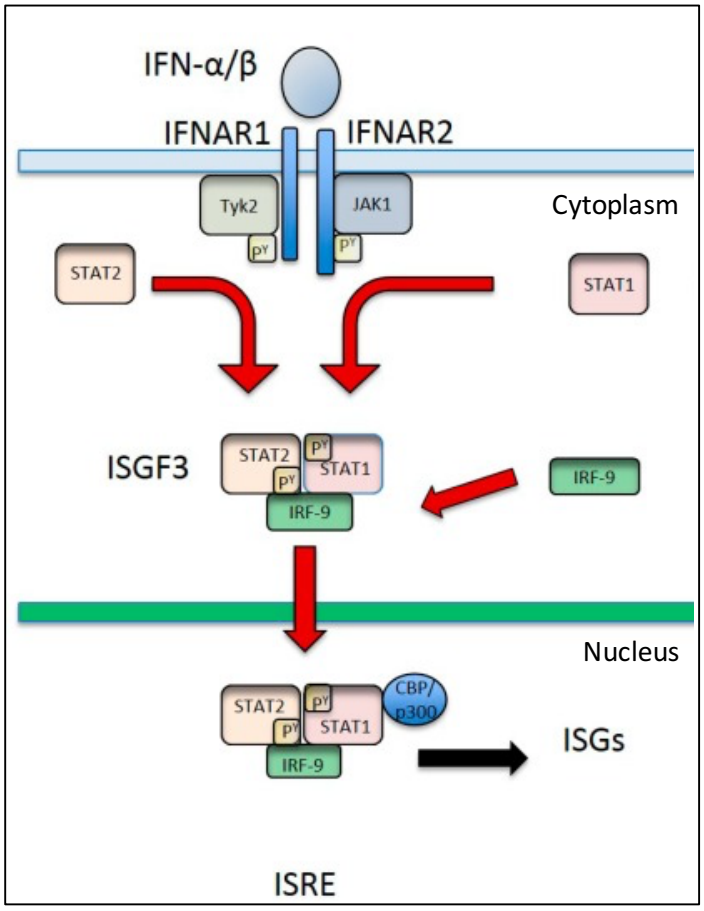

Figure 1.2: Overview of the IFN signalling cascade. IFN-β can trigger the activation of the JAK-STAT signalling pathway, inducing an 'antiviral state' in surrounding cells through the activation of many hundreds of Interferon stimulated genes (ISGs)(Fleming 2016).

1.4 Viral IFN antagonism

Viruses have developed an astonishing variety of IFN antagonists to counteract the induction, signalling or antiviral actions of the IFN system. Over 170 viral IFN antagonist has been described from 93 distinct viruses with most demonstrating a multifunctional role targeting multiple steps within the IFN response (Versteeg et al. 2010; Haller et al. 2006). Although each is unique, IFN antagonists counteract the cellular IFN response using common strategies that include i) broad-spectrum inhibition of cellular gene expression and ii) sequestration, proteolytic cleavage and proteasome-mediated degradation of key components of the IFN system (Versteeg et al. 2010).

1.4.1 Pleiotropic nature of viral IFN antagonists

The pleiotropic nature of IFN antagonists is dictated by restrictions on the viral genome. More specifically, RNA viruses have a relatively limited genome capacity in comparison to large dsDNA viruses, which drives a high-degree of multifunctionality of the IFN antagonists. This evolutionary pressure has resulted in the conservation of IFN antagonists within related RNA viruses whereas there is limited conservation in large dsDNA viruses (Versteeg et al. 2010). A prime example of this is the Non-structural, NS1, protein, which is conserved among Influenza A and B, and exhibits a plethora of different strategies to antagonise the IFN system (Hale et al. 2008). A second example of this is the Non-structural protein, NSs, protein which is a multifunctional IFN antagonist conserved among the Phleboviruses and Orthobunyaviruses (Elliott & Weber 2009).

1.4.2 Bunyamwera virus (BUN WT) and the IFN antagonist NSs

As BUN WT of the Orthobunyaviruses genus and the recombinant virus BUNΔNSs are used within a major part of this study we will discuss these viruses further, with particular focus on the functions of the IFN antagonist NSs. Bunyamwera virus is a prototypical virus within the *Bunyaviridae* family which contains pathogens of serious concern such as Rift Valley fever virus (RVFV) and Schmallenberg (SBV) (Fields et al. 2013; Garigliany et al. 2012). It possesses a tri-segmented negative sense RNA genome consisting of the Large (L), Medium (M) and Small (S) segments. The L segment encodes the viral RNA polymerase, the M segment encodes a polyprotein precursor, which is co-translationally cleaved to obtain the glycoproteins Gn and Gc and a non-structural protein NSm, and the S segment encodes the N protein and the NSs IFN antagonist in overlapping reading frames (Elliott and Blakqori 2011). For BUN WT, NSs is a non-essential small hydrophobic protein of 101 amino acids that is expressed from an internal, +1-shifted reading frame within the N gene of the S segment. The main function of this protein is attributed to globally inhibiting host mRNA transcription by blocking RNA polymerase II (RNAP II) through an interaction with Mediator complex subunit 8 (MED8), a complex required for mRNA production (Thomas et al. 2004; Leonard et al. 2006). Generation of a recombinant virus, BUNΔNSs, which does not express NSs demonstrated reduced plaque size and growth in IFN competent cells to approximately 10-fold lower titers compared to the wild-type virus (BUN WT). Furthermore, when inoculated intracerebrally into BALB/c mice, BUNΔNSs killed the mice in a slower time course than BUN WT (Bridgen et al. 2001). Indicating that although non-essential, expression of the NSs protein aids viral pathogenesis as the NSs

deficient virus is more sensitive to IFN and therefore attenuated compared to the wild-type virus.

1.5 IFN-sensitive viruses as Vaccines

With most, if not all, viruses encoding an IFN antagonist this opens up the opportunity for prophylactic intervention through the development of 'IFN-sensitive' viruses as live attenuated virus vaccines. A concept which has now been successfully verified for many viruses including Influenza A and B, RVFV and more recently Respiratory syncytial virus (RSV) (Bird et al. 2008; Jang & Seong 2012; Meng et al. 2014).

Live attenuated virus vaccines contain a mutant strain of a wild-type virus, whereby its ability to inhibit the hosts immune response has been weakened. This impairment can be associated with loss of a viruses IFN antagonist function or mutations within other proteins that slow viral replication such that it can be controlled by the IFN response. This attenuation does not prevent host infection but rather prevents the cause of severe disease. As the virus can still replicate within the host, it can produce numerous antigens causing a wide range of immune responses that later protect the host from subsequent infection from the wild-type virus.

1.5.1 Live Attenuated vaccine development

One of the first live attenuated vaccines to be developed was that against smallpox (variola virus)(reviewed in Minor 2015). In the 18th century it was well known among rural communities that workers who contracted cowpox were

subsequently resistant to smallpox. In 1976, Edward Jenner experimented by inoculating a young boy, James Phipps, with material from a cowpox-infected milkmaid. Seven weeks later he then injected the boy with material from a smallpox lesion and Phipps survived with no indication of infection (Jenner 1798). These initial investigations subsequently led to compulsory vaccination in the UK however debate over the quality of the production of the vaccine led to compulsion being dropped. Subsequently, in 1959 the World Health Organisation developed criteria for the production of a safer vaccine tackling major problems such as the possibility of bacterial contamination of the vaccine and also the transfer of syphilis (WHO 1959). Unbeknown to many the original constituent of the smallpox vaccine had mutated into what is now known as vaccinia virus. Whether this virus derived from cowpox or variola virus is unknown however its effectiveness is unquestionable (Elwood 1989; Petersen et al. 2016). In 1980 smallpox was declared eradicated making it one of the most successful human vaccines to date. Given that the infectious agent we now know as a virus was not described until 1898, it is not surprising that there was little influence of virology on the development of smallpox vaccines first investigated in 1798 (Minor 2015). This was not the case for the polio vaccine. This vaccine was obtained through a better understanding of viral pathogenesis and the virology of the poliomyelitis. Albert Sabin developed the Sabin type 1 vaccine from the serial passage of the wildtype virus through monkey testis cells (Sabin & Ward 1941). The type 2 and 3 strains were then isolated from clinical cases (Sabin & Boulger 1973). Many years later, following the introduction of the vaccines, sequence analysis of the vaccine strains then determined mutations affecting the virulence of each (Macadam et al. 1991; Westrop et al. 1989). Given

the success of this vaccine in decreasing polio to an unprecedented level it is not surprising that similar techniques including serial passage are still used today to try to obtain attenuated viruses for use as live attenuated vaccines.

1.5.2 Traditional methods to obtain attenuated viruses

Several approaches are used today to produce live attenuated viruses. One such technique is to passage the virus within a foreign host. Mutants generated with increased virulence in the foreign host typically lose virulence in humans and can therefore be analysed as a potential vaccine strain. This method has been shown to be a useful method with RNA viruses as they have a particularly high mutation rate. Alternatively, the virus can be grown in a different temperature to the human host, this can cause mutations to occur which adapt the virus to this new temperature but slow the viral growth in human cells enough for the adaptive immune response to fight infection (Baxter 2007; Minor 2015). A final approach is chemical mutagenesis which has been used to create potential vaccines for dengue and tuberculosis (Blaney et al. 2001; Collins 2000). These forward genetics approaches, firstly finding a mutated strain and then identifying what is making that strain attenuated have been a successful method to identify numerous vaccines against viruses such measles (MeV), mumps (MuV) and seasonal and pandemic strains of influenza (Fiore et al. 2009; Suguitan et al. 2006; Bankamp et al. 2011; Rubin et al. 2008). However, this process can be somewhat lengthy, as the virus needs to be passaged multiple times and then followed by pairing of genomic nucleotide changes with diminished virulence.

1.5.3 Rational design of live attenuated vaccines

Due to the difficulties associated with traditional empirical methods, the development of vaccines is currently moving towards rational design. Using this method known IFN antagonists can be directly mutated to attenuate the virus. This is typically completed by mutating the gene code to prevent the expression of the IFN antagonist or by editing specific sites to allow the expression of a non-functional protein (Rueckert et al. 2012). A prime example of this is the Bovela® attenuated virus vaccine produced by mutation of the IFN antagonists Npro Protease and E^{RNS} RNase of Bovine Viral Diarrhoeal virus (BVDV). This vaccine is now used successfully to prevent persistent infection of bovine with BVDV (Meyers et al. 2007). Recently, codon-pair de-optimisation has presented a novel approach to the attenuation of viral IFN antagonists. This method was first used to tackle the issue of genetic instability of live-attenuated poliovirus vaccines by incorporating the rarest codons in the human genome to lower translation of the capsid protein resulting in virus attenuation (Mueller et al. 2006). More recently this method has been used to attenuate RSV by codon de-optimization of the nonessential IFN antagonists NS1 and NS2 to create a potential live attenuated vaccine candidate (Meng et al. 2014). Importantly, this approach offers increased safety by decreasing the likelihood that the attenuated strain can revert to regain IFN antagonist function as well as improved immunogenicity. Despite the successes of attenuating a virus in this way, this process is by no means simple. Firstly, it relies on the notion that the IFN antagonist of the virus is already known which is not always the case. Secondly, it is particularly complicated for RNA viruses due to the multifunctional nature of most IFN antagonists, hence not

all rationally designed attenuations result in a viable live attenuated vaccine strain.

1.5.4 Vaccine production

Whether a virus has been developed by traditional methods or by rational design it is important to consider that the more attenuated the virus the more difficult it will be to produce for clinical use (Jang & Seong 2012). Currently, the default option for growth of IFN-sensitive viruses is limited to a select number of cell-lines such as Vero cells, that do not have an intact IFN system, however, as viruses exhibit host cell specificity not all viruses can be grown in such cells (Desmyter et al. 1968; Mosca & Pitha 1986). Previously we have developed cell-lines expressing IFN antagonists that enable blockage of the IFN response and can subsequently relieve host cell constraints on the virus, allowing virus growth (Young et al. 2003). However, development of these cell-lines is time consuming and creates regulatory problems during vaccine development, as each cell line has to be approved for use during production.

1.5.5 Experimental Objectives

To tackle this issue, it was hypothesised that blocking the IFN induction and signalling pathways using a small molecule inhibitor would offer a simple and flexible solution to increase viral growth, as an inhibitor could easily supplement the tissue culture medium of cell-lines of choice. To test this, eight inhibitors known to target different components of the IFN response (TBK-1, IKK-β and JAK1/2) were tested for their ability to block their corresponding pathways. Of these eight inhibitors, Ruxolitinib (Rux) the JAK1/2 inhibitor which blocks the IFN signalling pathway, was identified as the most effective inhibitor of the IFN

response (Stewart et al. 2014). Consequently, the first objective of my study was to further characterize the use of this IFN inhibitor, Rux, with respect to increasing the growth of IFN-sensitive viruses.

The second objective of my study then aimed to speed the process of traditional methods to identify attenuated viruses and allow selection of viable vaccine strains by developing a method to rapidly isolate potentially IFN-sensitive viruses from Paramyxoviruses, using fluorescent activated cell sorting (FACS). Following isolation, we could then employ the IFN inhibitor Rux to aid us in characterisation of potential IFN-sensitive viruses. As Paramyxoviruses are the main focus of this study, I will now outline the basic properties of the *Paramyxoviridae* family with particular focus on the prototypical virus Parainfluenza virus type 5 (PIV5) used throughout our experimental research.

1.6 Paramyxoviridae family

The family *Paramyxoviridae* are responsible for a range of acute respiratory diseases in both humans and animals. As a result, they are linked to a substantial mortality rate and cause a significant economic burden. The family is divided into the subfamilies *Paramyxovirinae* and *Pneumovirinae* (Table 1.1). The subfamily, *Paramyxovirinae,* is the largest group divided into 7 genera: *Aquaparamyxovirus, Avulavirus, Ferlavirus, Henipavirus, Morbillivirus, Respirovirus* and *Rubulavirus*. It contains many clinically important viruses such as MeV and MuV virus, which cause highly contagious viral diseases in human infants, in addition to, the newly emerging viruses Hendra (HeV) and Nipah virus (NiV) that are known to cause deadly diseases in both animals and humans. The

latter smaller subfamily, the *Pneumovirinae*, is divided into 2 genera the *Metapneumovirus* and the *Pneumovirus* and it contains viruses such as human RSV, which is the major cause of lower respiratory tract infection in infants (reviewed in Audsley 2013, Fields et al 2013).

Table 1.1: Paramyxoviridae subfamily and genus classification. (adapted from Audsley 2013, King et al 2012)

Subfamily	Genus	Virus
Paramyxovirinae	*Aquaparamyxovirus*	*Atlantic salmon paramyxovirus*
	Avulavirus	*Avian paramyxoviruses 2-9* *Newcastle disease virus*
	Ferlavirus	*Fer-de-Lance paramyxovirus*
	Henipavirus	*Hendra virus (HeV)* *Nipah virus (NiV)*
	Morbillivirus	*Canine distemper virus* *Measles virus (MeV)*
	Respirovirus	*Sendai virus (SeV)* *Human parainfluenza virus 1 and 3 (PIV1/3)*
	Rubulavirus	*Mumps virus (MuV)* *Parainfluenza virus 5 (PIV5)* *Human parainfluenza virus 2 and 4 (PIV2/4)*
Pneumovirinae	*Metapneumovirus*	*Human Metapneumovirus* *Avian Metapneumovirus*
	Pneumovirus	*Bovine respiratory syncytial virus (BRSV)* *Human respiratory syncytial virus (RSV)*

1.7 Paramyxovirus virion structure

Despite classification of paramyxoviruses into several genera, the basic paramyxovirus virion structure is consistent across all subtypes (Figure 1.3) (reviewed in Chang and Dutch 2012, Fields et al 2013, El Najjar et al 2014). It consists of pleomorphic (spherical or filamentous), enveloped particles ranging typically from 150 to 300nm in diameter (Kalica et al. 1973; Goldsmith et al. 2003; Loo et al. 2013). These particles encapsidate a non-segmented, negative sense, single stranded RNA that encodes for the necessary proteins required for replication of the virus. Genomic RNA is wrapped with nucleoprotein (NP), the phosphoprotein (P) and the large (L) protein forming what is termed a nucleocapsid structure, which is essential for RNA replication as well as transcription (Horikami et al. 1992; Noton & Fearns 2015). The L protein is the RNA dependent RNA polymerase allowing transcription and replication of the genomic RNA, aided by the P protein. NP is important for protecting the viral genome from cellular responses by encapsidating the RNA during RNA replication. Together this nucleocapsid interacts with the matrix (M) protein, a protein important in virion assembly, which lines the virion envelope. This envelope contains two surface glycoproteins, a trimeric fusion (F) protein and a tetrameric attachment protein- HN, H or G depending on the virus. The *Aquaparamyxoviruses*, *Avulaviruses*, *Ferlaviruses, Respiroviruses* and *Rubulaviruses* share a common attachment protein- Hemagglutinin–neuraminidase (HN) which has both Hemagglutinin (sialic acid binding) and neuraminidase (sialic acid cleaving) activity. These viruses can therefore use cellular surface sialic acid as their receptor (Chang & Dutch 2012). The

Morbilliviruses contain only Hemagglutinin (H) protein so can bind sialic acid but lack the ability to cleave it. Subsequently it has been shown that these viruses use cellular proteins such as signalling lymphocyte activation molecule (SLAM; also known as CD150) to gain entry to cells (Ono et al. 2001). The remaining families the *Henipaviruses* and both the *Metapneumoviruses* and the *Pneumovirus*es of the *Pneumovirinae* subfamily contain a G protein which facilitates attachment to cellular proteins such as Ephrin B2/B3 in the case of HeV and NiV (Negrete et al. 2006; Bonaparte et al. 2005), or nucleolin in the case of RSV (Tayyari et al. 2011).

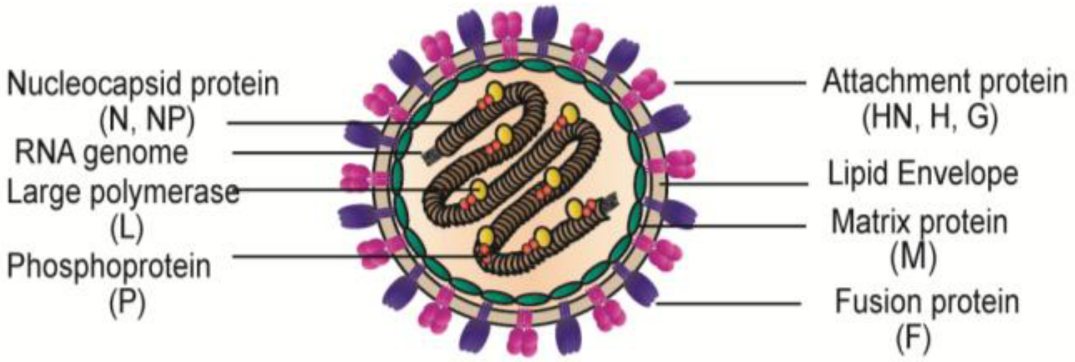

Figure 1.3: Paramyxovirus virion structure. All paramyxoviruses contain a nucleocapsid that comprises the negative sense RNA genome wrapped in nucleocapsid protein (NP), phosphoprotein (P) and the large (L) polymerase protein. This nucleocapsid is then enclosed in a lipid envelope that is lined with matrix proteins, which play an important role during virion assembly. The lipid envelope of the virion contains two surface glycoproteins: the attachment proteins (HN, H or G) and the fusion protein (F). These function to allow binding and entry to the host cell (El Najjar et al 2014)

1.8 Paramyxovirus replication cycle

As paramyxoviruses, like all viruses, are obligate parasites they must infect a host cell to replicate and produce new progeny virions (Figure 1.4). This cycle is initiated by binding of the attachment protein (HN, H or G) to the receptor on the host cell. The F protein then permits fusion of the envelope with the plasma membrane and allows release of the nucleocapsid into the cytoplasm (Bose et al. 2013; Chang & Dutch 2012). Once inside, transcription, protein synthesis and replication of the viral genome can occur within the cytoplasm of the host cell. Upon entry, the RNA polymerase, L protein, carried as part of the nucleocapsid can initiate transcription of the viral genome to form individual mRNAs in a transcription gradient that are subsequently transcribed to proteins (Abraham & Banerjee 1976). The most renowned model for switching to RNA replication then proposes that when enough unassembled nucleocapsid protein is present, the polymerase can then switch to transcribe full-length positive-sense anti-genomic RNA templates (Kolakofsky et al. 2004; Noton & Fearns 2015). This can then be used as a template to synthesise full length genomic RNAs. Notably most Paramyxoviruses obey the 'Rule of 6', i.e. their genome length must be exactly divisible by 6 to replicate efficiently due to restrictions on the wrapping of RNA with NP(Kolakofsky et al. 2004; Alayyoubi et al. 2015). Together with L, NP and P, the progeny RNA's form nucleocapsids, which associate with the M protein at the plasma membrane along with the viral glycoproteins (HN, H or G)(Ghildyal et al. 2006). Mature virions can then bud from the plasma membrane and exit to continue infection (reviewed in Fields et al 2013)

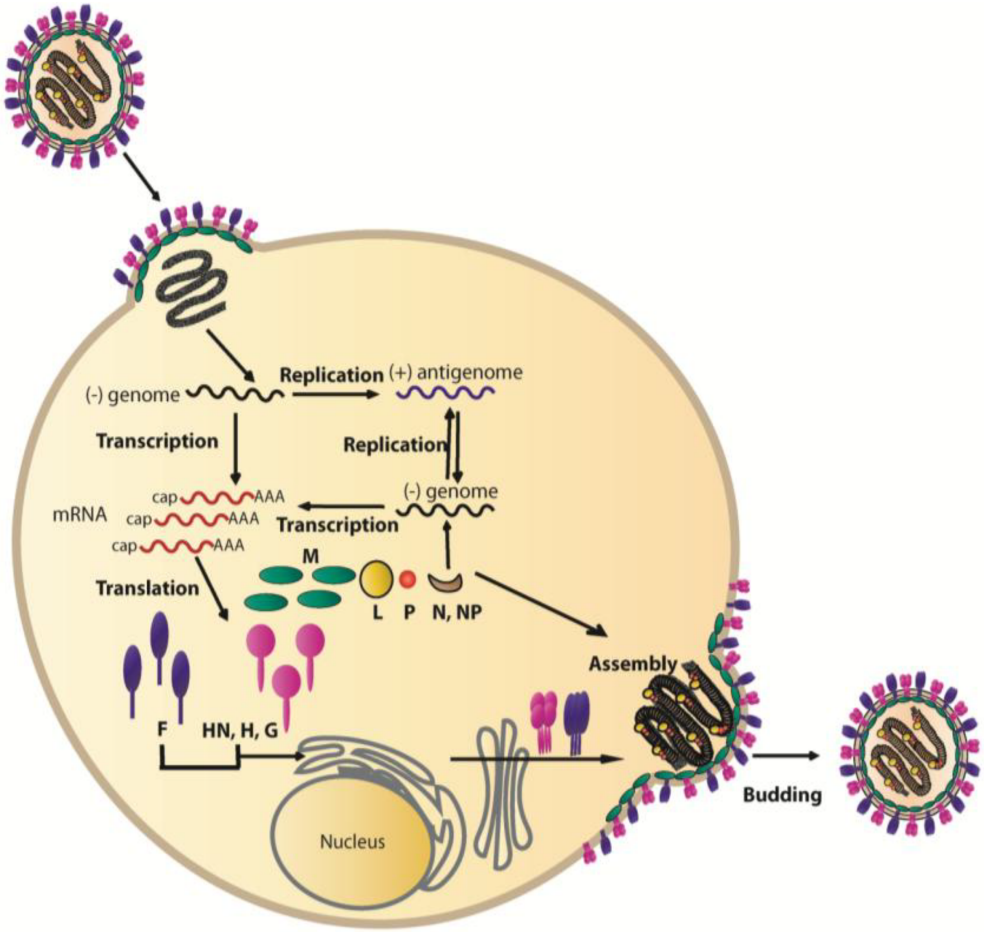

Figure 1.4: Paramyxovirus replication cycle. Entry to the cell is initiated by binding of the attachment protein to the cell (HN, H or G). The fusion protein can then instigate fusion of the viral envelope to the plasma membrane and allow release of the nucleocapsid to the cell cytoplasm. Inside the host the viral polymerase initiates transcription of viral mRNAs, which are then translated to proteins. The polymerase can also replicate the negative sense genome to a positive sense antigenome, which can then be used as a template to synthesise new progeny genomes. Together with L, P and NP, these newly synthesised RNA genomes form nucleocapsids, which by exploiting M protein can assemble with newly synthesised viral glycoproteins found at the cellular membrane into new virions. These new virions then bud from the host and exit to continue the spread of infection. (El Najjar et al 2014)

1.9 Additional proteins encoded by paramyxoviruses

Interestingly, in addition to the aforementioned proteins, a number of the *Rubulaviruses* and *Avulaviruses* and the entire *Pneumovirinae* subfamily produce a small hydrophobic (SH) protein that is thought to play a role in preventing apoptosis or protecting against the immune response (Li et al. 2013; Wilson et al. 2006). Furthermore, most paramyxoviruses can express a number of proteins from the P gene due to a number of overlapping open reading frames (ORFs). The *Morbillivirus*, *Respiroviruses*, *Henipaviruses* and *Avulaviruses* transcribe P mRNA however a process termed 'RNA editing' can allow the insertion of a G nucleotide into the transcript (Figure 1.5). This insertion creates a frameshift mutation in the downstream sequence, which thereby produces an mRNA that translates into a protein termed the V protein. This protein therefore shares a common N-terminus with the P protein but has a unique C terminus (Goodbourn & Randall 2009). The V protein is a cysteine rich protein termed as an interferon (IFN) antagonist as it is able to block the IFN immune response and allows the virus to propagate more easily within the cell (Andrejeva et al 2004, Didcock et al 1999, reviewed in Parks and Alexander-Miller 2013, Poole et al 2002). A second G residue insertion creates an mRNA that encodes proteins with different C-termini termed W, D or I. Intriguingly, it is the V protein of the *Rubulaviruses* such as PIV5 that is genomically templated and two G residues are inserted into the mRNA to produce the P protein. Furthermore, the addition of 1 or 4 G residues creates the I protein in certain viruses (reviewed in Parks and Alexander-Miller 2013, S. M. Thomas et al 1988)

In addition to RNA editing certain viruses such as the *Morbilliviruses*, *Respiroviruses* and *Henipaviruses* translate the P/V/W/D mRNAs by a process termed 'leaky scanning'. This occurs as the P/V/C mRNAs contain a number of weak start codons that result in several places for initiation of the ribosome. In SeV, for example, there are 4 distinct start codons which can generate C', C, Y1 and Y2 proteins with varying N-termini but share a common C-terminus (reviewed in Audsley 2013, Goodbourn and Randall 2009, Parks et al 2011). These proteins again have been linked to functions such as IFN antagonism and regulation of viral genome and antigenome RNA synthesis (Irie et al. 2008). Inversely, the P genes of the Pneumovirinae only encode 1 protein but some such as RSV encode 2 extra genes, namely NS1 and NS2, which have been shown to act as IFN antagonists (Elliott et al 2007, Goswami et al 2013, Lo et al 2005) .

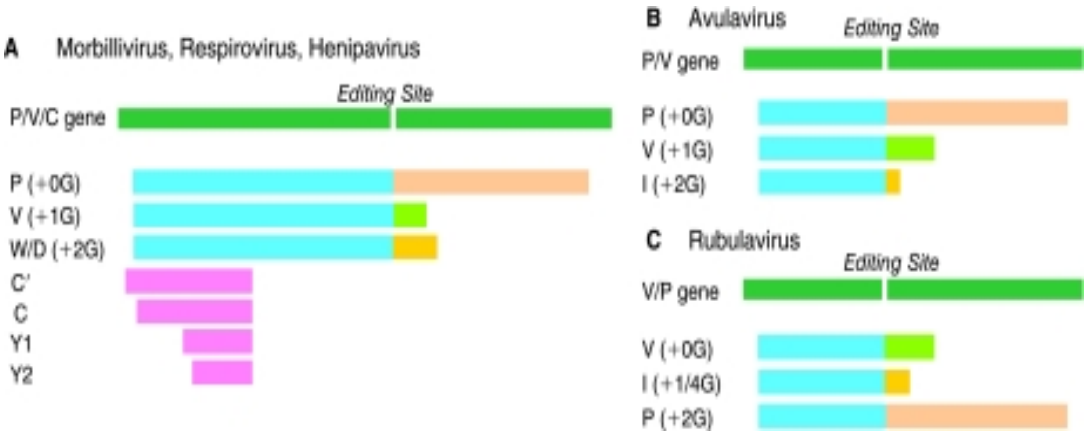

Figure 1.5: Accessory proteins produced by RNA editing and leaky scanning during paramyxovirus transcription and translation respectively. Those obtained by RNA editing are indicated in blue and those obtained by leaky scanning in pink. (Goodbourn & Randall 2009)

1.10 Parainfluenza virus 5 (PIV5)

For the purposes of this study, we shall now discuss the prototypical paramyxovirus, PIV5, in more depth. Many fundamental studies of paramyxoviruses are typically based on the analysis of PIV5. Initially isolated from rhesus monkey kidney cells the virus was named simian virus 5 (SV5)(Hull et al. 1956; Choppin 1964), however, since then, its isolation from a wide range of animals namely canine, porcine and human have led to the proposal that it be renamed parainfluenza virus 5 (PIV5) (Chatziandreou et al. 2004; Rima et al. 2014). Despite its isolation from a wide variety of animals, the virus remains avirulent in most cases including humans and its only known potential links to disease are to kennel cough in dogs and acute respiratory symptoms in pigs and calves (McCandlish et al. 1978; Heinen et al. 1998; Tong et al. 2002). What is more the virus also grows rapidly in tissue culture. Undoubtedly, these assets have facilitated its study as the prototypical paramyxovirus and many properties discovered from PIV5 studies, were later found to be common within the *Paramyxoviridae* family (Parks et al. 2011). In addition to aiding fundamental studies of paramyxoviruses, PIV5 has also recently gained interest as a tool for the development of vaccines. More specifically, many of its properties such as lack of pathogenicity in humans and rapidity of growth have led to the proposal that PIV5 is an ideal vaccine vector. For example, it has been shown that PIV5 can be engineered to expressed the H7 protein from the fatal H7N9 strain of influenza leading to an effective H7N9 vaccine that protected mice from lethal infection (Li et al. 2015; Li et al. 2013). Together these functions demonstrate

that despite causing no apparent illness in humans it is vital to continue our studies of PIV5.

Currently, one of the first strains of PIV5 to be isolated PIV5 W3 (or W3A) is routinely used in our laboratory to study the interactions of paramyxoviruses with the immune response. PIV5 W3 has a genome of 15,246 nucleotides, which contains 7 genes that encode for 8 known proteins (NP, V, P, M, F, SH, HN and L) (Figure 1.6)(He et al 2002, Parks et al 2011).

Figure 1.6: PIV5 W3 gene organisation. PIV5 W3A has a genome of 15,246 nucleotides and encodes for 8 proteins from its 7 genes (NP, V, P, M, F, SH, HN and L).

1.11 PIV5 proteins

1.11.1 Nucleoprotein (NP)

NP is the first gene encoded from the viral genome and plays a vital role in protecting the viral genome from degradation by encapsidating viral RNA. It consists of 502 amino acids and sequence analysis shows that it contains a central motif that is common among most paramyxovirus NP sequences. Notably, this motif has been shown in related viruses to be essential for self-assembly with RNA. Recently it has been shown that PIV5 genomic RNA associates with ~2600 copies of NP to form the helical nucleocapsid structure and each PIV5 NP binds six molecules of genomic RNA consistent with the rule of six (Alayyoubi et al. 2015). This feature allows NP to encapsidate the viral genome and

antigenome, which provides essential protection from nuclease degradation. NP also functions to create a functional promoter and is essential in the assembly of budding virions as part of the nucleocapsid (Parks et al. 2011). In addition to its interaction with RNA, soluble NP (NP^0) has been found to associate with P and V proteins, which may play a role in encapsidation of progeny RNA during replication (Precious et al. 1995; Randall & Bermingham 1996). More recently, evidence indicates that binding of NP with V protein could inhibit RNA replication meaning that V could play an important role in regulating viral replication during the initial stages of infection (Lin et al. 2005; Yang et al. 2015).

1.11.2 V protein (V)

The V protein is the second protein encoded for by the viral genome. It consists of 222 amino acids and plays a multifunctional role as an IFN antagonist, an inhibitor of viral RNA synthesis and it is also able to alter the cell cycle. As described previously, the V protein shares an N terminus of 164 amino acids with the P protein due to the unique process of RNA editing. Mutational analysis has determined that this region contains an NP binding domain, with another NP binding domain being found at the C terminus. Each site has been shown to negatively and positively affect RNA synthesis, respectively with L16 and I17 identified as critical sites within the NP binding domain for inhibition of viral RNA synthesis (Yang et al. 2015). The unique C terminus of V protein also contains 7 highly conserved cysteine residues that can bind two zinc ions creating a zinc finger-like structure (Paterson et al. 1995; Yang et al. 2015).

Arguably, the most renowned role of the V protein is its ability to block the IFN response by targeting both the IFN induction and signalling cascades. Indeed, it can block IFN induction via its interaction with Mda-5 and by sequestering IRF3 in the cytoplasm (Andrejeva et al 2004, Childs et al 2007, Biao He et al 2002). More recently it has been shown that the V protein can form a complex between RIG-I and the Laboratory of genetics and Physiology 2 (LGP2) protein that blocks the activation of RIG-I by RIG-I ligands again blocking activation of IFN induction (Childs et al 2012). Furthermore, the V protein can also block IFN signalling by targeting STAT1 for proteosomal degradation via its interaction with the damaged DNA binding protein (DDB1)(Didcock et al 1999, Precious et al 2005, Precious et al 2007). A PIV5 virus lacking the cysteine rich domain of the V protein was shown to be unable to block IFN induction or IFN Signalling (He et al 2002). Subsequently, the combination of Y26H, L50P and L102P mutations were identified to prevent V protein function against IFN signalling in the IFN-sensitive virus PIV5 CPI-, for the first time indicating a role for the V/P common N terminal domain in blocking IFN signalling (Chatziandreou et al. 2002). In addition to its roles in IFN antagonism, the C terminal region is also thought to be important in preventing apoptosis, as a recombinant virus lacking the C terminus induces a severe cytopathic effect (CPE) in tissue culture (Sun et al 2004). In addition, the expression of the V protein has been shown to delay the cell cycle and overexpression of DDB1 can partially restore this delay (Lin and Lamb 2000). Taken together these functions highlight the multifunctional role of the V protein in numerous roles within the virus life cycle (summarised in Figure 1.7).

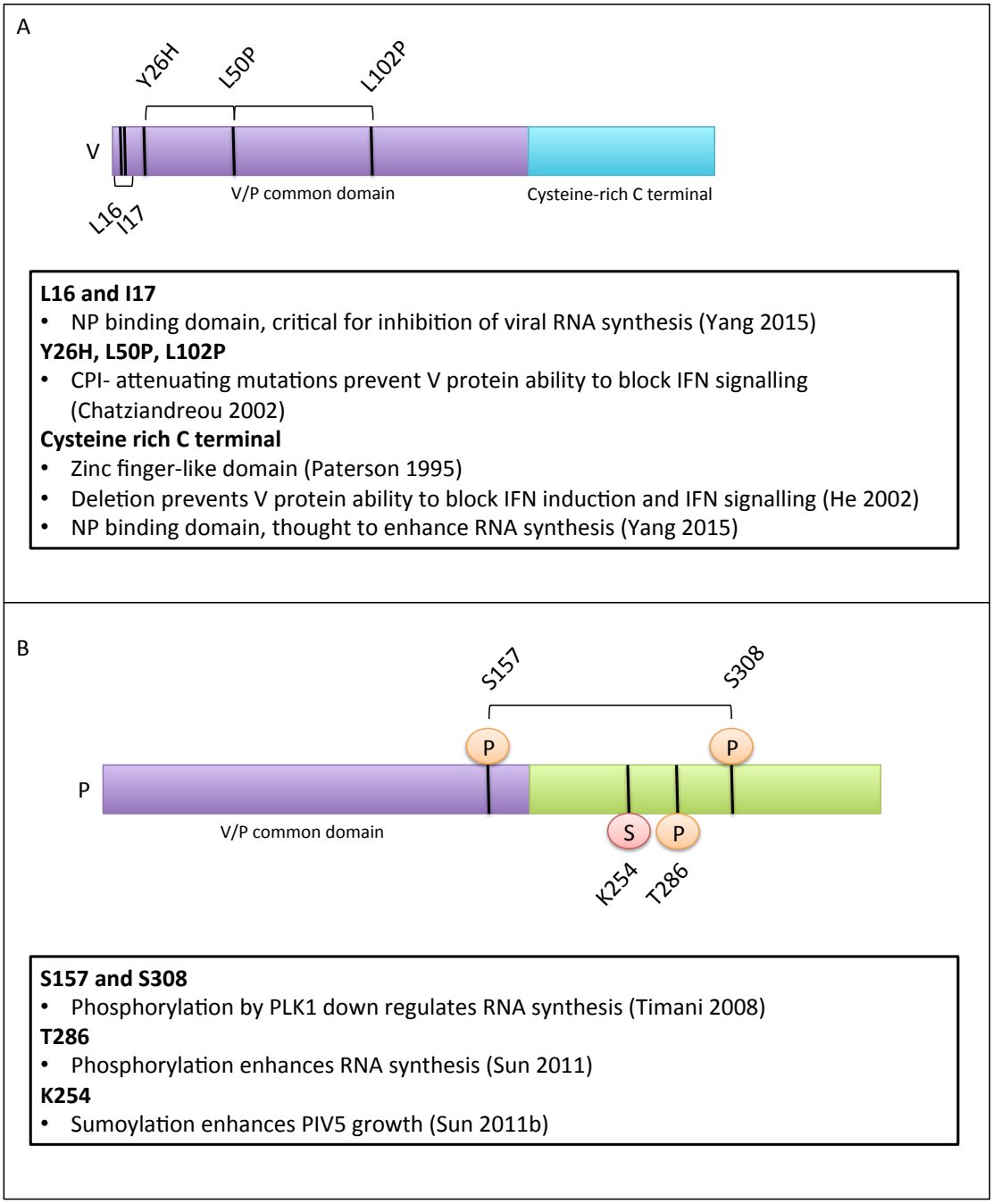

Figure 1.7: Summary of properties attributed to A) the V protein and B) the P protein of PIV5

1.11.3 Phosphoprotein (P)

The third protein, P, consists of 392 amino acids and it is thought that its main role is to aid RNA synthesis via its non-catalytic interaction with the viral RNA polymerase within the nucleocapsid complex. Numerous models attempt to explain the function of P however its exact role remains controversial. The most well supported model indicates that P tethers the catalytic L polymerase protein to the genomic RNA during RNA synthesis. Like all other paramyxovirus P proteins, the PIV5 P protein is heavily phosphorylated however the possible roles for this remain an enigma (Fuentes et al. 2010). Amongst the P proteins of the paramyxoviruses, the Sendai virus (SeV) and RSV are the best studied. Initial studies of SeV seemed to suggest that phosphorylation of the P protein did not play a major role in viral RNA synthesis (Hu & Gupta 2000; Hu et al. 1999; Byrappa et al. 1996). Studies of the RSV P protein then indicated that phosphorylation was dispensable for virus replication however more recent studies have recognised that phosphorylation of the P protein is essential for management of the viral protein M2-2 and its ability to mediate transcriptional inhibition (Lu et al. 2002; Asenjo & Villanueva 2016). Analysis of the PIV5 P protein suggests that phosphorylation at different sites can have both positive and negative effects on RNA synthesis (Sun et al 2011a)(summarised in Figure 1.7). One example of this shown to negatively regulate RNA synthesis is phosphorylation of serine 157 together with serine 308 by the host kinase Polo-like kinase 1 (PLK1) which when mutated to prevent phosphorylation was shown to elevate viral RNA synthesis (Sun et al 2009, Timani et al 2008). Another site shown to positively affect RNA synthesis is threonine 286 which when mutated lead to slowed viral mRNA synthesis and delayed protein

expression (Sun et al 2011a). Interestingly, sumoylation of the P protein at K254 is also thought to be important for PIV5 growth (Sun et al 2011b). Despite the debated model what is known is that the P protein is essential for RNA synthesis and it therefore plays a vital role in virus infection.

1.11.4 Matrix protein (M)

Next, the most abundant protein found within the PIV5 particle- the M protein contains 377 amino acids and is an organisational protein that orchestrates numerous proteins during assembly of the viral particle. During the replication cycle the M protein lines the inner surface of the host cell membrane and coordinates the interaction of host proteins such as caveolin-1 and angiomotin-like 1, viral glycoproteins and cytoplasmic nucleocapsids (Pei et al. 2011). These interactions lead to the formation and subsequent budding of infectious particles making it a vital protein in the viral life cycle (Parks et al. 2011).

1.11.5 Fusion protein (F)

The F protein is a 529 amino acid protein that firstly allows viral entry to the cell through fusion of the virion envelope with the host cell plasma membrane, secondly it promotes cell-cell fusion forming what is known as syncytia however cell-cell fusion is minimal in PIV5. The protein is initially synthesized as a precursor molecule Fo that is then glycosylated in the ER and forms homotrimers. Fo is then cleaved by an unknown host protease to F1 and F2 which results in a conformational change to a trimeric coiled coil that permits fusion (Welch et al. 2012). Interestingly mutations to the fusion peptide at positions 3, 7 and 12 resulted in hyperfusogenic F proteins that have been

subsequently harnessed for therapeutic applications such as increasing potency of oncolytic viruses (Gainey et al. 2008; Parks et al. 2011).

1.11.6 Small hydrophobic protein (SH)

Next, the smallest of all the proteins produced from the PIV5 genome, the SH protein, consists of only 44 residues many of which are hydrophobic. Its main role within the viral life cycle remains controversial with evidence suggesting that it could play roles in preventing apoptosis by blocking TNF-α as an SH knockout virus induced apoptosis in bovine and mouse cell-lines but not human A549 or Hela cells (Lin et al. 2003; He et al. 2001; Wilson et al. 2006). Other studies suggest that SH plays a role in counteracting immune responses but its exact role remains uncertain (Parks et al. 2011). Interestingly it has been shown in the related virus RSV that SH forms small pentameric ion channels which may function in a similar manner to influenza virus however there exact role is not certain (Gan et al. 2012).

1.11.7 Haemagglutinin-neuraminidase protein (HN)

Penultimately, HN is found on the outer surface of the virus particle and consists of 565 amino acids. Structurally, it is a type II membrane protein that has a large ectodomain, a transmembrane domain and a small N-terminal cytoplasmic tail. Functionally, it has been shown to be responsible for attachment of the virus particle to the host cell through its sialic acid binding activity (Bose et al 2011). This attachment is then thought to initiate a conformational change within the HN protein exposing the HN-stalk residues that interact with and trigger the F protein to initiate fusion with the host membrane (Bose et al 2013). PIV5 HN

also has enzymatic neuraminidase activity which is thought to function in aiding release of the virus (Merz et al. 1981; Welch et al. 2013).

1.11.8 Large protein (L)

Finally, the large protein L comprises a huge 2255 amino acids and is the essential catalytic subunit of the viral RNA dependent RNA polymerase. Tethered to the nucleocapsid template via the P protein this subunit is responsible for the replication and transcription of viral RNA (Parks et al. 2011). Interestingly, it has been shown that the L protein may have intrinsic kinase activity that enhances the phosphorylation of RAC-alpha serine/threonine-protein kinase (AKT1). Phosphorylated AKT1 can then phosphorylate the viral P protein, which as stated previously plays a vital role in the viral life cycle (Luthra et al. 2008).

1.12 PIV5 strains

1.12.1 PIV5 W3 and rPIV5mCh

In addition to PIV5 W3 a number of other wild-type and recombinant strains are routinely used within our study. PIV5 W3 was originally isolated by Hull and Minner in 1957. Subsequently a recombinant strain of PIV5 W3, namely rPIV5mCh, has been created, which contains the gene expressing mCherry fluorescent protein inserted between the HN and L polymerase of the viral genome. This virus therefore expresses mCherry fluorescent protein, which allows viral infection to be tracked easily via fluorescent microscopy techniques.

1.12.2 PIV5 CPI+/CPI-

The IFN-sensitive virus, canine parainfluenza CPI- is also routinely used within our study, which is antigenetically related to PIV5 W3. The parental strain CPI+

was isolated from the cerebrospinal fluid of a dog suffering with incoordination and impaired movement (Evermann et al. 1980). CPI- was later isolated from the brain of a dog during experimental work on CPI+. Most interestingly it has been shown that CPI- cannot block the IFN response due to three amino acid substitutions in the V protein, making it an ideal control of V protein functionality (Chatziandreou et al. 2002).

1.13 Research aims

1.13.1 Aim 1: Enhancing virus replication of IFN-sensitive viruses using the IFN inhibitor, Rux

The first aim of my study was to further characterize the use of the IFN inhibitor, Rux, which inhibits JAK1/2 of the IFN signalling pathway, with respect to growth of IFN-sensitive viruses.

1.13.2 Aim 2: Development of a novel method to rapidly select IFN-sensitive viruses using FACS

The second aim of this study was to develop a method to rapidly isolate IFN-sensitive viruses from paramyxoviruses using FACS. Following isolation, we then planned to employ the IFN inhibitor, Rux, to characterise selected mutants for IFN-sensitivity.

2 Materials and Methods

2.1 Cells, viruses, antibodies and IFN inhibitors

2.1.1 Mammalian cell-lines

All mammalian cell-lines used in this research are listed in Table 2.1. In addition to these basic cell-lines, a number of derivatives of A549 and MRC5 cells were used and these are listed in Table 2.2.

Table 2.1: List of mammalian cell-lines used in this study

Cell-line	Description
293T	Human embryonic kidney cell-line (provided by Professor Richard Iggo, University of Bordeaux)
A549	Human carcinomic alveolar basal epithelial cell-line (obtained from the European Collection of Authenticated Cell Cultures (ECACC))
BalB/C	Mouse embryonic fibroblast cell-line (ECACC)
MDBK	Madin-Darby bovine kidney cell-line (ECACC)
MDCK	Canine Cocker Spaniel kidney epithelial cell-line (ECACC)
PKIBRS2	Biological Institute renale swine 2 porcine kidney epithelial cell-line (Institute of Animal Health (House & House 1989))
RK.13	Rabbit kidney epithelial cell-line (ECACC)
Vero	African Green Monkey kidney cell-line (ECACC)
MRC5	Human lung fibroblast cell-line (ECACC)

Table 2.2: List of mammalian cell-line derivatives used in this study

Cell-line derivative	Description
A549.pr(ISRE).GFP	A549 cell-line that stably expresses GFP under the control of the Interferon stimulated response element (ISRE) element contained within an MxA promoter. It also contains inducible resistance to puromycin as puromycin-N-Acetyl-trasnferase (PAC) is expressed under the control of the ISRE element (Stewart et al. 2014; Gage et al. 2016)
A549.pr(ISRE).GFP/ ISG56^{-}/BVDV Npro	A549 cell-line that stably expresses GFP and PAC under the control of the ISRE element contained within an MxA promoter. Secondly, it stably expresses short-hairpin RNA (shRNA) to ISG56 and thirdly, it stably expresses the N-terminal protease (Npro) from Bovine Viral Diarrhoea Virus (BVDV). (See section 2.4 for generation of this cell-line)
A549/PIV5-V	A549 cell-line that stably expresses V protein from Parainfluenza virus 5 (Young et al. 2003)
MRC5/PIV5-V	MRC5 cell-line that stably expresses V protein from Parainfluenza virus 5 (Young et al. 2003)

2.1.2 Wild-type and recombinant viruses

All wildtype and recombinant viruses used in this study are listed in Table 2.3

Table 2.3: List of viruses used in this study

Virus	**Description**
ANAV	Anopheles A virus (provided by Professor Richard Elliot, University of Glasgow)
BUN-WT	Bunyamwera wild-type virus (provided by Professor Richard Elliot, University of Glasgow)
BUNΔNSs	A recombinant Bunyamwera virus that has the IFN antagonist, nonstructural protein (NSs), gene deleted (Weber et al. 2002)
BWAV	Bwamba virus (provided by Professor Richard Elliot, University of Glasgow)
CVV	Cache Valley Virus (provided by Professor Richard Elliot, University of Glasgow)
KRIV	Kairi Virus (provided by Professor Richard Elliot, University of Glasgow)
MDV	Main Drain Virus (provided by Professor Richard Elliot, University of Glasgow)
MeV	Measles Edmonson vaccine strain (obtained from The National Institute for Biological standards and controls (NIBSC))
MuV	Mumps Enders vaccine strain (NIBSC)
PIV5 CPI+	Canine PIV5 CPI+ strain (Southern et al. 1991)
PIV5 CPI-	Canine PIV5 CPI- strain that contains a non-functional IFN antagonist V protein (Southern et al. 1991)
PIV5 W3	Human Parainfluenza virus 5 W3A strain (Choppin 1964)
rPIV5mCh	A recombinant strain of PIV5 that contains mCherry fluorescent protein inserted between the HN and L genes within the viral genome (provided by Dr Biao He, University of Georgia)
SBV	Schmallenberg Virus (provided by Professor Richard Elliot, University of Glasgow)

2.1.3 Antibodies

All primary and secondary antibodies used in this study are listed in Table 2.4.

Table 2.4: List of Primary and Secondary antibodies used within this study

Primary Antibodies	**Manufacturer (catalogue number)**
Goat anti-IFIT1 (ISG56; polyclonal)	Santa Cruz Biotechnology (sc-82942)
Mouse anti-PIV5 HN (monoclonal)	Prof Richard Randall, University of St Andrews (Randall et al. 1987)
Mouse anti-PIV5 F (monoclonal)	Prof Richard Randall, University of St Andrews (Randall et al. 1987)
Mouse anti-PIV5 NP (monoclonal)	Prof Richard Randall, University of St Andrews (Randall et al. 1987)
Mouse anti-β-actin (monoclonal)	Sigma-Aldrich (A2228)
Mouse anti-STAT1 (monoclonal)	Santa Cruz Biotechnology (sc-8394)
Rabbit anti-Bunyamwera N protein antisera (polyclonal)	Provided by Richard Elliot, University of Glasgow
Rabbit anti-Mx1/2/3 (H285; MxA; polyclonal)	Santa Cruz Biotechnology (sc-166412)
Secondary Antibodies	**Manufacturer**
Goat anti-mouse Texas Red (TR)	Serotec® (103007)
Goat anti-mouse alkaline phosphatase (AP)-conjugated	Cell signalling technology (7056)
Goat anti-rabbit (AP)-conjugated	Cell signalling technology (7054)
IRDye®680RD goat anti-mouse	LI-COR (925-68070)
IRDye®680RD donkey anti-goat	LI-COR (925-68074)
IRDye®680RD goat anti-rabbit	LI-COR (925-68071)

2.1.4 IFN inhibitors

The IFN inhibitor Ruxolitinib (Rux) (INCB018424; Selleck chemicals) is a potent inhibitor of JAK1/2 with an IC_{50} of 3.3nM. Stocks were prepared in dimethyl sulfoxide (DMSO) at a concentration of 10mM and stored at -80°C.

2.2 Cell culture and Virological methods

2.2.1 Cell maintenance

All cells described above (Table 2.1 and Table 2.2) were cultured in 25cm^2, 75cm^2 or 175cm^2 tissue flasks (Greiner Bio-One) using Dulbecco's modified Eagle's medium (DMEM)(Thermo Fisher Scientific). This medium was supplemented with 10% [v/v] foetal bovine serum (FBS; Thermo Fisher Scientific) and 1% [v/v] penicillin and streptomycin (pen/strep). Cells were incubated at 37°C/5% CO_2 and routinely passaged when confluent using Trypsin/ethylenediaminetetraacetic acid (EDTA).

2.2.2 Cryopreserving and resuscitation of cells

Cells generated during this study were tested for mycoplasma, using PCR Mycoplasma Test Kit II, following manufacturer's instructions (Promokine) and only mycoplasma-negative cells were stored in liquid nitrogen. Cells were prepared for cryopreservation by trypsination of the cell monolayer, followed by re-suspension in 10% [v/v] FBS, 1% [v/v] pen/strep DMEM and pelleting at 1200rpm for 5min at room temperature (RT). Cells were then re-suspended in freezing medium (10% [v/v] DMSO, FBS), aliquoted into cryovials and frozen at -80°C before storage in liquid nitrogen. To resuscitate cells, cryovials were thawed rapidly at 37°C, centrifuged at 1200 rpm for 5min at RT and re-suspended and maintained in 10% [v/v] FBS, 1% [v/v] pen/strep DMEM at 37°C/5% CO_2. If necessary, the appropriate antibiotic selection (puromycin at 2µg/ml or blasticidin at 10µg/ml) was added following the first passage.

2.2.3 Preparation of virus stocks

All virus stocks used within this study were prepared using 90% confluent Vero cells. Cells were infected with the chosen virus at a multiplicity of infection (MOI) of 0.001 PFU/cell in 1ml serum-free DMEM per 25cm^2 flask or in 3mls serum-free DMEM per 75cm^2 flask. Following 1h on a rocking platform at 37°C 5% CO_2, the media volume was increased to 6mls per 25cm^2 flask or 11mls per 75cm^2 flask using serum-free DMEM and incubated for a further 3-4 days. Following incubation, the supernatant containing virus was harvested then clarified at 1500rpm for 5min before aliquoting into appropriate small volumes (<500µl) and storage at -80°C.

2.2.4 Virus infections

Monolayers of cells were infected at an appropriate MOI with virus suspended in a low volume of serum-free or 2% [v/v] FBS/DMEM (200µl for 6 well plate, 100µl for 12 well). After an initial adsorption period of 1h on a rocking platform at 37°C 5% CO_2 the virus inoculum was removed. Each monolayer was then washed with Phosphate-Buffered Saline (PBS), replaced with serum-free DMEM and incubated at 37°C 5% CO_2 until harvested.

2.2.5 Plaque assays

Plaque assays were used for several purposes during this study, firstly, to determine the titer of viral stocks following preparation and, secondly, to determine plaque development of viruses under different conditions such as in the presence of IFN inhibitor. Monolayers of cells were cultured in 6 or 12 well plates until 80-90% confluent. The virus stock was diluted 10-fold in DMEM 2% FBS with the exception of BUN WT and BUNΔNSs which was diluted in PBS 2%

New Calf Serum. Cells were then infected with low volume inoculum (200µl for 6 well plate, 100µl for 12 well) and incubated at 37°C 5% CO_2 for 1 hour with horizontal shakes every 15 min to prevent the monolayer from drying out. Inoculum was then removed and an appropriate volume of 2X overlay media (50ml 10X MEM, 10mls 100X Glutamax, 2% [v/v] Foetal calf serum (FCS), 14.5ml $NaCHO_3$ 7.5%, 170ml dH_2O) mixed with 2X avicel (final concentration 0.6% [w/v] avicel: Sigma-Aldrich®) was added. Where appropriate, IFN inhibitor Rux (4µM each) or the equivalent volume of DMSO was added directly to the overlay. Plates were then incubated for 1-6 days, without disturbing, until plaques were formed. Following incubation plaques were fixed in 5% [v/v] formaldehyde/PBS for 1hour at 4°C.

Plaques were visualised by either crystal violet (CV) staining or immunostaining. To visualise the plaques using CV staining, 0.15% [w/v] CV stain was added for 5 min on a rocking platform and then removed with water. Virus titre could then be determined using the following equation:

Equation 1: $\boldsymbol{Virus\ titer = number\ of\ plaques\ x\ dilution\ of\ virus\ stock}$

To visualize the plaques by immunostaining, fixed cells were permeabilised with 0.1% [v/v] Triton X-100/PBS for 30 min followed by addition of 500µl/well of appropriate primary antibody in 2% FBS/PBS (Table 2.4). Plates were then incubated for 1hour at RT on a rocking platform. Afterwards, cells were washed with PBS before addition of the appropriate secondary alkaline phosphatase (AP) conjugated antibody (Table 2.4). Monolayers were then washed and incubated with AP substrate (SIGMA*FAST*™ BCIP®/NBT, Sigma-Aldrich) prepared

in water until plaques were visible. The monolayers were then rinsed with water to stop any further reaction and the viral titer calculated as stated in Equation 1. When required measurement of plaque size was completed using Pixel stick (Plum Amazing) and significance calculated using an unpaired t test.

2.2.6 Multistep viral growth curves

Multistep viral growth curves were used to analyse virus growth of a number of viruses in several different cell-lines in the presence and absence of IFN inhibitor. Specifically, cells were seeded at $2x10^6$ cells per $25cm^2$ flask the day prior to infection. Virus infection was then added at an MOI of 0.001 PFU/ml in 10% [v/v] FBS, 1% [v/v] pen/strep DMEM and incubated on a rocking platform for 3 hours at 37°C 5% CO_2. The inoculum was then removed and the monolayer washed with PBS. Subsequently, 5mls of 10% [v/v] FBS, 1% [v/v] pen/strep DMEM was then added containing IFN inhibitor Rux (4μM) or equivalent volume of DMSO. Subsequently, 300μl of virus supernatant was then collected at each time point and titered on Vero cells using a plaque assay (see section 2.2.5).

2.3 IFN Signalling GFP reporter assay to assess the stability of the IFN inhibitors Rux

An IFN signalling GFP reporter assay was used to determine the stability of the IFN inhibitor Rux. Initially, the inhibitor Rux (4μM) or equivalent volume DMSO were incubated individually in 5mls of 10% [v/v] FBS, 1% [v/v] pen/strep DMEM on A549 naïve cells and 300μl samples of the supernatant were taken for 7 days. Each sample was then analysed by assessment of GFP knockdown on A549:pr(ISRE).GFP reporter cells, using an IFN signalling GFP reporter assay.

To conduct an IFN signalling GFP reporter assay, A549.pr(ISRE).GFP reporter cell-lines were seeded in triplicate per treatment at $3x10^4$ cells/well in 96 well plates (see Table 2.2 for a description of these cell-lines). Notably, this reporter cell-line requires activation to enable production of GFP expression. To activate the ISRE element in A549.pr(ISRE).GFP cell-lines, cells were treated with $1x10^4$ Units/ml of purified IFN-α (Roferon, NHS) in DMEM and incubated for 48 hours at 37°C 5% CO_2 before measuring GFP expression. GFP expression was measured using TECAN infinite 200 plate reader (TECAN) set to an excitation of 488nm and emission of 528nm or imaged by EVOS® microscope (Thermo Fisher Scientific). Data was then analysed using Magellan data analysis software (TECAN) and presented using Graphpad Prism 6 (Graphpad software).

2.4 Generation of the A549.pr(ISRE).GFP/ISG56-/BVDV Npro cell-line using pdl'shISG56.blast and pdl'BVDV Npro.puro lentivirus

To develop a method to isolate IFN-sensitive viruses using flow cytometry a derivative of the A549/pr(ISRE).GFP cell-line (Table 2.2) was generated that constitutively expresses both ISG56 and BVDV Npro. The A549/pr(ISRE).GFP/ISG56$^-$/BVDV Npro cell-line (Table 2.2) was generated using second-generation lentivirus system that enables stable expression of the inserted gene of interest within target cells. This system required two parts: i) generation of lentivirus particles by transfection of 293T cells with three lentiviral plasmids and ii) transduction of target cells with the lentivirus to create a stably expressing cell-line.

2.4.1 Generation of pdl'shISG56.blast and pdl'BVDVNpro.puro lentiviruses

The generation of the lentiviruses pdl'shISG56.blast and pdl'BVDV Npro.puro required three lentiviral plasmids each. The first two plasmids, CMV-R and VSV-G, are known as the packaging plasmids. CMV-R encodes the HIV gag structural protein and HIV pol gene encoding enzymes for replication (Zufferey et al. 1997). VSV-G encodes the vesicular stomatitis virus (VSV) envelope protein (Naldini et al. 1996). A third plasmid, known as the transfer vector, contains the gene of interest as well as all the necessary elements to allow the delivery of the gene including: long terminal repeats regions (LTRs), the ψ packaging site, the rev response element (RRE), the central polypurine tract (cPPT) and an spleen focus-forming virus (SFFV) promoter. It also contains antibiotic selection markers to allow selection of successfully transduced target cells. In this case, the BVDV Npro expressing plasmid, pdl'BVDVNpro.puro, expresses PAC which confers puromycin resistance and the shISG56 expressing plasmid, pdl'shISG56.blast, expresses blasticidin-S deaminase which confers blasticidin resistance (kindly provided by Dr Lena Andrejeva, University of St Andrews). Together with the CMV-R and VSV-G plasmids, each of these transfer vectors was combined to create two lentivirus's, the first of which expresses BVDV Npro and the second of which expresses shISG56. Specifically, each of the plasmids were prepared (6µg CMV-R, 6µg VSV-g and 10µg transfer vector) in 1.5mls OptiMEM and incubated for 5min. Subsequently, 1.5mls of OptiMEM containing 4% [v/v] Lipofectamine 2000 (Thermo Fisher) was added to the plasmid mix and incubated for a further 30min at RT. Two 75cm^2 flasks of 50% confluent 293T cells in 10% [v/v] FBS DMEM without antibiotics were then transfected with each plasmid mix and incubated at 37°C/5% CO_2 for 5 hours. Following

incubation, the media was replaced with 10% [v/v] FBS DMEM without antibiotics. Subsequently, 48h post transfection the supernatant containing the lentivirus was harvested, clarified at 1500rpm for 10min, filtered using a 0.45μM filter, aliquoted into 1ml fractions and stored at -80°C.

2.4.2 ii) Transduction of A549.pr(ISRE).GFP cells with pdl'shISG56.blast and pdl'BVDV Npro.puro lentivirus

To create a cell-line which expressed both shISG56 and BVDV Npro, A549.pr(ISRE).GFP cells were transduced firstly with the lentivirus expressing shISG56 and selected using blasticidin. Surviving cells were then transduced again with the lentivirus expressing BVDV Npro and selected for a second time using both puromycin and blasticidin. Specifically, one aliquot of lentivirus was combined with 1ml of serum-free DMEM and polybrene (8μg/ml) and added to a 25cm^2 flask containing 50% confluent target cells. The cells were then incubated for 2.5hours before topping up media with 2ml 10% [v/v] FBS DMEM without antibiotics and incubating the flask for a further two days. Antibiotic selection (puromycin 2μg/ml for 2days and blasticidin 10μg/ml for 4 days) was then added to select cells that had been successfully transduced with the target lentivirus. The resultant cell-line then remained under antibiotic selection until required for further experiments.

2.4.3 Characterization of A549.pr(ISRE).GFP/ISG56-/Npro cells using western blot analysis

The newly generated cell-line, A549.pr(ISRE).GFP/ISG56-/Npro, was characterized using western blot for expression of ISG56, MxA and PIV5 NP following infection with PIV5 CPI-. Western blot analysis contains two steps: i)

separation of the proteins by sodium dodecyl sulphate polyacrylamide gel electrophoresis (SDS-PAGE) and ii) transfer of the proteins to a PVDF membrane that can then be probed with antibodies to detect specific proteins. Specifically, A549/pr(ISRE).GFP and A549.pr(ISRE).GFP/ISG56-/Npro cells were pre-treated for 8 hours with IFN at $1x10^4$Units/ml or left untreated before cells were mock infected or infected with PIV5 CPI- at MOI 5. Cell monolayers were then lysed 18hours post infection in disruption buffer containing: 10M urea, 20% [w/v] SDS, 15% [v/v] β-mercaptoethanol and a few crystals of bromophenol blue. Cell lysates were then sonicated twice for 5 seconds and heated for 10min at 95°C to denature protein structure. Prepared samples were then loaded onto 12% hand-cast polyacrylamide gels (30% Protogel, as per manufacturer's instructions, National Diagnostics) for separation by SDS-PAGE alongside a ladder of proteins with known molecular weight (PageRular Plus Prestained Protein Ladder; Thermo Fisher Scientific). Gels were run using 1X TGS running buffer (25mM Tris, 192mM glycine, 0.1% [w/v] SDS, pH8.3) at 110V in Bio-Rad electrophoresis tanks until clear separation of the protein ladder was obtained. Following SDS-PAGE electrophoresis, the proteins were transferred using the Bio-Rad Trans-blot Turbo Transfer System onto methanol activated polyvinylidene difluoride (PVDF) membrane using 1X NuPage transfer buffer (500mM Bis-Tris, 500mM Bicine and 20.4mM EDTA). The membrane was then blocked for 1 hour at RT in blocking buffer (PBS, 5% [w/v] skimmed milk powder and 0.1% [v/v] Tween-20). Once blocked, the membrane was incubated with appropriate primary antibody diluted in blocking buffer (Table 2.4). Here, Goat anti-IFIT1 (ISG56), rabbit anti-MxA, mouse anti-PIV5 NP and mouse anti-Actin antibodies were used sequentially at a dilution of 1:1000 overnight at 4°C. Following incubation with

each primary antibody, the membrane was washed six times using PBS 0.5% [v/v] Tween-20 for 5 min each to remove unbound antibody. The membrane was then incubated with the appropriate LiCOR IRDye® fluorescent secondary antibody (donkey anti-goat, goat anti-rabbit and goat anti-mouse) diluted 1:10000 in blocking buffer. Afterwards, each membrane was then washed again before visualisation using the Odyssey CLx Imaging system (LiCOR Biosciences).

2.5 Florescence activated cell sorting (FACS) analysis

2.5.1 Preparation of cells for FACS analysis

Fluorescence activated cell sorting (FACS) analysis was used to accurately measure GFP, mCherry and texas red fluorescence from live cells following infection of GFP reporter cells, A549.(ISRE).GFP or A549.pr(ISRE).GFP/ISG56$^-$/BVDV Npro. All cells to be examined by FACS analysis were prepared using the same method. In brief, A549.(ISRE).GFP or A549.pr(ISRE).GFP/ISG56$^-$/BVDV Npro reporter cells were seeded into 12 well plates at $3x10^5$ cells/well and allowed to adhere overnight. The following day, cells were infected with virus (rPIV5mCh, PIV5 W3 or a mutant derived from these viruses) at the specified MOI, in 200µl serum-free DMEM and incubated at 37°C, 5% CO_2 on a platform rocker for 1 hour. Following infection, the inoculum was removed and the monolayers washed with PBS before addition of 1ml serum-free DMEM. After 6-8 hours, primary antibody (anti-PIV5 HN and anti-PIV5 F) was added at a dilution of 1:1000 to prevent infection with progeny virus and IFN-α was added to the appropriate wells at $1x10^4$Units/ml to induce GFP expression. The following day cell monolayers were prepared for FACS analysis. Each monolayer was trypsinised, re-suspended in 10% [v/v] FBS/DMEM, centrifuged at 1500rpm

for 5min and re-suspended in 1ml serum-free DMEM. Thereafter, cells in suspension were filtered using a 40μm cell strainer (Corning), collected in polypropylene tubes (Corning) and kept on ice until FACs analysis and/or sorting.

2.5.2 Set up of the BD FACSJazz™ cell sorter and FACS analysis

FACS analysis/sorting was accomplished using a FACSJazz™ Cell sorter (Becton Dickinson and company, BD) and FACS sortware sorter software (BD). In brief, a FACS analyzer organizes cells using hydrodynamic force into a single-file stream. Lasers are then aligned to this stream forming an interrogation point. At this point the lasers excite the fluorochromes expressed within each cell and the light emitted known as the emission spectra is detected and measured. Following interrogation, the stream is forced to form droplets by application of an acoustic wave through a piezoelectric device. Application of a positive or negative charge to these droplets then allows specific cells to be sorted using charged deflection plates. These deflection plates attract droplets of the opposite charge and can therefore guide droplets containing cells of interest into specified plates. To set up the FACSJazz™ cell sorter, the stream was aligned and focused by eye using the inbuilt pinhole camera. The two lasers (488nm and 561nm) that allow excitation of each fluorochrome were then aligned to the stream using SPHERO™ Rainbow Calibration Particles (BD) (as per manufacturer's instructions). Following this, FACS™ Accudrop Beads (BD) were used to determine the drop delay (as per manufacturer's instructions). This parameter is defined as the time between analysis of a cell at the interrogation point and application of the charge to the droplet. Measurement of this parameter is vital

to ensure that the charge applied to each drop is applied at the correct time so that the drops formed contain the cell selected for sorting. After alignment, a control sample of non-fluorescent cells is then loaded onto the machine. This allows specific gating to be applied to exclude debris and doublets of cells (Figure 2.1). Following gating, fluorescent controls positive for GFP and mCherry or Texas red only are used to apply compensation to the workspace. Notably, all fluorochromes emit a range of wavelengths known as the emission spectra and within a FACS analyzer, this emission spectra is selected by a bandpass filter. However, when measuring two fluorochromes simultaneously the emission spectra can overlap and the fluorescence from one can distort the measurement of the other. To correct for this distortion, fluorescence compensation is applied. This allows the measurement of two different fluorochromes from one cell as it excludes the spectral overlap of one fluorochrome from the other. Notably, the spectral overlap between GFP and mCherry/texas red is very small (~2%). GFP was measured using excitation from a 488nm laser and selected using a 530/40 bandpass filter. mCherry and texas red were measured using excitation from a 561nm laser and detected using a 610/20 bandpass filter. Following set up of the machine each sample was loaded and analysed. Measurement of GFP and mCherry or texas red fluorescence was taken from 10000 cells within each sample.

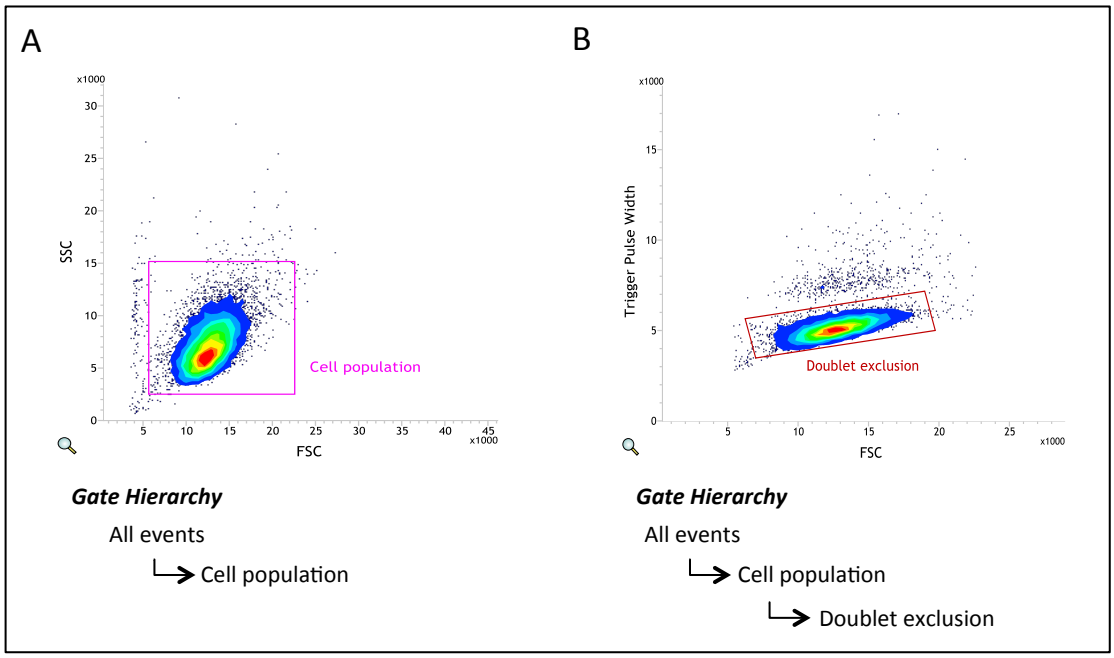

Figure 2.1: Cell sorter gating applied to all samples to exclude debris and doublets A) Shows 'all events' of a typical sample on a graph that demonstrates forward scatter (FSC) of each of the cells versus side scatter (SSC). Notably, FSC indicates the relative size of the cells and SSC indicates the relative granularity of the cells. The gate applied then selects the cell population from 'all events' and excludes debris. **B)** Shows FCS versus trigger pulse width for the gated cell population. The gate applied here selects for the single cell population and excludes doublets due to their appearance at double the trigger pulse width of a single cell. Notably, the trigger pulse width is a measurement of the time it takes for the cell to pass the detector. Consequently, doublets take double the time to pass the detector than a single cell and can therefore be excluded as they appear at double the trigger pulse width of a single cell. Following doublet exclusion samples are then analysed and gated for sorting based on fluorescence.

2.6 Isolation of IFN-sensitive mutants from rPIV5mCh using flow cytometry

2.6.1 Selection and sorting of potentially IFN-sensitive rPIV5mCh mutants into 96 well plates

A method to isolate IFN-sensitive mutant viruses from a rPIV5mCh wild-type stock using the newly generated GFP reporter cell-line, A549/pr(ISRE).GFP/ISG56$^-$/BVDV Npro was developed. To select and sort IFN-sensitive rPIV5mCh mutants, A549/pr(ISRE).GFP/ISG56$^-$/BVDV Npro cells were infected with a rPIV5mCh stock at MOI 1 and prepared for FACS analysis as stated previously (see section 2.5). During analysis, cells positive for both GFP and mCherry (potentially infected with an IFN-sensitive virus), were then selected and sorted onto 96 well plates containing a monolayer of A549/pr(ISRE).GFP/ISG56$^-$/BVDV Npro cells, using a 1.0-drop pure single cell sort setting. These sort settings provide the most stringent cell sorting as they ensure that only one droplet is sorted containing a single cell. Following sorting, each 96 well plate was then incubated for 3-4 days (depending on the level of cytopathic effect (CPE) seen) and then subjected to further analysis.

2.6.2 Preparation of working stocks of potentially IFN-sensitive rPIV5mCh mutant viruses

Supernatant from FACS sorted cells (see above 2.6.1) was removed and stored in a new 96 well plate at -80°C. Following supernatant removal, cells were incubated in the presence of $1x10^4$ Units/ml IFN for 18h and then analysed using a fluorescent microscope (EVOS; Thermo Fisher Scientific). As before, wells

containing cells positive for both GFP and mCherry were identified as containing a potential IFN-sensitive mutant virus. Subsequently, stored supernatant corresponding to each GFP and mCherry positive well was then used to create a working stock of the potential IFN-sensitive mutant virus. Specifically, virus working stocks were prepared by inoculating Vero cells using 5µl of the previously selected supernatant in 5ml 10% [v/v] FBS, 1% [v/v] pen/strep DMEM. Following 3-4 days the supernatant containing virus was then harvested and clarified as stated previously (see section 2.2.3).

2.6.3 Confirmation of potentially IFN-sensitive rPIV5mCh mutant viruses using flow cytometry

Potential mutants (see section 2.6.2) were screened for IFN sensitivity using flow cytometry. A549/pr(ISRE).GFP/ISG56^{-}/BVDV Npro cells were infected with each potential mutant virus stock in the same manner as the primary selection experiment (See section 2.6). Note, to expedite the process of mutant virus identification, mutant stocks were not titered for analysis using flow cytometry but were instead estimated at 1x10^{7} PFU/ml. Following analysis via flow cytometry mutants displaying an attenuated phenotype (i.e. were unable to block the IFN signalling pathway) were then titered on Vero cells using a plaque assay (see section 2.2.5). Following titration each mutant was then prepared for sequencing of the V/P gene.

2.6.4 Sequencing of the V/P gene of potentially IFN-sensitive mutant viruses

2.6.4.1 RNA Extraction using TRIzol

Viral RNA from potentially IFN-sensitive rPIV5mCh mutant viruses was extracted using TRIzol. Briefly, a 25cm^2 flask containing 90% confluent Vero cells was infected with each potential mutant at MOI 5 in 1ml serum-free DMEM. The cells were then incubated for 1hour on a rocker before the inoculum was replaced with 5mls 10% [v/v] FBS, 1% [v/v] pen/strep DMEM. After 18hours the supernatant was removed and 3mls of TRIzol was added to the cell monolayer. This was then rocked for 5min at RT before collecting and aliquoting into snap lock tubes (1ml each). Subsequently, 200µl of chloroform was added per aliquot, mixed well and incubated at RT for 2-3min. After incubation, each sample was centrifuged at 12000g for 15min at 4°C to separate the aqueous and organic phases. Specifically, 300µl of the upper aqueous phase containing both cellular and viral RNA was transferred to a clean tube and 1µl Glycoblue was added. Next, 500µl of 100% Isopropyl-alcohol (IPA) was added to each sample and incubated at -20°C for 30min. Samples were then centrifuged at 12000g for 10min at 4°C and the supernatant removed. The remaining blue pellet containing RNA was washed with 1ml 75% Ethanol and centrifuged at 7500g for 5min at 4°C. This step was then repeated a second time, followed by removal of the EtOH to allow the pellet to air dry. The pellet was then re-suspended in Nuclease free water and RNA concentration determined by measuring absorbance at 260nm (A260) using a NanoDrop 1000 UV spectrophotometer (Thermo Fisher Scientific). The purity of each sample was determined by A260/A280 and

A260/A230 ratio, with both ratios above 1.8 considered acceptable for further study. Each sample was then stored at -70°C

2.6.4.2 First strand cDNA synthesis

A primer specific to the PIV5 V/P gene was used during first strand cDNA synthesis to specifically reverse transcribe genomic V/P RNA to cDNA using Moloney Murine Leukemia Virus Reverse Transcriptase (M-MLV RT, Promega). The sequence of the specific primer used was 5'-GGTTCCTGCCTACCATCGG-3'. Each reaction contained 1.5µl of 100µM specific primer, 2µg of RNA and 3.5µl of nuclease free H_2O. This was then heated at 70°C for 5minutes to remove secondary structure within the template RNA. Next, the following components were added 5µl of M-MLV 5x Reaction buffer, 5µl of deoxynucleotide (dNTPs; containing 10mM each nucleotide), 0.5µl of Recombinant RNasin® Ribonuclease Inhibitor (25units), 3.5µl nuclease free H_2O and 1µl M-MLV RT (200units). This mix was then incubated for 60mins at 42°C after which the resulting cDNA was then stored at -20°C.

2.6.4.3 Polymerase Chain reaction (PCR)

PCR was used to amplify V/P cDNA from cDNA samples. All PCR reactions were completed using KOD hot start DNA polymerase (Merck Millipore) and the forward and reverse primers as follows:

PIV5 V/P primers

Forward primer 1 5'-GGTTCCTGCCTACCATCGG-3'

Reverse primer 1 5'-GTTCGGGCTTATTTATCGTTAATC-3'

The expected PCR product using these primers consisted of 1364bp. Each reaction comprised of the following 50µl mix: 5µl 10x polymerase buffer, 3µl

25mM $MgSO_4$, 5µl 2mM dNTPs, 1.5µl of 10µM PIV5 V/P forward and reverse primers, 100ng of template DNA and 1µl KOD hot start DNA polymerase (1Unit/µl). Each reaction was carried out in a thermocycler (Biometra®, T-gradient) using the following cycling conditions: polymerase activation at 95°C for 5min, denaturation at 95°C for 30sec, annealing at 55°C for 30sec and extension at 68°C for 20sec. The denaturation, annealing and extension steps were then repeated for 30 cycles before holding samples at 4°C for storage.

2.6.4.4 Gel Electrophoresis

PCR products were analysed using gel electrophoresis to identify if the correct size of PCR product had been obtained. In this case the expected size of the mutant V/P PCR product was ~1400bp. Gels were prepared containing 1% agarose and 1µg/ml Ethidium Bromide in 1X TBE buffer (1M Tris base, 1M Boric acid and 0.02M EDTA). Each 50µl PCR sample was prepared in 6X DNA loading buffer (Promega) and loaded onto the gel. Samples were run at 90V in TBE buffer for 30 minutes and visualised under UV light. DNA ladders of known size (1kb and 100bp ladders; Promega) were run alongside the samples to ensure that the PCR product obtained was the correct size. The PCR product was then excised and purified using QIAquick Gel Extraction Kit (following manufacturer's instructions;QIAGEN) and the DNA concentration determined by measuring absorbance at 260nm (A260) using a NanoDrop 1000 UV spectrophotometer (Thermo Fisher Scientific). The purity of each sample was determined by A260/A280 ratio, with a ratio above 1.8 considered acceptable for further study.

2.6.4.5 Ligation and transformation

Extracted V/P cDNA was blunt end cloned into the vector pJET 1.2, which confers ampicillin resistance (Thermo Fisher Scientific). Each reaction included 40ng of purified PCR product, 10µl of 2X reaction buffer, 1µl of pJET 1.2 vector, 7µl nuclease free H_2O and 1µl of T4 DNA Ligase (3 Weiss Units/µl). This mixture was then incubated at RT for 5min before transformation into competent cells. Following incubation, the mixture was transformed into 100µl ultra-competent *E. coli* cells (JM109) primed using the Z-competent™ *E. coli* transformation kit (as per manufacturer's instructions, ZYMO Research). Transformants were then plated onto agar plates containing ampicillin overnight at 37°C. Successfully transformed bacteria containing the ligated plasmid express ampicillin resistance and consequently form colonies on the ampicillin containing agar plate.

2.6.4.6 Colony PCR

Colony PCR using GoTaq® green mastermix (Promega) was used to identify colonies containing plasmids with a correctly ligated V/P sequence. This reaction comprised of a mastermix of 5µl GoTaq mastermix, 0.5µl of each of the forward and reverse primers (supplied with the pJET1.2 plasmid kit; Thermo Fisher Scientific) and 4µl of distilled H_2O. The primers supplied with the pJET1.2 plasmid flank the region before and after the insertion site therefore only vector containing an insert would produce a PCR product. A minimum of 6 colonies were selected from each plate using a sterile tip and dipped into the mastermix. The same tip was also used to dip into a fresh ampicillin agar plate, numbered to allow easy identification and recovery of positive colonies. This fresh ampicillin

plate was then incubated at 37°C for a maximum of 8hours. During this time the colony PCR was run on the thermocycler using the same conditions as stated previously, with the exception of extending the extension time to 1min 20sec (see section 2.6.4.3). Each reaction was then run directly on a 1% agarose gel and analysed under U.V light to identify if they contained the correct PCR product as previously stated (see section 2.6.4.4). Reactions producing a band at ~1400bp in length were identified as positive as they contained a band consistent with the size of the V/P sequence. The corresponding colonies, stored previously on the fresh Ampicillin plate, were then cultured to prepare enough plasmid DNA for sequencing. At least three positive colonies were prepared for sequencing from each potential mutant virus. Each colony was inoculated into 5ml Luria-Bertani (LB) broth supplemented with 50mg/ml ampicillin (Sigma) and incubated overnight in an orbital shaker (225rpm, 37°C). Plasmids were then extracted using QIAprep Spin miniprep Kit (as per manufacturer's instructions, QIAGEN®). Afterwards, sequencing was completed using pJET1.2 primers (Thermo Fisher Scientific) during capillary electrophoresis dye-terminator sequencing (performed by Dundee Sequencing services).

2.6.5 Adaption of the method to isolate IFN-sensitive viruses from the wild-type non fluorescent virus PIV5 W3

In addition to isolation of viral mutants from rPIV5mCh, we adapted our method to isolate mutants from the wild-type non-fluorescent virus PIV5 W3. This involved adding in two PIV5 HN and F immunostaining steps to our method. These immunostaining steps were added i) to identify PIV5 W3 infected cells before FACS analysis and cell sorting and ii) to identify potentially IFN-sensitive

mutants following incubation of sorted cells i) Initially, A549.pr(ISRE).GFP/ISG56-/Npro cells were infected with PIV5 W3 at an MOI 0.5 for 1 hour. After 6-8hours, IFN and primary anti-PIV5 HN/F antibody was added as previously stated (see section 2.5). After 18 hours, immunostaining for PIV5 HN and F was then completed. Each monolayer was washed once with PBS and then incubated for 1hour at 4°C in 400µl of secondary goat anti-mouse texas red antibody diluted 1:200 in ice cold 3% [v/v] FBS/PBS. Following staining, cells were then collected for FACS analysis and dual GFP and texas red positive cells were sorted into 96 well plates as previously stated (see section 2.6). ii) The second immunostaining step was added to identify potentially IFN-sensitive mutant viruses following incubation of sorted cells in 96 well plates. Initially, the supernatant (potentially containing IFN-sensitive mutant viruses) was collected from each well and the remaining monolayers of infected cells were incubated with IFN, as previously stated (see section 2.6.2). Cells were then fixed in 5% [v/v] formaldehyde/PBS for 30mins prior to permeabilisation using 0.1% [v/v] Triton X-100/PBS for 30min. Afterwards, cells were incubated for 1hour with primary anti-PIV5 HN and F antibody diluted 1:1000 in 2% [v/v] FBS/PBS. Monolayers were then washed thrice with 2% [v/v] FBS/PBS and incubated for 1hour with goat anti-mouse texas red antibody diluted 1:200 in 2% [v/v] FBS/PBS. Each well was then analysed using a fluorescent microscope (EVOS). Those containing GFP and texas red positive cells were then identified as containing a potentially IFN-sensitive mutant and the virus stock previously stored from that well used to create a working stock. The V/P gene of this virus was then sequenced as previously stated (see section 2.6.4).

2.6.6 Methods required for characterization of IFN-sensitive viral mutants following isolation

Following sequencing, three mutant viruses, rPIV5mCh-α, rPIV5mCh-β and PIV5 W3-γ, were identified. Subsequently, these mutants were characterized in a number of assays:

i) FACS analysis of potentially IFN-sensitive mutants at different MOI

ii) Western blot for STAT1 degradation

iii) IFNβ induction and IFN signalling luciferase assays to analyse mutant V protein activity

iv) FACS analysis and serial passage to assess mutant stability of the IFN-sensitive mutants rPIV5mCh-α and PIV5-W3-γ

v) DAPI staining to assess fusogenicity and apoptosis of the IFN-sensitive mutants rPIV5mCh-α and PIV5-W3-γ

vi) Full genome sequencing

2.6.6.1 i) FACS analysis of potentially IFN-sensitive mutants at different MOI

Initially, each mutant virus was analysed by FACS using the method as described in section 2.5 with the following modifications. Specifically, A549/pr(ISRE).GFP/ ISG56-/ BVDV Npro cells were infected at MOI 0.1, 1, 5 or 10 for 1hour with rPIV5mCh, rPIV5mCh-α, rPIV5mCh-β, PIV5 W3 and PIV5 W3-γ. After 8 hours, IFN treatment ($1x10^4$Units/ml) and anti-PIV5 HN and F antibody (1:1000) was added. Following 18hours, each sample was then collected, immunostained if necessary (see section 2.6.5) and analysed by FACS.

2.6.6.2 ii) Western blot analysis of STAT1

The functionality of each mutant V protein was assessed by analysis of STAT1 degradation following infection using a western blot. Specifically, A549: naïve cells were mock infected or infected with the viruses PIV5 W3, rPIV5mCh, PIV5 CPI-, rPIV5mCh-α, PIV5mCh-β and PIV5 W3-γ at MOI 10 for 12 hours followed by a 16 hour IFN treatment ($1x10^4$ Units/ml). Following incubation, cells were collected in disruption buffer, run on an SDS-PAGE gel and transferred to a PVDF membrane as previously stated (See section 2.4.3). The blot was then probed using mouse anti-STAT1, mouse anti-PIV5 NP and mouse anti-Actin antibodies sequentially at a dilution of 1:1000, overnight at 4°C. Following incubation with each primary antibody, the membrane was washed with PBS 0.5% [v/v] Tween-20 as previously stated (See section 2.4.3). Each membrane was then incubated with goat anti-mouse LiCOR IRDye® fluorescent secondary antibody at a dilution of 1:10000 and washed again using PBS 0.5% [v/v] Tween-20 before visualisation using the Odyssey CLx Imaging system (LiCOR Biosciences).

2.6.6.3 iii) IFN-β induction and IFN signalling luciferase reporter assays to analyse mutant V protein activity

Mutant rPIV5mCh-α, rPIV5mCh-β and PIV5 W3-γ V protein sequences were excised from pJET1.2 by enzyme digest using XhoI and XbaI (as per manufacturer's instructions; Promega) and ligated into the pcDNA3.1- expression vector (Thermo Fisher Scientific) using T4 DNA ligase (Promega). V protein functionality was then analysed using two luciferase reporter assays.

A luciferase assay was used to analyse the effects of mutant rPIV5mCh-α, rPIV5mCh-β and PIV5 W3-γ V protein on the IFN induction pathway. This assay required a plasmid containing firefly luciferase under the control of the IFN-β promoter (pIFΔ(-116)lucter; provided by Dr Lena Andrejeva, University of St Andrews) and a second plasmid expressing Mda5 (pEF.mda-5; provided by Dr Lena Andrejeva, University of St Andrews). When expressed together, Mda5 activates the induction of the IFN-β promoter and subsequent luciferase expression. A third plasmid containing β-galactosidase (pJATlacZ; provided by Dr Lena Andrejeva, University of St Andrews) was used as a transfection control and enabled the data to be normalised to a standard. A transfection mix including all three plasmids (250ng/well each) as well as a plasmid that expresses one of the V proteins to be assessed (wild-type, rPIV5mCh-α, rPIV5mCh-β or PIV5 W3-γ V protein) (750ng/well each) and 4% [v/v] Lipofectamine 2000 (Thermo Fisher Scientific) was prepared in 500µl OptiMEM and incubated for 30 mins. Subsequently, 90% confluent monolayers of 293T cells in 12 well plates were then transfected with this mix and incubated at 37°C/5% CO_2 for 5 hours. Following incubation, 1ml of 10% [v/v] FBS DMEM without antibiotics was added and cells were incubated for 48hours before collection in 100µl lysis buffer (Promega). Each lysate was then clarified at 1500rpm for 5mins and 20µl each transferred into two fresh tubes for analysis of both firefly luciferase and β-galactosidase activity. To measure firefly luciferase activity, the luminometer (GloMax) was programmed to automatically add 100µl of firefly luciferase substrate (Promega) to one aliquot of the lysate and measure luminescence following a 10 second incubation. To measure β-galactosidase activity, 100µl of β-glo substrate (Promega) was added to the second aliquot of

lysate and incubated for 30mins at RT. The luminescence was then measured using the luminometer and used to normalise the luciferase activity of each sample. Each sample was set up in triplicate allowing standard deviation to be calculated and added to each graph created using Graphpad Prism 6 (Graphpad Software).

A second luciferase assay was used to analyse the effects of mutant rPIV5mCh-α, rPIV5mCh-β and PIV5 W3-γ V protein on the IFN signalling pathway. This assay required a plasmid (p(9-27)4tkΔ(-39)lucter; provided by Dr Lena Andrejeva, University of St Andrews) containing firefly luciferase under the control of four tandem repeat sequences of the ISRE from the IFN-inducible gene 9-27 (Didcock et al. 1999). This element is found within the promoters of hundreds of ISGs and is activated upon the addition of IFN. Thus in this assay addition of IFN following transfection with this plasmid results in the expression of luciferase. This plasmid was therefore transfected along with the plasmid expressing β-galactosidase and another that expresses one of the mutant V proteins (wild-type, rPIV5mCh-α, rPIV5mCh-β or PIV5 W3-γ V protein; 250ng/well each) in the same manner as described above. Following transfection and incubation for 48hours, IFN treatment (10^4Units/ml) was added for 6 hours. Samples were then collected and analysed as previously stated.

2.6.6.4 iv) FACS analysis and serial passage to assess the ability of the IFN-sensitive viruses rPIV5mCh-α and PIV5-W3-γ to regain IFN antagonist function

Ability of the mutant viruses rPIV5mCh-α and PIV5-W3-γ to revert to regain IFN antagonist function was assessed using two methods i) FACS analysis and ii) serial passage of each virus. i) Firstly, we infected A549:pr(ISRE).GFP cells with both rPIV5mCh-α and PIV5-W3-γ at MOI 1. Samples were then prepared and subjected to FACS analysis as previously stated (see section 2.5). Following analysis of PIV5-W3-γ, texas red only positive cells were sorted and the V/P gene sequenced from 10 samples as stated previously (see section 2.6). Notably, following analysis of rPIV5mCh-α, very few mCherry only positive cells were present. Further analysis of the selected viruses then showed that viruses were still unable to block IFN signalling and were therefore not sequenced ii) rPIV5mCh-α and PIV5-W3-γ were also passaged through A549:pr(ISRE).GFP cells for 60 days following an initial infection at an MOI 5. Following 60 days, each population of cells was seeded at $3x10^5$ cells/well in a 12 well plate and allowed to adhere overnight. The next day cells were treated with IFN for 18hours. Following incubation, samples containing rPIV5mCh-α infection could be collected directly and analysed by FACS. By contrast, samples containing PIV5-W3-γ virus were immunostained and analysed by FACS as previously stated (See section 2.5 and 2.6.5).

2.6.6.5 v) DAPI staining to assess fusogenicity and apoptosis of the IFN-sensitive mutants rPIV5mCh-α and PIV5-W3-γ

Mutants rPIV5mCh-α and PIV5-W3-γ were analysed for i) fusogenicity and ii) apoptosis using DAPI (4',6-diamidino-2-phenylindole) staining following viral

infection. i) To analyse for fusogensity, Vero cells seeded onto coverslips (1mm thick) were mock infected or infected with rPIV5mCh, PIV5 W3, PIV5mCh-α and PIV5 W3-γ at MOI 10 for 1 hour in 200µl serum-free DMEM. The virus inoculum was the replaced with 1ml serum-free DMEM and incubated for 48hours. Following incubation, cells were fixed in 5% [v/v] formaldehyde/PBS for 30min. Fixed cells were then washed thrice with 2%[v/v] FBS/PBS and permeabilised using 0.1% [v/v] Triton X-100/PBS for 30min. Following a second wash step, 30µl DAPI stain diluted 1:200 was added and incubated for 20mins. The coverslips were then washed for a final time before inversion and mounting multiple coverslips onto large glass slides using citifluor (Citifluor Ltd). Afterwards, images were taken at 10X Magnification using Microphot-FXA immunofluorescence microscope (Nikon). ii) To analyse for apoptosis, A549 naïve cells seeded onto coverslips were infected with rPIV5mCh, PIV5 W3, PIV5mCh-α and PIV5 W3-γ at MOI 10 for 1 hour in 200µl SF-DMEM. The virus inoculum was then replaced with serum-free DMEM -/+ 4µM Rux or equivalent volume DMSO and incubated for 48 or 72 hours. Afterwards, cells were stained using DAPI staining, mounted onto glass slides and analysed using a fluorescence microscope as previously stated. Note images were taken at 20X Magnification.

2.6.6.6 vi) Full genome sequencing of each mutant virus

Full genome sequencing of each viral mutant was completed by Elizabeth Wignall-Fleming at the University of Glasgow. In brief, each viral mutant was prepared for directional sequencing by RNA extraction (see section 2.6.4.1). A library preparation for each mutant was then completed using TruSeq stranded

Total RNA with Ribo-Zero Gold (Illumina) and sequenced using MiSeq (Illumina). Bioinformatics analysis was then completed to separate genomic and antigenomic RNA reads. Following this, a consensus sequence was generated from the wild-type PIV5 W3 and rPIV5mCh sample. Subsequently, the genomic reads from each mutant virus preparation were aligned to the appropriate reference sequence using Burrows-Wheeler-Alignment (BWA) or Bowtie2. Each alignment was then analysed to identify mutations within the viral genome.

3 Chapter 3

3.1 Inhibitors of the IFN response enhance virus replication in vitro

3.1.1 Introduction and aims

Manipulation of a virus's capacity to circumvent the IFN response is an essential tool used to advance our knowledge of viruses and how they interact with the immune system. As well as being of fundamental interest, this ability may also have many practical applications such as facilitating the design of live-attenuated vaccines. Despite the many benefits of disabling a virus's capacity to circumvent the IFN response, these IFN-sensitive viruses are often difficult to grow to high titer as many cell-lines produce and respond to IFN (Young et al. 2003). The default option for growth of these viruses is therefore limited to a select number of cell-lines such as Vero cells, that do not have an intact IFN system, however, as viruses exhibit host cell specificity not all viruses can be grown in such cells (Desmyter et al. 1968; Mosca & Pitha 1986). To tackle this issue, we have previously engineered cell-lines with an intact IFN response to express IFN antagonists that inhibit this IFN response, such as the BVDV Npro protein from BVDV, which blocks the IFN induction pathway by targeting IRF3 for proteasome-mediated degradation, or the V protein from PIV5, which blocks the IFN signalling pathway by targeting STAT1 for proteasome-mediated degradation (Young et al. 2003; Didcock et al. 1999; Hilton et al. 2006). However, the creation of genetically engineered cell-lines is time consuming and the use of such cells can create regulatory problems in vaccine production. Consequently, our laboratory set out to attain another, more flexible method to improve viral growth.

Prior to my study, it was hypothesised that blocking the IFN induction or signalling pathways using a small molecule inhibitor would offer a simple and flexible solution to increase viral growth, as an inhibitor could easily supplement the tissue culture medium of cell-lines of choice. To test this, eight inhibitors known to target different components of the IFN response (TBK-1, IKKβ and JAK1) were tested for their ability to block their corresponding pathways. Of these eight inhibitors, Rux, which blocks the JAK1/2 component of the IFN signalling pathway, was identified as the most effective inhibitor of the IFN response (Stewart et al. 2014). Specifically, it was shown to increase growth of numerous IFN-sensitive viruses that were sensitive to IFN due to i) loss of function of the viral IFN antagonist or ii) mutations that slowed virus replication enough to allow the IFN response to overcome the infection. This was demonstrated using a diverse range of viruses, including, viruses with disabled IFN antagonists that exemplify live-attenuated vaccine candidates (RSV and Influenza virus), traditionally attenuated vaccine strains (MuV Enders strain and MeV Edmonston strain) and a slow growing wild-type virus (RSV) (Stewart et al 2014).

My study aimed to further characterise the use of the IFN inhibitor, Rux, using a number of assays including:

i. Monitoring the stability of the inhibitor *in vitro*

ii. Analysing its effect on virus growth in Vero cells

iii. Analysing the effect on virus growth of pre-treating cells with the inhibitor prior to infection

iv. Analysing the effect of the inhibitor on virus growth:

    a) in multiple cell-lines

    b) of other previously untested viruses.

The results of such studies are outlined in the following chapter.

3.1.2 Monitoring the stability of Rux in vitro

Further characterisation of the IFN inhibitor, Rux, in the context of virus infection required that experiments be performed over several days. Therefore, we firstly set out to analyse the activity of the inhibitor over time to decipher whether chemical degradation or cellular metabolism reduced the drugs ability to inhibit the IFN response. To test inhibitor stability over time, the inhibitory activity of Rux was analysed, following incubation of the inhibitor in the media of A549 naïve cells, using an IFN signalling GFP reporter assay. Specifically, we incubated 4μM of the drug, Rux, in the culture medium of A549 naïve cells and harvested samples of the culture medium at numerous time-points for 7 days. Collected Rux test samples were then added to an IFN signalling GFP reporter assay to analyse for loss in inhibitor activity.

The assay commenced with the addition of each test sample to the IFN signalling GFP reporter cell line, A549:pr(ISRE).GFP. This cell-line contains GFP under the control of the mouse Mx1 promoter, which is activated following induction of the IFN signalling pathway. Subsequently, the IFN signalling pathway and thus GFP expression was optimally activated by addition of IFNα/β. Notably the Mx1 promoter contains an ISRE element, which is found within the promoters of many ISGs. Hence, when IFN-α/β is added to A549:pr(ISRE).GFP cells, this activates the IFN signalling pathway which switches on the Mx1 (ISRE containing) promoter and results in expression of GFP. Importantly, previous work has demonstrated that addition of the IFN inhibitor, Rux (4μM) to the IFN signalling GFP reporter assay, results in a significant reduction in GFP expression by blocking the IFN signalling pathway. Consequently, this enabled us to examine

the stability of the activity of the inhibitor present in the test samples, as any reduction in inhibitor activity following their incubation in A549: naïve cells would result in a regain of GFP expression. The results from the IFN signalling GFP reporter assay demonstrated that there was no regain in GFP expression following addition of the incubated Rux test samples (Figure 3.1). In summary, this indicates that there was no loss in inhibitor activity of Rux over time and therefore the drug was considered stable in cell culture for up to 7 days.

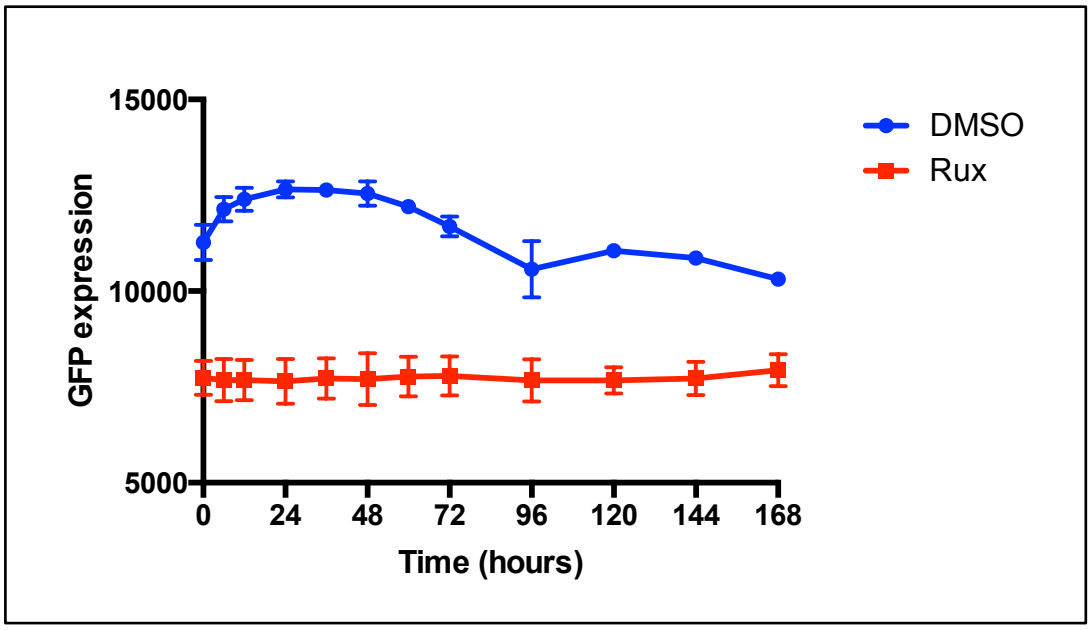

Figure 3.1: Analysis of the stability of the IFN inhibitor Rux *in vitro*. A549 naïve cells were cultured in the presence of media supplemented with Rux (4μM) or equivalent volume of DMSO. Samples of the medium were then harvested at numerous time-points for 7 days. The inhibitory activity of culture medium containing Rux was then tested in A549:pr(ISRE).GFP reporter cells using an IFN signalling GFP reporter assay. Briefly, the A549:pr(ISRE).GFP reporter cell-line was activated with purified IFN, following incubation with the test samples, and GFP measured 48 hours post-IFN treatment.

3.1.3 Analysis of growth kinetics of the IFN-sensitive virus, BUNΔNSs, in A549 naïve and Vero cells supplemented with the IFN inhibitor, Rux

Throughout the following studies BUNΔNSs was used as a model virus to study the effects of the IFN inhibitor Rux on the IFN response within different cell-lines. Notably, BUNΔNSs is IFN-sensitive as the IFN antagonist NSs protein has been deleted, consequently, it is unable to grow efficiently in the presence of an active IFN response (Bridgen et al. 2001). Blockage of the IFN response by the IFN inhibitor, Rux, could therefore be assessed by analysing increased growth of this virus.

Previously it has been shown that the IFN inhibitor Rux can increase the growth of the IFN-sensitive virus BUNΔNSs in A549 cells using both plaque assays and multistep viral growth curves (Stewart et al. 2014). Following this, the effect of the IFN inhibitor, Rux, on BUNΔNSs plaque development was then compared in A549 naïve and Vero cells (Figure 3.2). Notably, Vero cells are currently one of a limited number of cell-lines approved in vaccine production therefore any improvement on viral growth achieved in these cells may be of interest to vaccine manufacturers (Barrett et al. 2009). Interestingly, this comparison demonstrated two intriguing effects i) Firstly, BUNΔNSs plaque size appeared slightly increased in Vero cells supplemented with inhibitor compared to Vero cells supplemented with the equivalent volume of DMSO (Figure 3.2). ii) Secondly, BUNΔNSs plaque development was significantly faster in A549: naïve cells supplemented with the IFN inhibitor, Rux, than in Vero cells (Figure 3.2). In this section we set out to quantify these effects using multistep viral growth curves to identify if virus growth of the IFN-sensitive virus BUNΔNSs i) is

increased in the presence of the IFN inhibitor, Rux, in Vero cells compared to Vero cells supplemented with the equivalent volume of DMSO and ii) is faster in A549 naïve cells supplemented with IFN inhibitor compared to Vero cells.

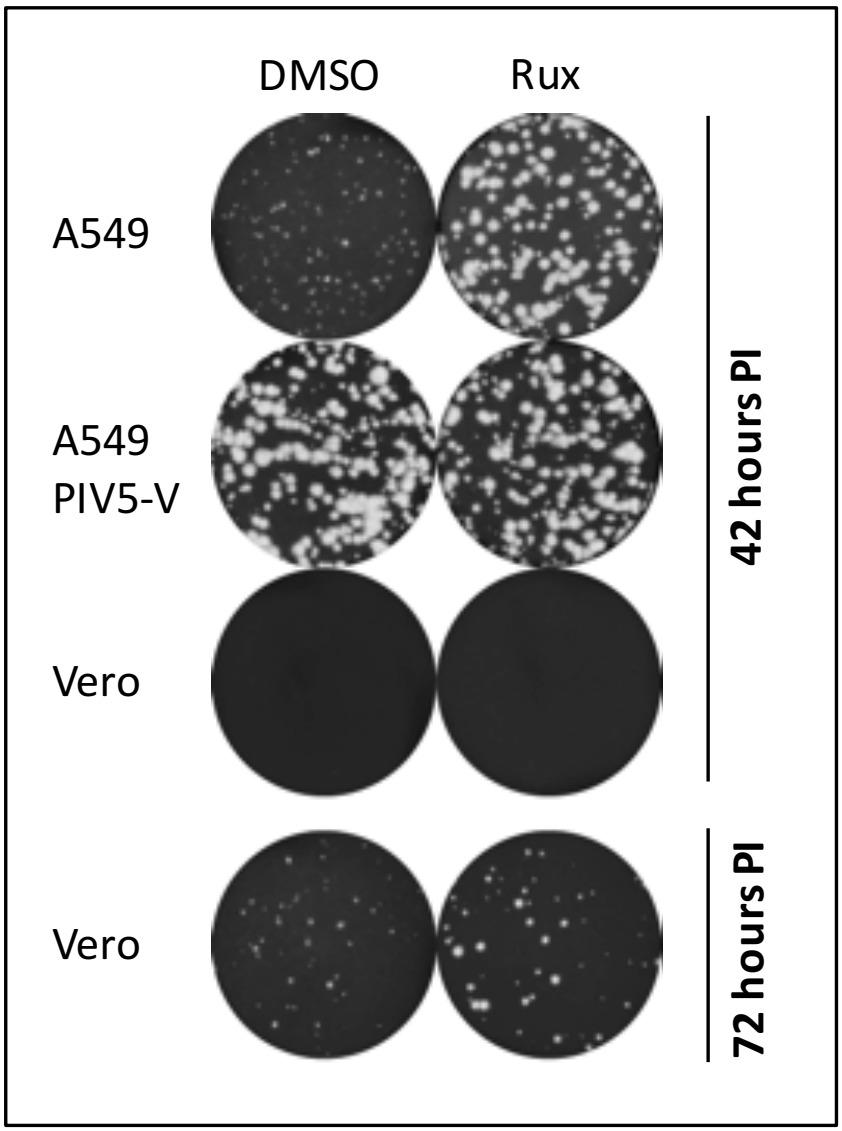

Figure 3.2: BUNΔNSs plaque development in A549 naïve, A549/PIV5-V and Vero cells supplemented with Rux. BUNΔNSs plaque formation was analysed following 42 or 72-hour incubation in the presence of the IFN inhibitor Rux (4μM) or the equivalent volume of DMSO on A549, A549/PIV5 V or Vero cells. Plaques were visualised using CV stain (Data prepared by C. Adamson).

Firstly, we set out to identify if virus growth of the IFN-sensitive virus, BUNΔNSs, is increased in the presence of the IFN inhibitor, Rux, in Vero cells. Previously, it had been shown that plaque size was slightly increased in Vero cells supplemented with the inhibitor, Rux, compared to Vero cells supplemented with the equivalent volume of DMSO (Figure 3.2). This was intriguing as it has been shown previously that Vero cells do not have an intact IFN response (Desmyter et al. 1968), therefore addition of IFN inhibitor should have no effect. It was therefore decided to quantify this effect using a multistep viral growth curve. Specifically, BUN Δ NSs growth in the presence of Rux (4μM) or equivalent volume of DMSO was compared in Vero cells. The results indicated that there was no significant increase in viral titre in Vero cells in the presence of the inhibitor, Rux, compared to the control, DMSO (Figure 3.3). In summary, this indicates that the IFN inhibitor, Rux, has no effect on viral growth in Vero cells therefore the slight increase seen previously in plaque development appears to be insignificant.

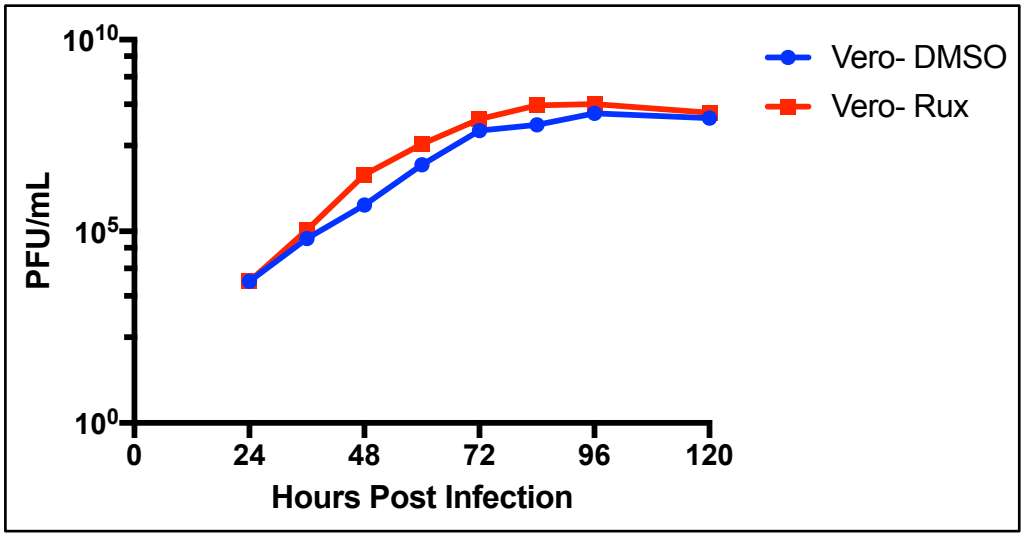

Figure 3.3: Analysis of the effect of the IFN inhibitor, Rux, on BUNΔNSs growth in Vero cells using a multistep viral growth curve. BUNΔNSs growth was monitored for 5 days in Vero cells following infection at MOI 0.001 in the presence of the IFN inhibitor, Rux (4μM), or equivalent volume of DMSO. Samples of the media were taken at numerous time-points. PFU/ml was then determined by titration of these samples on Vero cells using a plaque assay. (Data representative of two independent repeats with a lower limit of detection of 1x 10^3 PFU/ml)

Secondly, we set out to identify if virus growth of the IFN-sensitive virus, BUNΔNSs, is faster in A549 naïve cells supplemented with the IFN inhibitors, Rux, compared to growth in Vero cells in the absence of IFN inhibitor. Previously, it was noted that BUNΔNSs plaque development was significantly faster in A549 naïve cells supplemented with the IFN inhibitors, Rux, than in Vero cells in the absence of IFN inhibitor (Figure 3.2). It was therefore decided to quantify this using a multistep viral growth curve. Specifically, growth of BUNΔNSs in A549 naïve cells supplemented with the IFN inhibitor, Rux, was compared to growth in Vero cells (Figure 3.4). Note, that A549/PIV5-V cells were used as a positive control in this experiment as they express the IFN antagonist V protein from PIV5 and have previously demonstrated that blockage of the IFN response can result in an increase in viral growth of IFN-sensitive viruses (Young et al. 2003). The results demonstrate that the viral titer of BUNΔNSs was ~2 logs higher in A549 naïve cells supplemented with Rux than in Vero cells without IFN inhibitor when compared at 48 hours post infection. Vero cells in the absence of IFN inhibitor then achieved a similar titer to that seen in A549 naïve cells supplemented with Rux 24hours later (Figure 3.4). Notably, the increased growth of BUNΔNSs in A549: naïve cells in the presence of Rux was comparable to the positive control cell line, A549/PIV5-V, at 48hours post infection indicating that other host-cell constraints must limit infection in Vero cells. In summary, growth of the IFN-sensitive virus, BUNΔNSs, is much faster in A549 naive cells supplemented with Rux than in Vero cells.

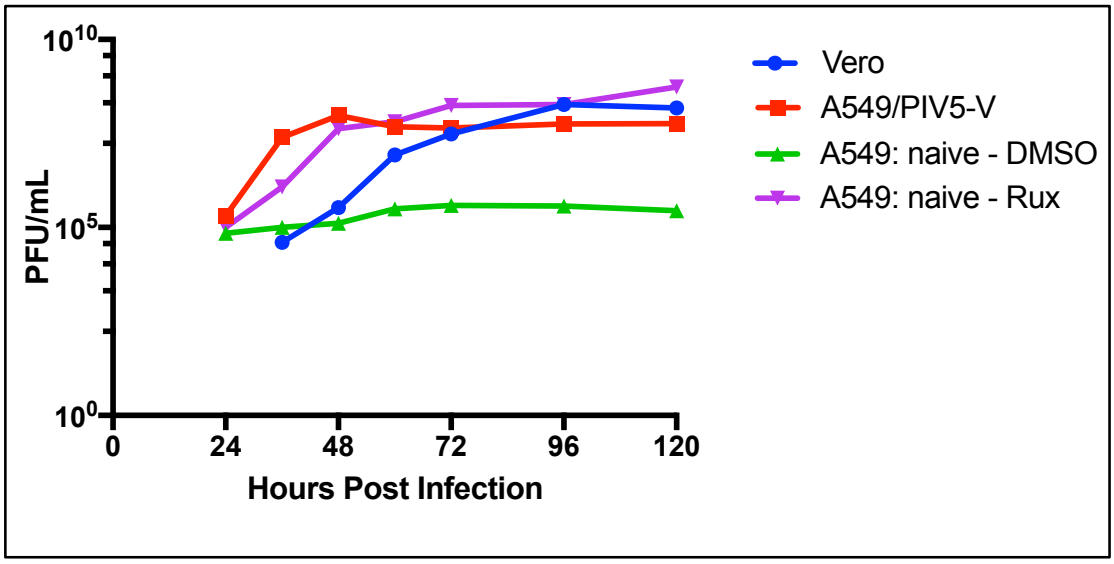

Figure 3.4: Comparison of growth of the IFN-sensitive virus, BUNΔNSs, in A549: naïve cells supplemented with Rux compared to growth in Vero and A549/PIV5-V cells using a multistep viral growth curve. BUNΔNSs growth was monitored over 5 days following infection at MOI 0.001 in A549 naïve cells in the presence of 4μM Rux or the equivalent volume of DMSO in comparison to Vero and A549/PIV5-V cells. Samples of the media were taken at numerous time-points. PFU/ml was then determined by titration of these samples on Vero cells using a plaque assay (Data representative of two independent repeats with a lower limit of detection of 1x 10^3 PFU/ml).

Interestingly, it was noted that growth of BUNΔNSs was slightly faster in the engineered cell-line, A549/PIV5-V, than in A549 naïve cells supplemented with Rux (~1 log greater at 36hours post infection)(Figure 3.4). We therefore hypothesised that as V is constitutively expressed and hence shut off of the IFN response is present in A549/PIV5-V cells prior to infection then this may provide a significant advantage over addition of IFN inhibitor zero hours post infection. We therefore sought to determine if pre-treating the cells with the inhibitor, Rux, prior to infection would result in increased growth of BUNΔNSs that matches the speed seen in A549/PIV5-V cells. Specifically, A549 naïve cells were incubated in the presence and absence of the IFN inhibitor Rux for 24hours before infection with BUNΔNSs. Subsequently these cells were then analysed in comparison to A549/PIV5-V cells via a multistep viral growth curve (Figure 3.5). The results demonstrate that there was no increase in viral growth in A549 naïve cells pre-treated with Rux for 24hours compared to A549 naïve cells where Rux was added 0hours post infection. In summary, this indicates that pre-treatment of A549 naïve cells with Rux, prior to infection with BUNΔNSs, has no effect on viral growth and cannot increase the speed of viral growth to that seen in A549/PIV5-V cells.

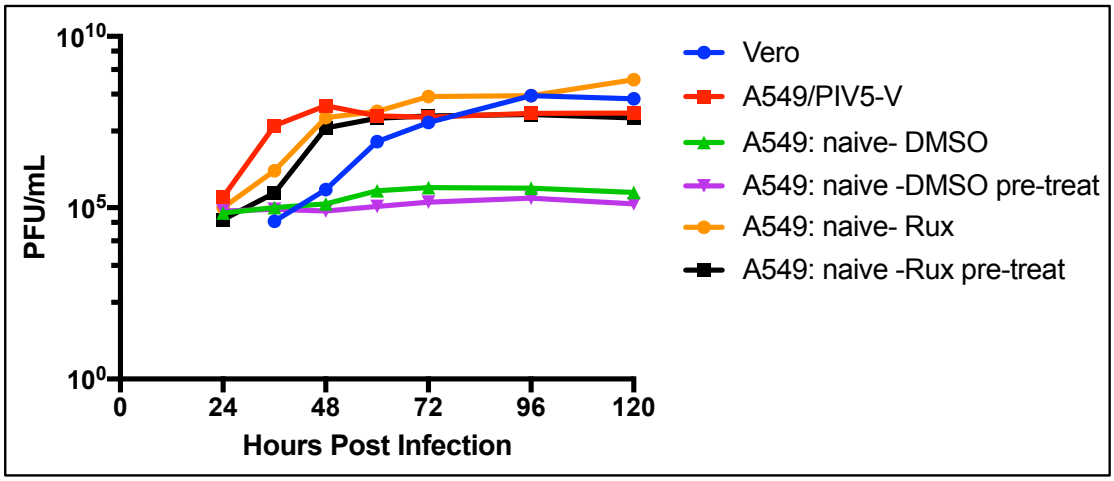

Figure 3.5: Analysis of the effect of pre-treatment of A549: naïve cells with the IFN inhibitor, RUX, on BUNΔNSs growth, using a multistep viral growth curve. BUNΔNSs growth was monitored for 5 days following infection at MOI 0.001 in A549: naïve cells pre-treated with Rux (4μM) for 24hours before infection. This was compared to growth of BUNΔNSs following infection at MOI 0.001 in A549: naïve cells treated with Rux at 0hours post infection and growth in A549/PIV5-V cells and Vero cells. Samples of the media were taken at numerous time-points. PFU/ml was then determined by titration of these samples on Vero cells using a plaque assay. (Data representative of two independent repeats with a lower limit of detection of 1x 10^3 PFU/ml)

To summarize, we have demonstrated that supplementing the media with the IFN inhibitor, Rux, had no effect on growth of the IFN-sensitive virus BUNΔNSs in Vero cells. Reiterating that Vero cells do not have an intact IFN response. We then demonstrated that BUNΔNSs growth was much faster in A549 naïve cells supplemented with Rux than in Vero cells. Indicating that inhibiting the IFN response within mammalian cells with IFN inhibitors may provide a valuable alternative to the current method used for Vaccine production. Expanding on this, it was noted that growth of BUNΔNSs in A549/PIV5-V cells was faster than in A549: naïve cells supplemented with the inhibitor Rux. We then demonstrated that pre-treatment of A549: naïve cells with Rux did not increase viral growth to that seen in A549/PIV5-V cells. Thus indicating that expression of the IFN antagonist V protein may provide other advantages to increase viral growth. Despite this, addition of the IFN inhibitor, Rux, may provide the best alternative to growth in Vero cells for the manufacture of vaccines as the use of genetically engineered cell-lines can create regulatory problems for vaccine manufacturers.

3.1.4 Effects of Rux on replication of various viruses from the Bunyaviridae family in a range of cell-lines derived from different mammalian species

In the following section we set out to further characterise the use of the IFN inhibitor, Rux, by examining its effect on growth of BUNΔNSs, BUN WT and several other viruses from the *Bunyaviridae* family, on MRC5 (human foetal lung fibroblast) cells and a number of other cell-lines derived from different mammalian species.

3.1.4.1 Analysis of the effects of the IFN inhibitor, Rux, on BUNΔNSs growth in MRC5 cells

Currently, only a few cell-lines are approved for use in vaccine production, for example, Vero and MRC5 cells (Barrett et al. 2009). As we have already examined the effects of Rux on the growth of BUNΔNSs in IFN incompetent Vero cells, we then extended our study to analyse its effect on viral growth in the IFN competent MRC5 cell-line, and compared this to growth in the engineered IFN incompetent MRC5/PIV5-V expressing cell-line. To examine this, plaque development of the IFN-sensitive virus, BUNΔNSs, was analysed following incubation with Rux (4μM) or equivalent volume of DMSO in each of the cell-lines. Notably, we also included A549: naïve and A549/PIV5-V cells as a comparable positive and negative control. The results demonstrate that addition of Rux increased BUNΔNSs plaque size in the IFN competent MRC5 naïve cells equivalent to that seen in the engineered cell line MRC5/PIV5-V in the absence of inhibitor, but had no effect on plaque size in IFN incompetent MRC5/PIV5-V cells (Figure 3.6). This demonstrates that Rux can block the IFN response in MRC5 naïve cells to allow an increase of viral growth equivalent to expression of the PIV5-V protein. Furthermore, as the IFN response in MRC5/PIV5-V cells is already blocked by expression of PIV5-V we see no further increase in plaque size in the presence of inhibitor. As MRC5 cells are commonly used in vaccine production (in addition to Vero cells) the use of the IFN inhibitor Rux may be of interest to vaccine manufacturers to increase viral growth of vaccine strains.

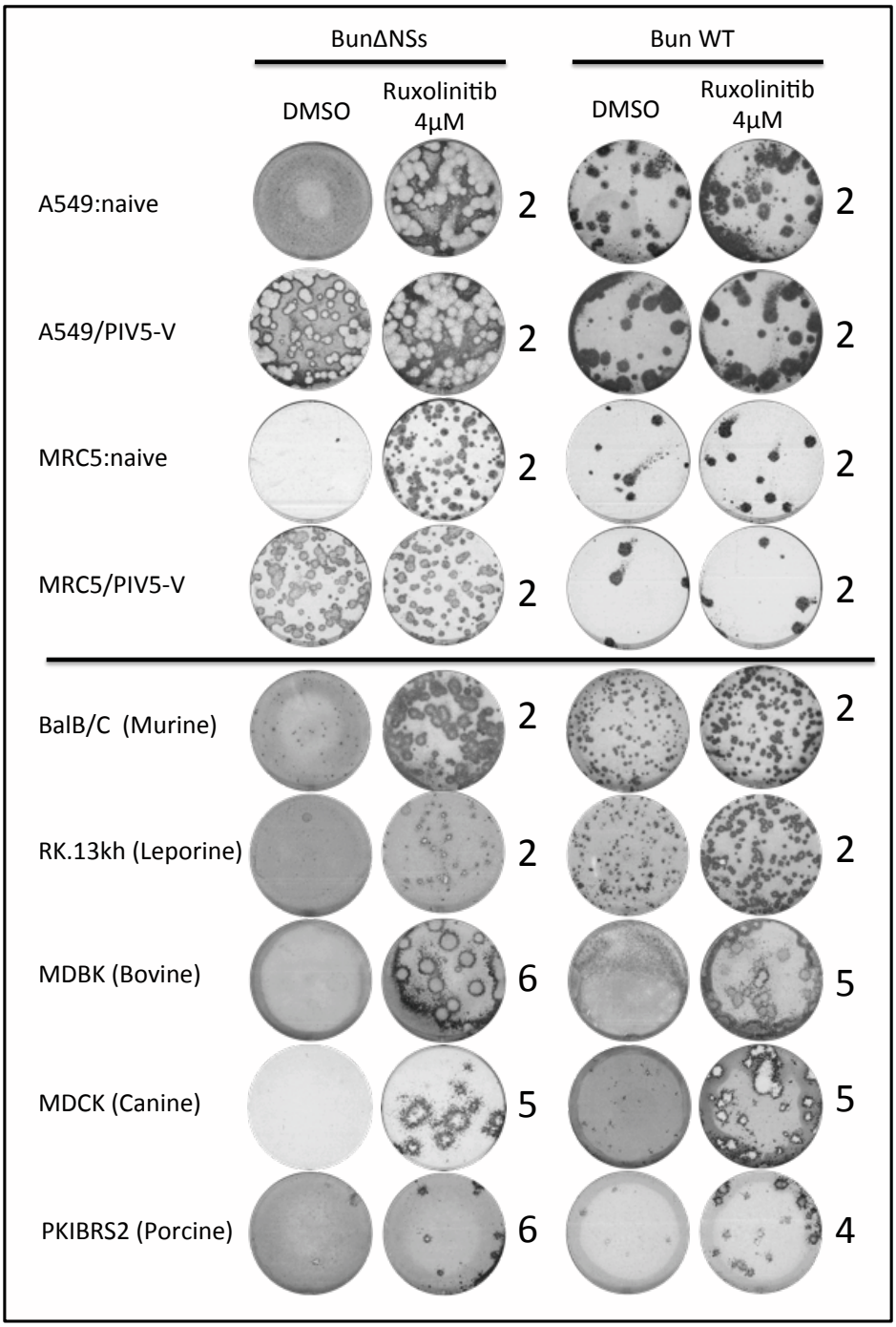

Figure 3.6: Effects of IFN inhibitor, Rux, on BUNΔNSs and BUN WT plaque formation in a range of mammalian cell-lines. BUNΔNSs and BUN WT plaque size was determined following incubation with 4μM Rux in A549, A549/PIV5 V, MRCV, MRC5/PIV5 V, BalB/C, RK.13, MDBK, MDCK and PKIBRS2 cells. Plaques were fixed on the day indicated and visualized by immunostaining for Bunyamwera N protein (Data representative of three independent repeats).

3.1.4.2 Analysis of the effects of the IFN inhibitor, Rux, on BUN ΔNSs growth in a number of different mammalian cell-lines

Next we set out to further characterise the use of the IFN inhibitor, Rux, by examining its effect on viral growth of BUNΔNSs in a number of cell-lines derived from different mammalian species. Specifically, plaque development of the IFN-sensitive virus, BUNΔNSs, was analysed following incubation with Rux (4μM) or equivalent volume of DMSO in five commonly used mammalian cell-lines, namely BalB/C (murine fibroblast), RK.13 (leporine kidney epithelial cells), MDBK (bovine kidney epithelial cells), MDCK (canine kidney epithelial cells) and PKIBRS2 (porcine kidney epithelial cells). The results demonstrated that, Rux increased plaque size, to a varying degree, in all mammalian cell-lines tested (Figure 3.6). Thus indicating that Rux can block the IFN response in each of these cell-lines. In summary, this provides further evidence that supplementing the media of IFN competent cells with Rux provides a flexible approach to increase viral growth of IFN-sensitive viruses in a cell-line of choice.

3.1.4.3 Analysis of the effects of IFN inhibitor, Rux, on BUN WT infection in A549, MRC5 and five other commonly used mammalian cell-lines

Next we sought to analyse the effects of the inhibitors on BUN WT. This virus can infect humans and contains an IFN antagonist (NSs), which blocks the IFN response successfully in human derived cell-lines. Here we set out to analyse the host cell range of the NSs protein further by examining BUN WT plaque development following addition of IFN inhibitor, Rux, in several different mammalian cell-lines (A549: naive, A549/PIV5 V, MRCV: naive, MRC5/PIV5 V, BalB/C, RK.13, MDBK, MDCK and PKIBRS2). Specifically, plaque development of

BUN WT was analysed following incubation with Rux (4μM) or equivalent volume of DMSO in each of the cell-lines (Figure 3.6).

As expected, the results demonstrate that the presence of inhibitor, Rux, had no effect on BUN WT plaque size in any of the human derived cell-lines (A549: naïve, A549/PIV5-V, MRC5: naïve and MRC5/PIV5-V) as the IFN antagonist NSs is functional within human cell-lines, therefore there can be no further increase in viral growth in the presence of inhibitor. Next it was noted that in the absence of Rux, BUN WT grew well in RK.13 and BalB/C cell-lines and when Rux was added there was only a slight increase in plaque size (Figure 3.6). These results suggest that the NSs protein is functional within RK.13 and BalB/C cells as growth occurs in the absence of inhibitor and is only moderately increased by the presence of inhibitor. Interestingly, in the absence of inhibitor BUN WT grew poorly in MDCK and PKIBRS2 cells however, when the inhibitor, Rux, was added there was a substantial increase in plaque size. This indicates that the NSs protein is not functional in these cell-lines as addition of the IFN inhibitor relieves the strain of the IFN response and this allows viral growth. Finally, the results from analysis of growth of BUN WT in the presence and absence of Rux in MDBK cells represented an interesting case, which we then chose to investigate further

3.1.4.3.1 Further analysis of viral growth of BUN WT in MDBK bovine cells in the presence and absence of the IFN inhibitor, Rux.

In the previous analysis of plaque development of BUN WT in the presence and absence of Rux, plaques were visualised by immunostaining for Bunyamwera N

protein following fixation. Looking closely at the MDBK cell monolayer following staining it was noted that in the absence of the inhibitor, Rux, large holes in the monolayer remained unstained. These holes looked identical to the size of plaques that were stained in monolayers in the presence of Rux. It was therefore hypothesised that Bunyamwera infection had begun to grow and form plaques but following incubation, the MDBK cells had been able to overcome the infection. These plaques then remained unstained at the time of immunostaining because infected cells were no longer present. To examine this further, viral plaque formation of BUN WT was analysed over 7 days with and without the IFN inhibitor, Rux, in MDBK cells. The monolayers were then immunostained for Bunyamwera N protein to visualise infected cells and then subsequently stained with CV stain to visualise holes within the monolayer (Figure 3.7A). The results show that consistently, in the absence of Rux, immunostained plaques would be present and increase in size until day 3. From Day 3, these plaques would then begin to reduce in size and also gradually become undetectable by immunostaining for Bunyamwera N protein. By contrast, in the presence of Rux, plaque size would increase until the monolayer was destroyed by day 7. We therefore hypothesised that the NSs protein is non-functional (or has a limited function) in MDBK bovine cells or the IFN response in MDBK bovine cells is particularly powerful, and therefore infection can be overcome under these conditions. Subsequently, viral growth of BUN WT in A549 naïve and MDBK bovine cells was quantified in the presence or absence of the inhibitor, Rux, using a multistep viral growth curve (Figure 3.7B). Conversely, the results showed that growth in MDBK bovine cells was not restricted in the absence of Rux and was also not increased by the presence of Rux. These conflicting results indicate that

the NSs protein is functional in this cell-line or that the MDBK bovine cell line does not have a more powerful IFN response. In summary, the ability to regress BUN WT virus appears to be dependent on the conditions of the assay and further studies would be required to elucidate this feature.

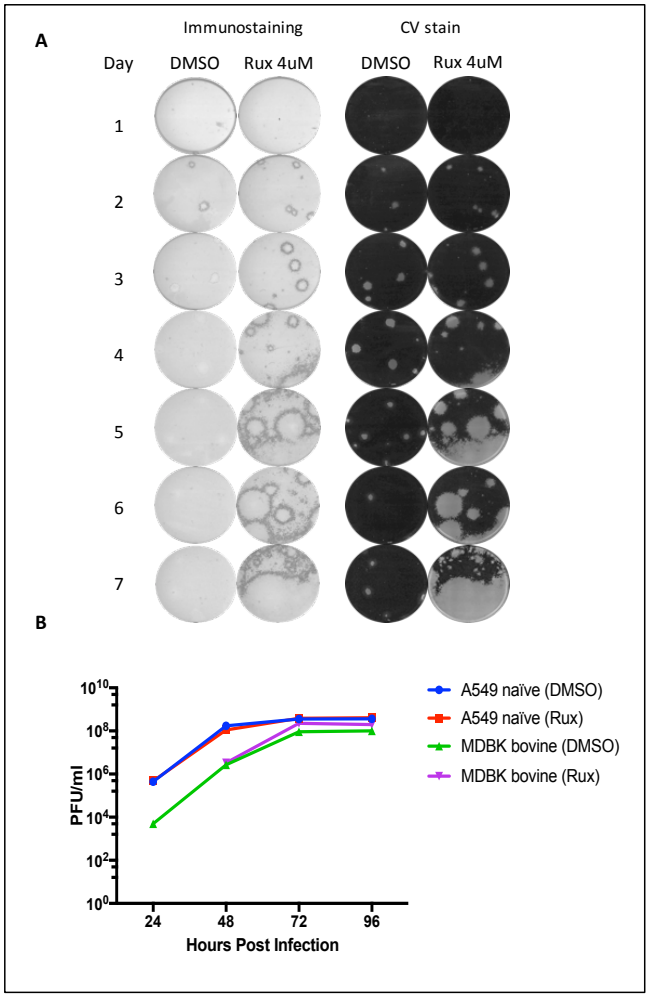

Figure 3.7: BUN WT growth in MDBK bovine cells. A) BUN WT plaque formation was analysed in MDBK bovine cells for 7 days in the presence of Rux or equivalent volume of DMSO, visualized firstly by immunostaining for Bunyamwera N protein followed by CV staining. B) BUN WT virus growth was monitored in the presence of 4µM Rux or equivalent volume of DMSO in A549 naïve cells and MDBK bovine cells (Data representative of three independent repeats with a lower limit of detection of 1x 10^3 PFU/ml).

As BUN WT growth in MDBK cells had produced an interesting result in both the plaque assay and multistep viral growth curve it was important to demonstrate that this was an isolated case and all other mammalian cell types did not produce a similar effect. Consequently, we decided to analyse BUN WT growth in all other mammalian cell-lines (BalB/C, RK.13, MDCK and PKIBRS2) using a multistep viral growth curve. Specifically, BUN WT growth was analysed following incubation with Rux (4μM) or equivalent volume of DMSO, in each of the mammalian cell-lines using a multistep viral growth curve (Figure 3.8).

As expected, the results indicate that BUN WT growth is increased in the presence of IFN inhibitor, Rux, in both MDCK and PKIBRS2 cells. The effect is most prominent in PKIBRS2 cells, as BUN WT is unable to grow until Day 5 in the absence of Rux but reaches titers of ~$1x10^8$ in the presence of Rux. Furthermore, there is an increase in viral titer of ~2logs at 48hours post infection in MDCK cells. Lastly, there was no significant increase in BUN WT viral growth seen in BalB/C and RK.13 cells. This was expected as the previous plaque analysis of BUN WT growth in these cell-lines demonstrated only a small increase in plaque size in the presence of Rux (Figure 3.6). In summary, the results from each BUN WT viral growth curve reflect the previous analysis of BUN WT growth using a plaque assay. This confirmed that viral growth was significantly increased in MDCK and PK1BRS2 cells but not in BalB/C or RK.13 in the presence of Rux. Importantly this confirms that the interesting effect on BUN WT growth in MDBK cells, in the presence and absence of Rux (Figure 3.7), is an isolated case.

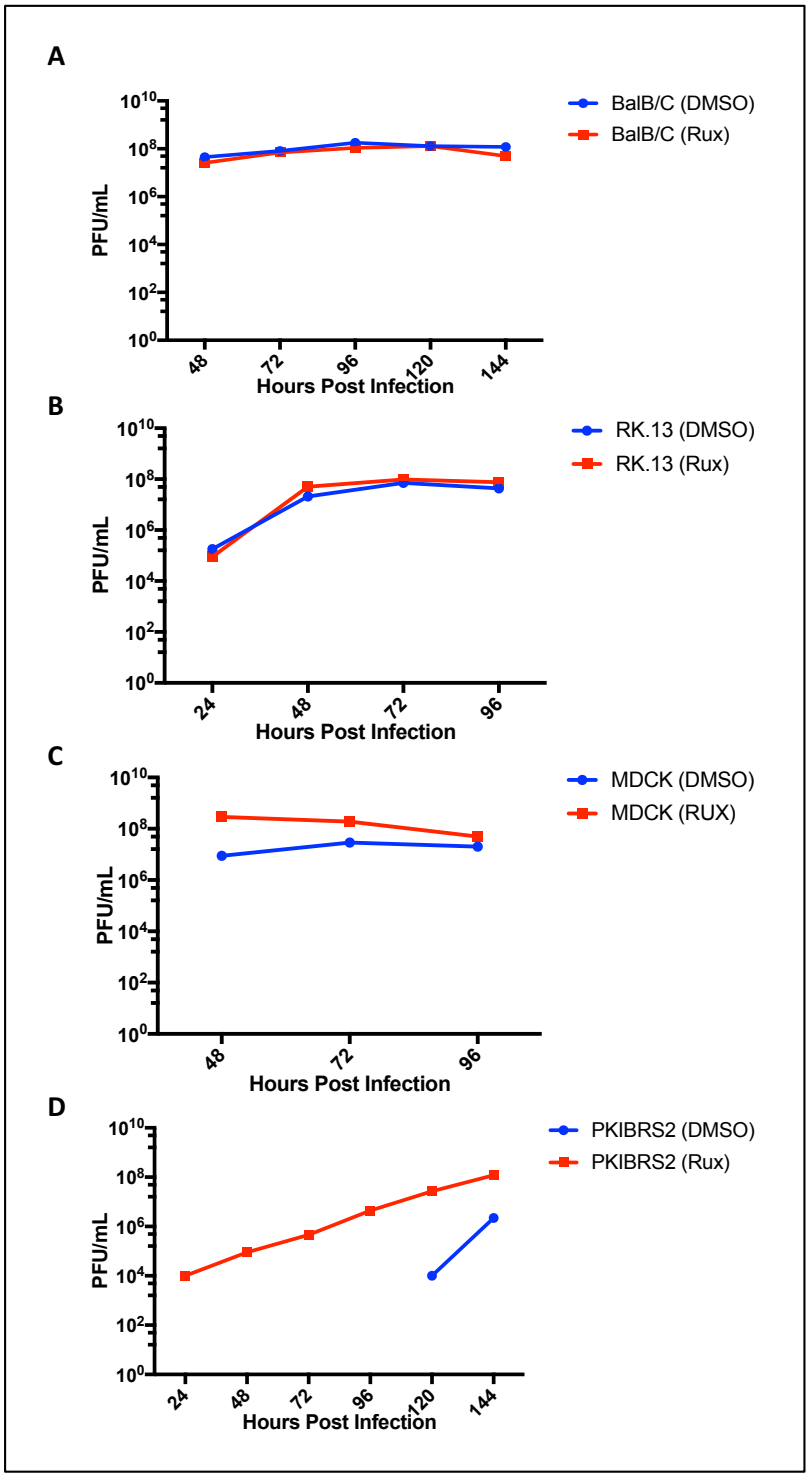

Figure 3.8: Viral growth curves of BUN WT in the presence of IFN inhibitor Rux (4µM) or equivalent volume DMSO. A) BalB/C murine cells B) RK.13 leporine cells. C) MDCK canine cells. D) MDBK bovine cells. (Data representative of two independent repeats with a lower limit of detection of 1x 10^3 PFU/ml).

In summary, addition of the inhibitor, Rux, had no effect on plaque development of BUN WT in the human derived cell-lines A549 or MRC5. This suggests that the NSs protein is functional within these cell-lines. Furthermore, addition of Rux only moderately increased growth in RK.13 and BalB/C cells. Thus indicating that the NSs protein is also functional within these mammalian cell-lines. By contrast addition of Rux substantially increased viral growth in MDCK and PKIBRS2 cells. This striking difference indicates that the NSs protein is non-functional in these cell-lines as addition of the inhibitor has relieved the strain of the IFN response and allowed a significant increase in viral growth. Interestingly, these results demonstrate that the use of IFN-inhibitors may offer a general approach to initiate fundamental studies to investigate species-specific constraints on viral IFN antagonist function.

3.1.4.4 Effects of the IFN inhibitor, Rux, on several viruses from the Bunyaviridae family

Finally, we extended our study to analyse the effect of the inhibitor, Rux, on growth of several viruses from the *Bunyaviridae* family in a number of mammalian cell-lines. In particular, we examined plaque development of Anopheles A virus (ANAV), Bwamba virus (BWAV), Cache Valley virus (CVV), Kairi virus (KIRV), Main Drain virus (MDV) and SBV in the presence and absence of Rux in each of the following cell-lines: A549 naïve, BalB/C, MDBK, MDCK, NBL-6 and RK.13. Notably, the NBL-6 (equine) cell-line was added as MDV has been shown previously to infect horses (Emmons et al. 1983). Furthermore, all viruses express an IFN antagonist, NSs protein, with the exception of ANAV. This virus has been shown to be unable to block the IFN induction pathway and

consequently leads to the induction of IFN-α/β (Mohamed et al. 2009). Specifically, plaque development of each virus was examined following incubation with Rux (4μM) or equivalent volume of DMSO in each of the cell-lines (Figure 3.9). Note that virus titre was kept constant across all cell-lines to enable comparison between growth in different cell-lines however viral titre is not the same for each virus so comparisons between viruses cannot be made. Next we will outline the results for each virus across each cell line individually.

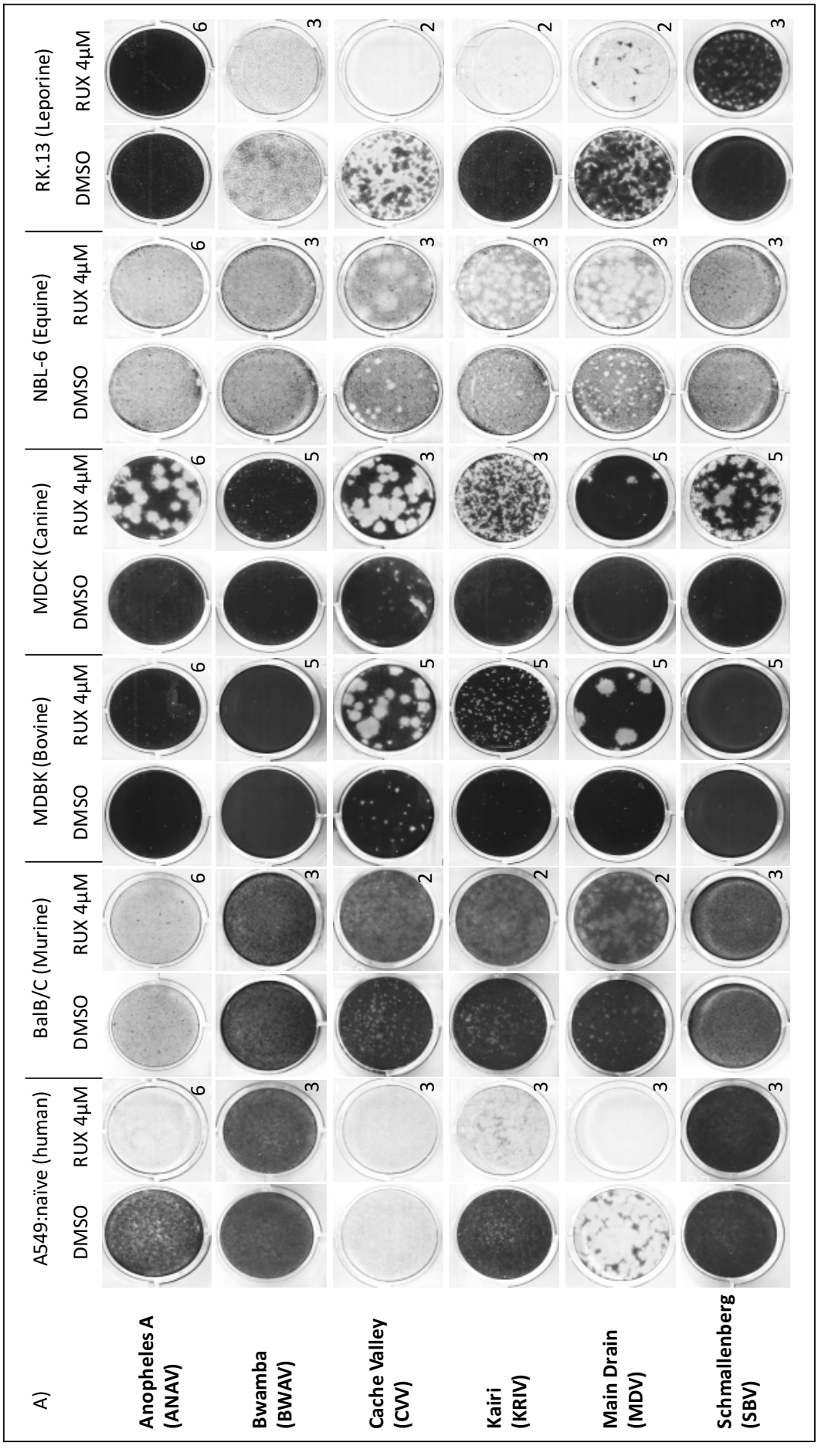
A)
A549:naïve (human)
BalB/C (Murine)
MDBK (Bovine)
MDCK (Canine)
NBL-6 (Equine)
RK.13 (Leporine)
DMSO
RUX 4μM
Anopheles A (ANAV)
Bwamba (BWAV)
Cache Valley (CVV)
Kairi (KRIV)
Main Drain (MDV)
Schmallenberg (SBV)

B)

	A549: naïve (Human)		BalB/C (Murine)		MDBK (Bovine)		MDCK (Canine)		NBL-6 (Equine)		RK.13 (Leporine)	
	DMSO	Rux 4µM	DMSO	Rux 4µM	DMSO	Rux 4µM	DMSO	Rux 4µM	DMSO	Rux 4µM	DMSO	Rux 4µM
ANAV	+	++	-	-	-	-	-	++	-	-	-	-
BWAV	-	-	-	-	-	-	-	++	-	-	+	++
CCV	+*	++*	+	++	+	++	+	++	+	++	+	++
KRIV	+	++	+	++	+	++	+	++	+	++	+	++
MDV	+	++	+	++	+	++	+	++	+	++	+	++
SBV	-	-	-	-	-	-	+	++	-	-	-	++

*results based on Figure 3.10

Figure 3.9: Plaque development of seven different viruses from the *Bunyaviridae* family (ANAV, BWAV, CVV, KRIV, MDV and SBV) in six mammalian cell-lines (A549 naïve, BalB/C, MDBK, MDCK, NBL-6 and RK.13). A) Plaques were fixed at the day indicated and stained using CV stain B) This table summarizes the results from each plaque assay. '-' indicates that the virus did not produce plaques in that cell line, '+' indicates that the virus produced plaques at least pin point plaques in that cell line and '++' indicates that plaque size increased in the presence of the IFN inhibitor Rux in comparison to growth in the absence of inhibitor. (Data representative of three independent repeats).

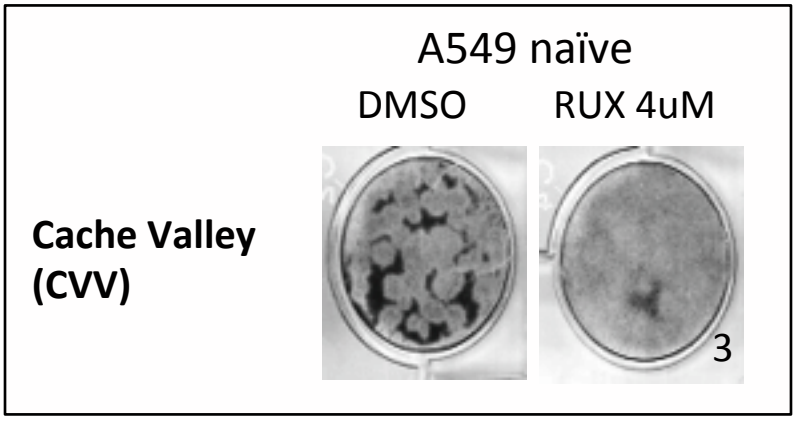

Figure 3.10: Plaque development of Cache Valley virus in A549 naïve cells. Plaques were fixed at the day indicated and stained using CV stain. (Data representative of three independent repeats).

The results demonstrate that ANAV did not grow in BalB/C, MDBK, NBL-6 or RK.13 cells in the presence or absence of Rux. In contrast, ANAV did grow small plaques in the absence of Rux in A549: naïve cells and in the presence of Rux plaque size is increased dramatically. Finally, ANAV did not plaque in MDCK cells in the absence of inhibitor but in the presence of inhibitor larger plaques appear. This indicates that the presence of an active IFN response restricts growth of the virus in A549: naïve and MDCK cells as addition of the IFN inhibitor, Rux, can increase viral growth. However, other constraints must also limit ANAV infection in BalB/C, MDBK, NBL-6 or RK.13, as addition of IFN inhibitor had no effect on viral growth.

Likewise, BWAV did not grow in A549: naïve, BalB/C, MDBK or NBL-6 cells in the presence or absence of Rux. By contrast, it did grow in RK.13 cells in the absence of inhibitor with a small increase in plaque size in the presence of inhibitor. Finally, BWAV did not plaque in MDCK cells in the absence of inhibitor but in the presence of inhibitor small plaques appeared. Hence differences in NSs target proteins may limit host cell range in MDCK and RK.13 cells as addition of IFN inhibitor can increase viral growth in such cells. However, other host cell constraints must restrict BWAV infection within A549: naïve, BalB/C, MDBK and NBL-6 cells as addition of IFN inhibitor had no effect on viral growth.

Next CVV, KRIV and MDV produced similar results across all cell-lines with growth of all viruses in the absence of inhibitor increased in the presence of inhibitor. Note that both monolayers of A549: naïve cells were destroyed using the original dilution of CVV therefore a second lower dilution of CVV was set up

to enable us to determine if plaque size was increased in the presence of inhibitor (Figure 3.10). This demonstrated that CVV infection can grow in the absence of inhibitor but growth is also increased in the presence of inhibitor. Together this demonstrates the CVV, KRIV and MDV are not as restricted as ANAV and BWAV by host cell constraints as they can grow well in each cell-line in the absence of inhibitor. However, each virus is restricted by the IFN response in all cell-lines, as the presence of inhibitor increases growth in all cases.

Finally, SBV did not grow in any of the cell-lines in the absence of inhibitor with the exception of MDCK cells where SBV produced pin point plaques. In the presence of inhibitor plaques are greatly increased in MDCK cells and appear in RK.13 cells. Hence differences in NSs target proteins must limit host cell range in MDCK and RK.13 cells as addition of IFN inhibitor can increase viral growth in such cells. However, other host cell constraints must also restrict BWAV infection within A549: naïve, BalB/C, MDBK and NBL-6 cells as addition of IFN inhibitor had no effect on viral growth.

In summary, the presence of inhibitor, Rux, has increased viral growth of a number of these viruses in different cell-lines. Importantly, these results demonstrate that use of the inhibitor, Rux, could aid fundamental studies of these viruses as high titer virus stocks can be produced by addition of the IFN inhibitor, Rux, to an appropriate cell-line. Furthermore, the use of the IFN inhibitor Rux could also be used to initiate the fundamental study of host cell constraints as these results demonstrate that other host cell constraints exist aside from the IFN response that prevent the infection of a number of these

viruses in different cell-lines. Finally, these results also support the concept that addition of Rux provides a flexible method to improve techniques to isolate emerging viruses by improving virus growth of a number of different viruses in a range of cell-lines derived from different mammalian species.

To summarise, in this section we have further characterised the IFN inhibitor, Rux by investigating its effect on growth of BUNΔNSs, BUN WT and several other members of the *Bunyaviridae* family, in a number of mammalian cell-lines. Firstly, we have demonstrated that addition of IFN inhibitor can increase growth of BUNΔNSs in MRC5 cells, which are commonly used in vaccine production. Thus providing further evidence that the IFN inhibitor could be useful in vaccine production. Secondly, we have demonstrated that addition of the IFN inhibitor, Rux, increased viral growth of BUNΔNSs in several mammalian cell-lines (BalB/C, RK.13, MDBK, MDCK and PKIBRS2). This supports the concept that supplementing the media with Rux provides a flexible approach to increase growth of IFN-sensitive viruses in a cell-line of choice. Thirdly, we have demonstrated that addition of IFN inhibitor increases growth of BUN WT significantly in PKIBRS2 and MDCK cells. Thus indicating that species-specific constraints on the function of the IFN antagonist, NSs protein, exist in these cell-lines. These results therefore demonstrate that the use of IFN-inhibitors may offer a general approach to initiate fundamental studies to investigate species-specific constraints on viral IFN antagonist function. Notably the effects of Rux on growth of BUN WT in MDBK cells represented an interesting case that also initiated further investigation into NSs function and host cell constraints. Finally, we have demonstrated that addition of the IFN inhibitor, Rux, increased viral

growth of several viruses from the *Bunyaviridae* family in several mammalian cell-lines. These results therefore indicate that the addition of the IFN inhibitor, Rux, can aid i) fundamental studies of these viruses and the host cell constraints that prevent their infection and ii) isolation of emerging viruses.

3.1.5 Conclusions

To conclude, in this chapter we have further characterised the use of the IFN inhibitor, Rux, by demonstrating its effectiveness in numerous assays. Specifically, we have demonstrated i) that addition of the IFN inhibitor, Rux, could provide a faster and therefore more efficient alternative for growth of IFN-sensitive vaccine strains than Vero cells, which are used widely in vaccine production and ii) that addition of the IFN inhibitor, Rux, can increase growth of the IFN-sensitive virus BUNΔNSs, BUN WT and several other viruses from the *Bunyaviridae* family in a number of cell-lines derived from different mammalian species. Thus indicating that addition of IFN inhibitors could aid in practical applications such as vaccine production and techniques to isolate emerging viruses. Furthermore, we have demonstrated that i) growth of BUN WT can be significantly increased in cell-lines where species-specific constraints limit IFN antagonist function (PKIBRS2 and MDCK cells) and ii) other host cell constraints aside from the IFN response limit the infection of several viruses from the *Bunyaviridae* family in cell-lines derived from different mammalian species. Thus demonstrating that addition of IFN inhibitor can initiate fundamental studies into species-specific host cell constraints on IFN antagonists as well as investigation of other host cell constraints that limit virus growth. Together, these findings highlight that supplementing the media with IFN inhibitor could

become a valuable technique that could aid in numerous aspects of virological research.

Following this study, the IFN inhibitor, Rux, was used to aid characterisation of several IFN-sensitive viral mutants following their isolation using FACS. In the following chapters, we will discuss the development of this method to isolate IFN-sensitive mutants using FACS and the subsequent characterisation of each IFN-sensitive viral mutant.

4 Chapter 4

4.1 Development of A Novel Method to Isolate IFN-Sensitive Viruses Using FACS

4.1.1 Introduction and aims

Circumventing the host IFN response is an essential component of all viruses, with most viruses producing at least one IFN antagonist. Consequently, this opens up opportunities for prophylactic intervention through the development of 'IFN-sensitive' viruses as attenuated virus vaccines. Current methods to obtain live attenuated vaccines include i) traditional methods such as serial passage of the virus in a foreign host or at abnormal temperatures or ii) rational design. However, traditional methods can be lengthy and rational design can result in an over-attenuated virus that is not viable for vaccine production, particularly in RNA viruses where the IFN antagonists are often multifunctional in nature. Here we aimed to develop a novel method to rapidly select IFN-sensitive viruses from stocks of paramyxoviruses using flow cytometry, utilizing PIV5 as our experimental model for defining parameters of selection. This method would not only speed the process of traditional methods but also allow selection of naturally occurring mutant viruses within the population. Primarily, this method would further our understanding of paramyxoviruses and their interaction with the IFN response. Specifically, we would expect that mutations would occur within the IFN antagonist V protein. This would potentially allow us to map areas within the IFN antagonist where no function had been assigned and give us a greater understanding of structural and functional relationships of the antagonist. Furthermore, we may also find mutations within other areas of the

viral genome. This would allow us to gain insight into other aspects of the biology of these viruses, such as the control of virus transcription and replication. In summary, not only would this method lead to insights into paramyxovirus interactions with the IFN system but it may also have applications in vaccine manufacture as the IFN-sensitive viruses obtained may be further developed as potential IFN-sensitive live attenuated vaccine candidates.

4.1.2 Method concept

To develop this method we utilized the IFN-responsive GFP reporter cell-line, A549/pr(ISRE).GFP, which as explained previously, was engineered within our laboratory to contain a GFP gene under the control of the Mx1 promoter. This promoter contains an ISRE, which is the universal element found in the promoters of hundreds of ISGs. Hence, upon activation of the IFN signalling pathway, via addition of IFN, this promoter is activated and results in the expression of GFP. The basic method concept used to isolate IFN-sensitive viruses using these cells is outlined in Figure 4.1. Briefly, A549/pr(ISRE).GFP cells would be infected using a stock of the paramyxovirus PIV5 and then treated with IFN to optimally activate the IFN signalling pathway and subsequent GFP expression. The cells would then be analysed by FACS and sorted based on GFP expression. As the wild-type virus blocks IFN signalling via the IFN antagonist V protein, GFP expression would also be blocked. Consequently, GFP negative cells would be discarded, as they would be infected with a wild-type virus. In contrast, GFP positive cells may be infected with an IFN-sensitive attenuated virus unable to block the IFN signalling pathway due to either mutation in the V protein or

mutations elsewhere in the viral genome (e.g. those that slow virus replication). These GFP positive cells could then be selected and sorted onto preformed monolayers of cells in 96 well micro-titre plates for isolation of potentially IFN-sensitive mutant viruses unable to block IFN signalling.

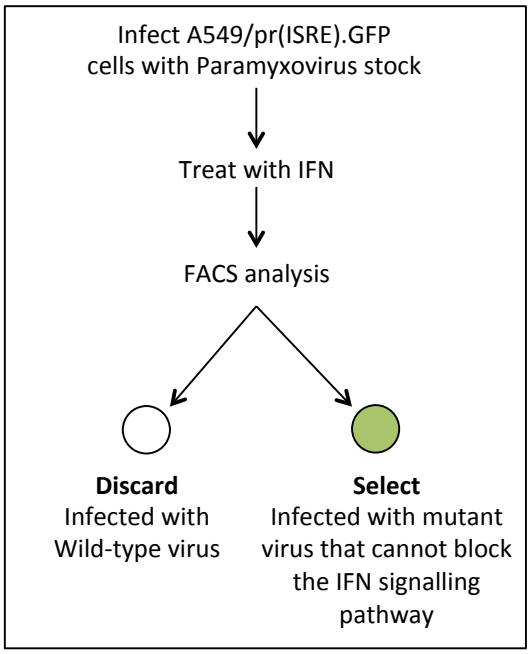

Figure 4.1: Method concept to isolate IFN-sensitive viruses using FACS. Following infection of A549/pr(ISRE).GFP cells with the paramyxovirus PIV5 and subsequent treatment with IFN, cells are then subjected to FACS analysis and sorted based on GFP expression. If the cell is infected with a wild-type virus, then the viral IFN antagonist V protein blocks the IFN signalling pathway and subsequent expression of GFP following IFN treatment. If the cell is infected with an IFN-sensitive virus, then this virus is unable to block the activation of the IFN signalling pathway and consequently, GFP is expressed following addition of IFN. GFP negative cells will be discarded while the GFP positive cells selected and sorted in 96 well micro-titre plates during FACs analysis for isolation of potentially IFN-sensitive mutant viruses unable to block IFN signalling.

Following the creation of this method concept it was evident that a number of elements within the method would require optimisation. The optimisation of this method concept is therefore discussed further in the following section.

4.1.3 Optimisation of the method concept

4.1.3.1 Optimising the time of IFN treatment following infection

A number of steps in the method concept required optimisation. Firstly, it was important to determine the optimum time to treat cells with IFN following their infection with PIV5. IFN addition is required to up-regulate GFP expression following infection allowing us to determine if the cell is infected with an IFN-sensitive virus or not. However, if IFN is added too early, then cells may start to produce GFP, indicating an active IFN signalling response, before the virus has had time to block IFN signalling. As GFP has a half-life of around 26hours (Corish & Tyler-Smith 1999), then this could result in cells being positive for GFP even though they might have been infected by a wild-type virus. Subsequently these cells would be selected as false positives. By contrast, if IFN were added much later, then the length of the experiment would have to be increased to allow sufficient time for the induction of GFP. Consequently, this may mean that cells infected with IFN-sensitive viruses may subsequently become infected with progeny virus, including wild-type viruses, from other infected cells within the population. It was therefore important to identify the optimum timeframe to add IFN.

To analyse the optimum time to add IFN, GFP expression was monitored following mock or PIV5 CPI+ infection combined with treatment of IFN

(1x10^{4}Units/ml) at different time points post infection (Figure 4.2). Note here that this analysis was carried out using PIV5 CPI+, a wild-type strain of PIV5 commonly used within the laboratory. Following mock infection, maximal GFP expression (>93%) was observed after 16-24 hours IFN treatment. Following PIV5 CPI+ infection at MOI 5 all cells should be infected and block the expression of GFP, however, 12% of cells express GFP following IFN treatment at 0 hours post infection (PI). This then dropped to below 5% if IFN was added at 4,8 or 12 hours PI. It was therefore decided to add IFN 6-8 hours PI to allow infection to establish and then to incubate with IFN overnight for 18hours to allow maximal GFP expression within a 24hour experimental timeframe.

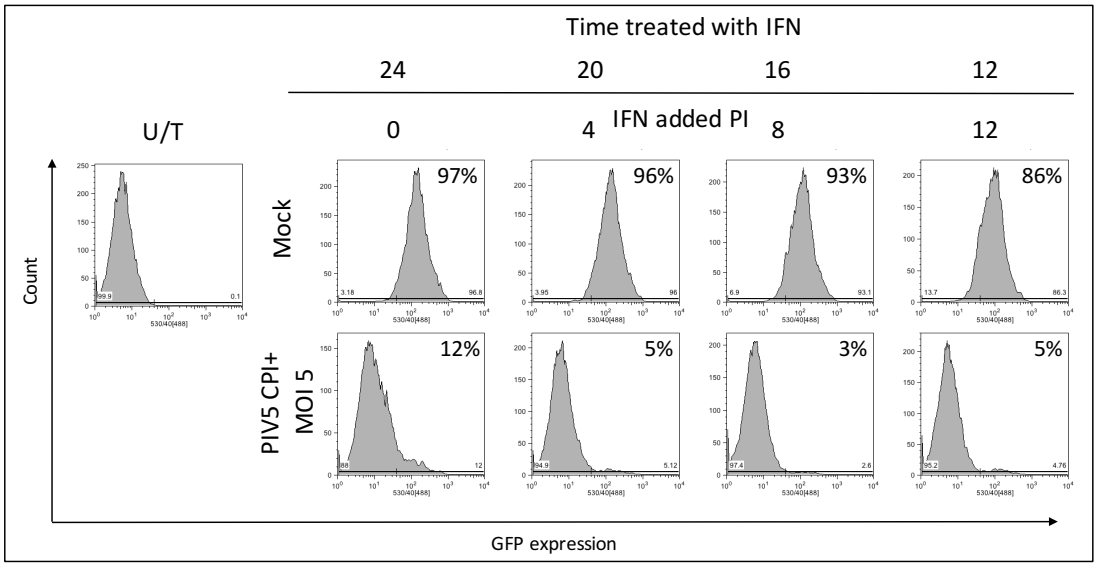

Figure 4.2: Determining the optimum time to treat cells with IFN following infection. A549/pr(ISRE).GFP cells were mock infected and infected with PIV5 CPI+ at MOI 5 for 1 hour before addition of IFN at 0, 4, 8 and 12 hours PI. Cells were then collected 24hours PI and immunostained for PIV5 HN protein before analysis for GFP using flow cytometry. Gating was applied using the untreated (U/T) sample as the no fluorescence control. (Data representative of two independent repeats).

4.1.3.2 Generation of the A549/pr(ISRE).GFP/ISG56-/BVDV Npro to create a more suitable environment to propagate IFN-sensitive viruses

Initially A549/pr(ISRE).GFP cells were used in our method to isolate IFN-sensitive viruses. However, it was quickly realised that upon addition of IFN to these cells, to induce GFP expression following infection, hundreds of ISGs would also be expressed creating an antiviral state within the infected cells. This would therefore create a difficult environment for an attenuated virus to propagate. To tackle this issue we further developed the A549/pr(ISRE).GFP cell-line to create a cell-line that was more suitable to propagate IFN-sensitive viruses. Previous studies have shown that expression of ISG56 is primarily responsible for the IFN-induced inhibition of PIV5 replication (Andrejeva et al. 2013; Young et al. 2016). We therefore used a lentivirus expressing shRNA to ISG56 to knockdown expression of ISG56 in A549/pr(ISRE).GFP cells. In addition, we reasoned that infection with an IFN-sensitive virus might also rapidly activate the IFN induction pathway resulting in production of IFN, before the addition of exogenous IFN. As this might have also inhibited the replication of IFN-sensitive attenuated viruses we further engineered the cell line so that it was unable to produce IFN. Previously, BVDV NPro protein has been shown to block IFN induction by targeting IRF3 for proteasomal degradation (Hilton et al. 2006). We therefore created a dual cell-line that constitutively expressed BVDV Npro and shRNA targeting ISG56 (Figure 4.3). Analysis of the newly engineered cell-line, A549/pr(ISRE).GFP/ISG56-/BVDV Npro, demonstrated that IFN still induced the expression of GFP in this cell-line (Figure 4.3A). Furthermore, BUNΔNSs plaqued on the A549/pr(ISRE).GFP/ISG56-/BVDV Npro but not in the parental cell-line, A549/pr(ISRE).GFP (Figure 4.3B). As BUNΔNSs does not replicate in cells that

can produce and respond to IFN (Hilton et al. 2006), this result shows that constitutive expression of BVDV/Npro in these cells has knocked out the IFN system as predicted. Lastly, knockdown of ISG56 using shRNA facilitated the replication of the ISG56-sensitive strain of PIV5, termed CPI- (Chatziandreou et al. 2002), within cells pre-treated with IFN (Figure 4.3C). In summary, these changes provide a more suitable environment for IFN-sensitive viruses to propagate by preventing the antiviral responses that may inhibit the replication of IFN-sensitive mutants of PIV5.

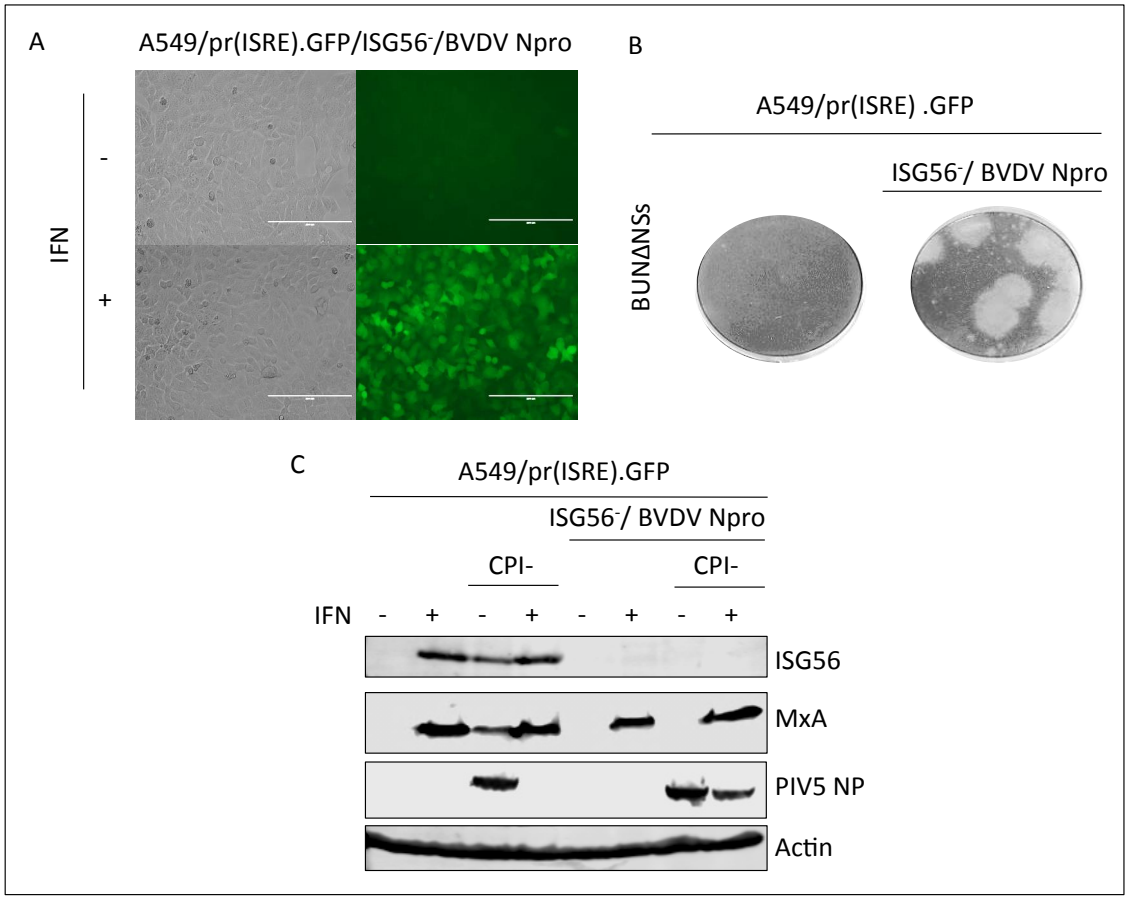

Figure 4.3: A549/pr(ISRE).GFP/ISG56-/BVDV Npro cell-line analysis. A) A549/pr(ISRE).GFP/ISG56-/BVDV Npro cells were (+) or were not (-) treated with IFN for 48 hours before GFP images were taken using an EVOS microscope at 10x magnification. **B)** Plaque development of the IFN-sensitive virus BUNΔNSs was compared in A549/pr(ISRE).GFP and A549/pr(ISRE).GFP/ISG56-/BVDV Npro cells. Cells were then fixed 3 days post infection and stained using CV stain **C)** A549/pr(ISRE).GFP and A549/pr(ISRE).GFP/ISG56-/BVDV Npro cells were (+) or were not (-) pre-treated for 8 hours with IFN before cells were mock infected or infected with PIV5 CPI- at MOI 5. Samples were then harvested 18 hours post infection and analysed by western blot for ISG56, MxA, PIV5 NP an Actin.

4.1.3.3 Use of rPIV5mCh virus to distinguish between uninfected cells and cells infected with a virus unable to block IFN signalling

Rationally, it was decided to infect A549/pr(ISRE).GFP/ISG56-/BVDV Npro cells with virus at an MOI 0.5 so that it would be unlikely that the same cell would be infected with more than one virus. However, at an MOI 0.5, according to Poisson's distribution, around 60% of the cells in this population would remain uninfected. We therefore needed a way to distinguish between cells that were GFP positive, because they were uninfected and those that were GFP positive because they had been infected with a virus unable to block IFN signalling. To initially tackle this issue, we used a recombinant PIV5 virus, termed rPIV5mCh, in which a gene expressing the mCherry fluorescent protein (mCherry) had been inserted between the HN and L genes in the viral genome. Theoretically, this would allow us to easily distinguish between uninfected cells and cells infected with a potentially IFN-sensitive virus; as uninfected cells would be positive only for GFP whereas cells infected with a potentially IFN-sensitive virus would be positive for both GFP and mCherry. This method is summarised in Figure 4.4.

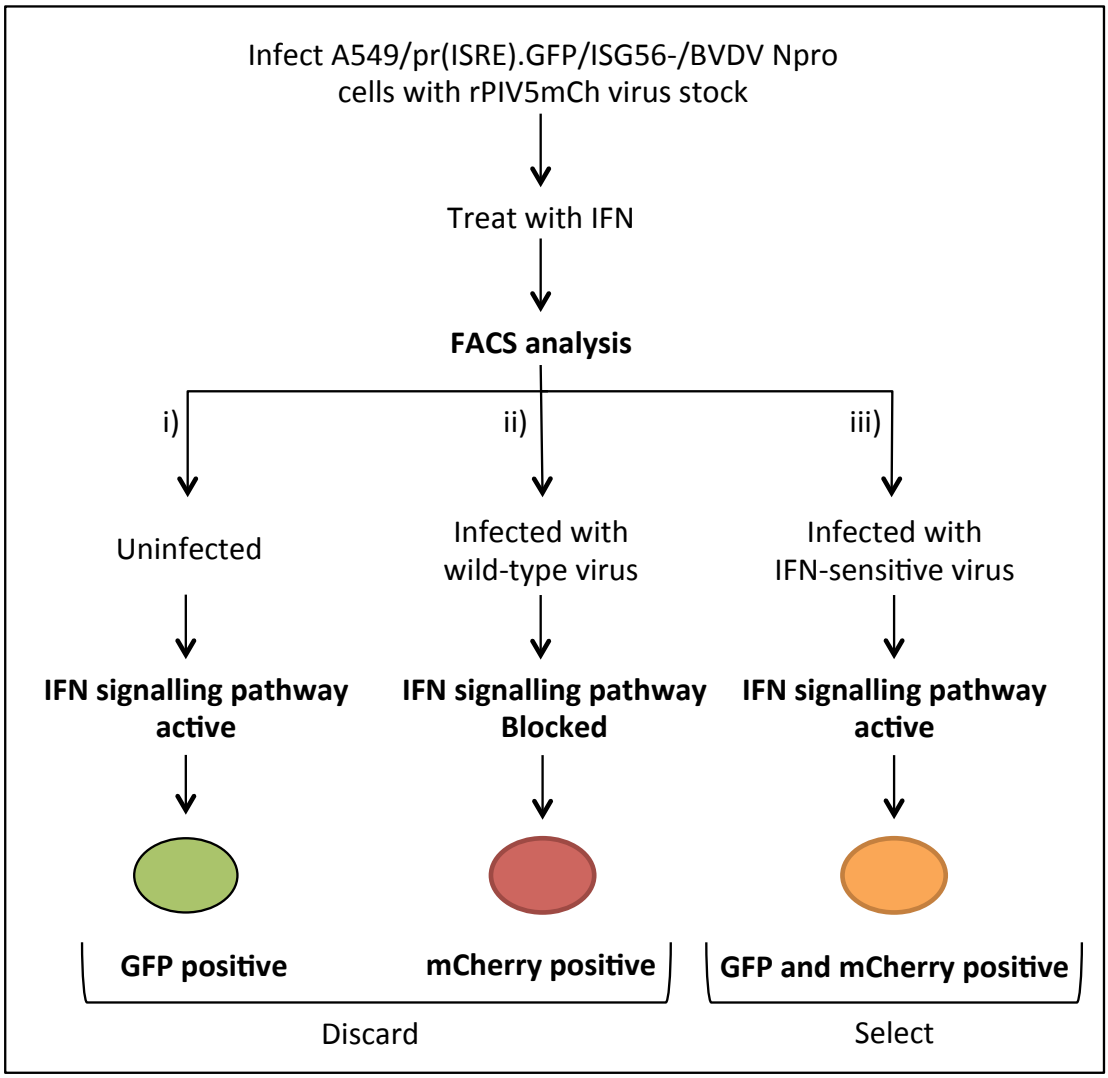

Figure 4.4: Method outline for isolation of IFN-sensitive mutants viruses from rPIV5mCh. Following infection of A549/pr(ISRE).GFP/ISG56-/BVDV Npro cells with rPIV5mCh and subsequent treatment with IFN, cells are then subjected to FACS analysis and three different fluorescent outcomes are identified **i)** If the cell remains uninfected then the IFN signalling pathway is activated following IFN treatment and the cell produces GFP. **ii)** If the cell is infected with a wild-type rPIV5mCh virus, the viral IFN antagonist V protein blocks the IFN signalling pathway and subsequent expression of GFP following IFN treatment. These cells are therefore mCherry positive but GFP negative **iii)** If the cell is infected with a

potentially IFN-sensitive virus, then this virus is unable to block the activation of the IFN signalling pathway and consequently, GFP is expressed following addition of IFN. These cells are therefore positive for mCherry and for GFP expression. Consequently, GFP positive only and mCherry positive only cells will be discarded while the GFP and mCherry dual positive cells selected and sorted in 96 well micro-titre plates during FACs analysis for isolation of potential mutant viruses unable to block IFN signalling.

4.1.3.4 Use of neutralising antibody to inactivate progeny viruses released from infected cells

During analysis of rPIV5mCh infected cells it was noted that the intensity of mCherry fluorescence varied widely from cell to cell (Figure 4.5, panel A). As mCherry expression is used as a marker for infection, this indicated that there was variation in the stage of infection within the population of cells analysed. It was therefore hypothesised that cells were becoming infected at later stages during the experiment due to the release of progeny viruses from the originally infected cells. This problem could result in false positives, as cells already expressing GFP due to IFN treatment may subsequently become infected with progeny wild-type viruses, resulting in the cell becoming positive for both GFP and mCherry. To solve this problem high titres of neutralizing antibody were added to each sample during the experiment (PIV5 anti-HN and anti-F antibodies), thereby inactivating any progeny virus from the infected cells. Such a procedure enabled us to clearly distinguish between infected and uninfected cells (Figure 4.5, compare panels A and B). Next, rPIV5mCh infected A549/pr(ISRE).GFP/ISG56-/BVDV Npro cells were incubated in the presence of

IFN in combination with the presence and absence of neutralising antibody (-/+Ab) (Figure 4.5, compare panels C and D). As observed previously, in the absence of neutralizing antibody there is a wide range of mCherry fluorescence intensities seen following infection and subsequent IFN treatment. However, in the presence of neutralizing antibody the four populations of cells are clearly defined i.e. non-fluorescent cells in Q4, cells infected with wild-type virus Q1, dual fluorescent cells potentially infected with viruses unable to block IFN signalling in Q2 and uninfected cells in Q3. Thus, the presence of neutralizing antibody has reduced the number of false positive cells by neutralizing progeny virus released by initial infection. In summary, the optimized concept for isolating mutant PIV5 viruses unable to block IFN signalling is shown in Figure 4.6.

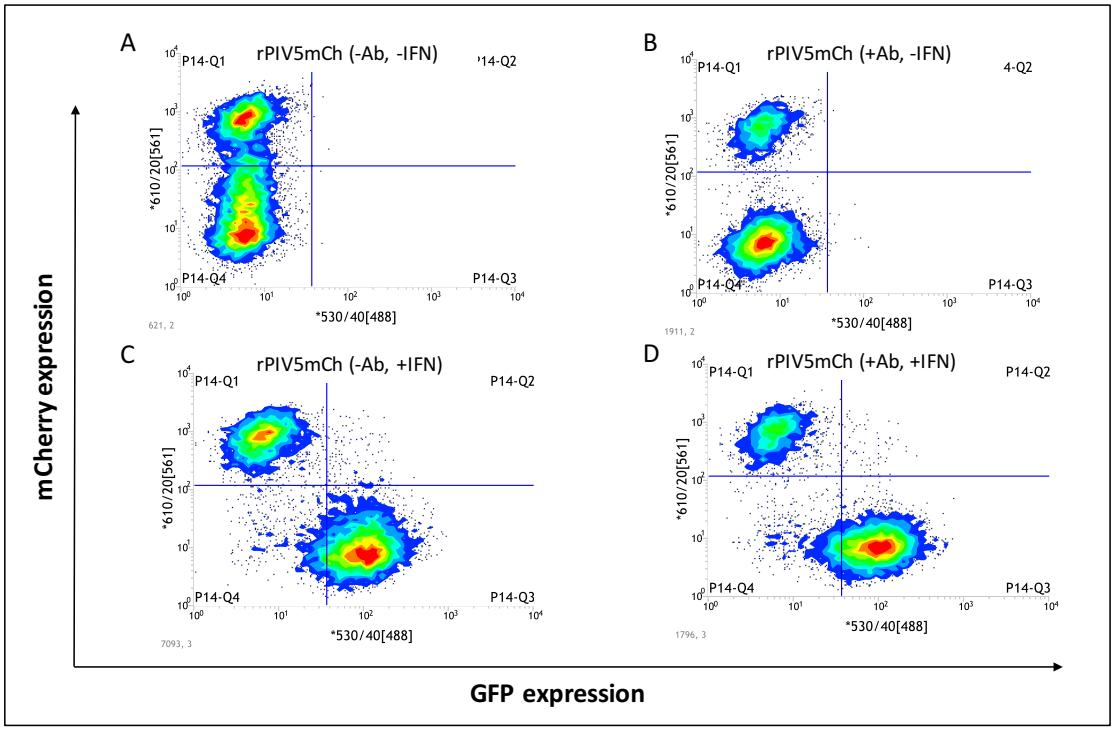

Figure 4.5: Addition of neutralising antibody to inactivate progeny viruses released by infected cells. A549/pr(ISRE).GFP/ ISG56^{-}/ BVDV Npro cells were infected at MOI 0.5 for 1 hour on a rocking platform in 5% CO_2 at 37°C. The inoculum was then removed, cells washed with PBS and replaced with serum free-media. After 6 hours, a mixture of anti-HN antibody and F monoclonal antibodies and/or IFN treatment was added as indicated (-/ + Ab and - /+ IFN respectively). After 24 hours, single cell suspensions were made from rPIV5mCh infected cells incubated in the absence of antibody and IFN (panel A, -Ab, -IFN), in the presence of neutralizing antibody (panel B, +Ab, -IFN), in the presence of IFN (panel C, -Ab, +IFN) and in the presence of both neutralizing antibody and IFN (panel D +Ab, +IFN) prior to FACS analysis.

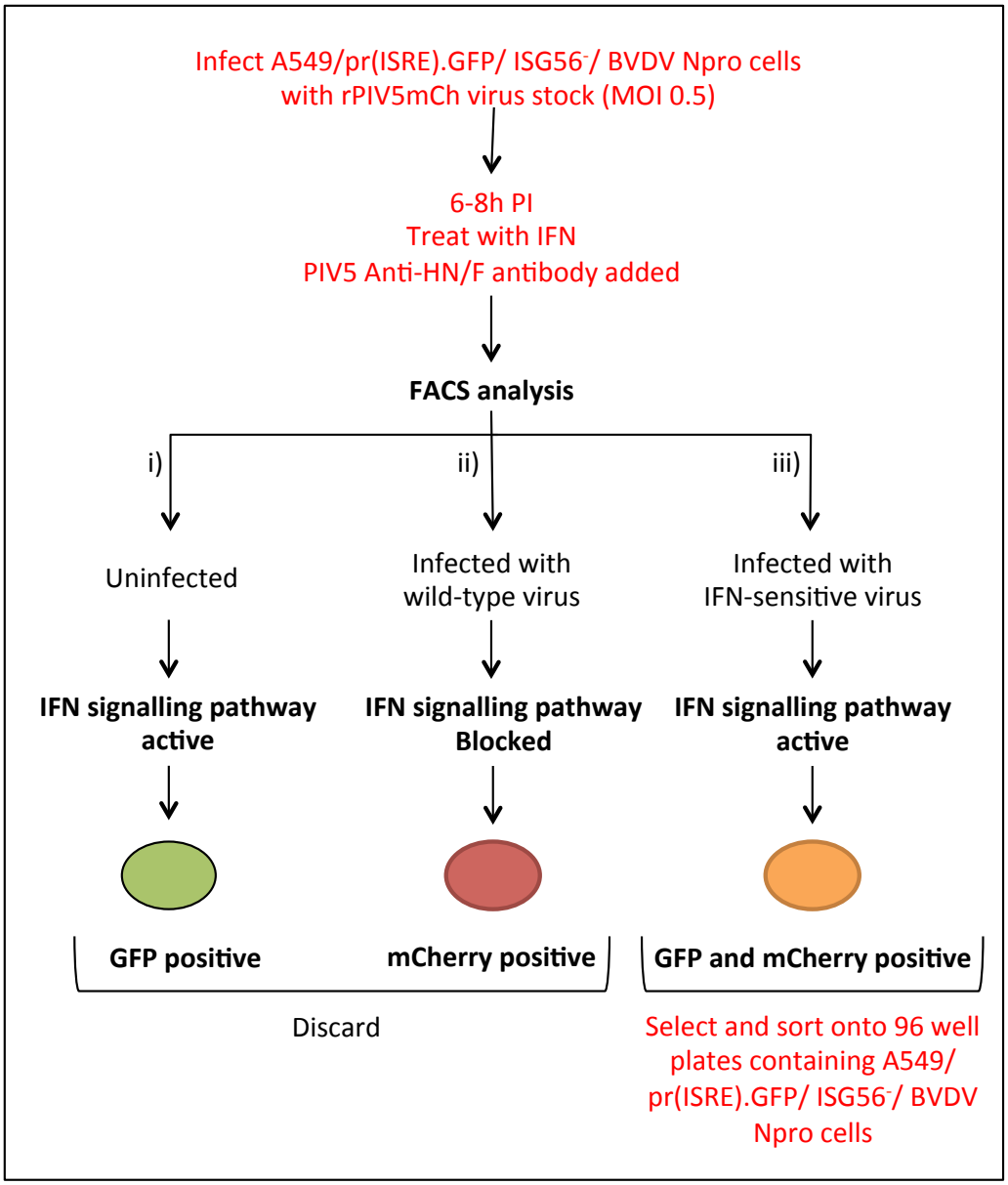

Figure 4.6: Optimised method concept for isolation of IFN-sensitive viruses from rPIV5mCh via FACS. Initially, A549/pr(ISRE).GFP/ISG56^{-}/BVDV Npro cells are infected with rPIV5mCh at MOI 0.5. Following 6-8h, IFN and a mixture of PIV5 anti-HN and anti-F antibodies are added to initiate GFP expression and to neutralise progeny viruses, respectively. Following 24h, GFP and mCherry positive cells are then selected and sorted onto 96 well plates containing A549/pr(ISRE).GFP/ ISG56^{-}/ BVDV Npro cells, to facilitate the growth and isolation of mutant viruses unable to block IFN signalling.

5 Chapter 5

5.1 Isolation of potentially IFN-sensitive mutant viruses using FACS

5.1.1 FACS analysis and selection of potentially IFN-sensitive mutant viruses from rPIV5mCh

Following optimisation, we then implemented this method to isolate potentially IFN-sensitive mutant viruses from rPIV5mCh. A total of four samples were prepared, three control samples plus one experimental sample. The three control samples consisted of mock infected A549/pr(ISRE).GFP/ISG56^{-}/BVDV Npro cells that were (+) or were not (-) treated with IFN (1x10^{4}Units/ml) and rPIV5mCh infected A549/pr(ISRE).GFP/ISG56^{-}/BVDV Npro cells that were not treated with IFN (-IFN). The experimental sample consisted of rPIV5mCh infected A549/pr(ISRE).GFP/ISG56^{-}/BVDV Npro cells treated with IFN which would subsequently be used for selection of cells containing potentially IFN-sensitive mutant viruses.

Examination of the mock infected controls indicated that in the absence of IFN, all cells were GFP and mCherry negative (Figure 5.1, panel A) and in the presence of IFN, 95% of cells were GFP positive (Figure 5.1, panel B). Importantly, these two controls demonstrated that the cells were uninfected and remained responsive to IFN in the absence of infection. Examination of the rPIV5mCh infected control, indicated that in the absence of IFN, 24% of cells were mCherry positive only (P14-Q1) and the rest (76%) of the cells were both GFP and mCherry negative (P14-Q4) (Figure 5.1, panel C). Importantly, this control demonstrates that infection leads to the production of mCherry but does

not induce IFN signalling and subsequent GFP expression. Following analysis of the controls, the experimental sample was then used to select cells that could contain potentially IFN-sensitive mutant viruses (Figure 5.1, panel D). Specifically, 21% of cells in this sample were mCherry positive only (P14-Q1), 70% of cells were GFP positive only (P14-Q3) and a further 9% of cells were both GPF and mCherry negative (P14-Q4). The latter indicates that these cells were infected with a virus that is unable to produce mCherry, which can occur if the recombinant virus mutates so that it no longer expresses mCherry. Most importantly, 1% of cells were positive for both GFP and mCherry (P14-Q2). This indicated that these cells could contain a potentially IFN-sensitive mutant virus, as the infecting virus could not block GFP expression. Consequently, these cells were selected and single cell sorted into 96 well micro-titer plates containing confluent monolayers of A549/pr(ISRE).GFP/ISG56-/Npro cells that facilitate the growth and isolation of IFN-sensitive viruses. These plates were then incubated for 3-4 days to allow virus amplification for further analysis, which is outlined in the following section.

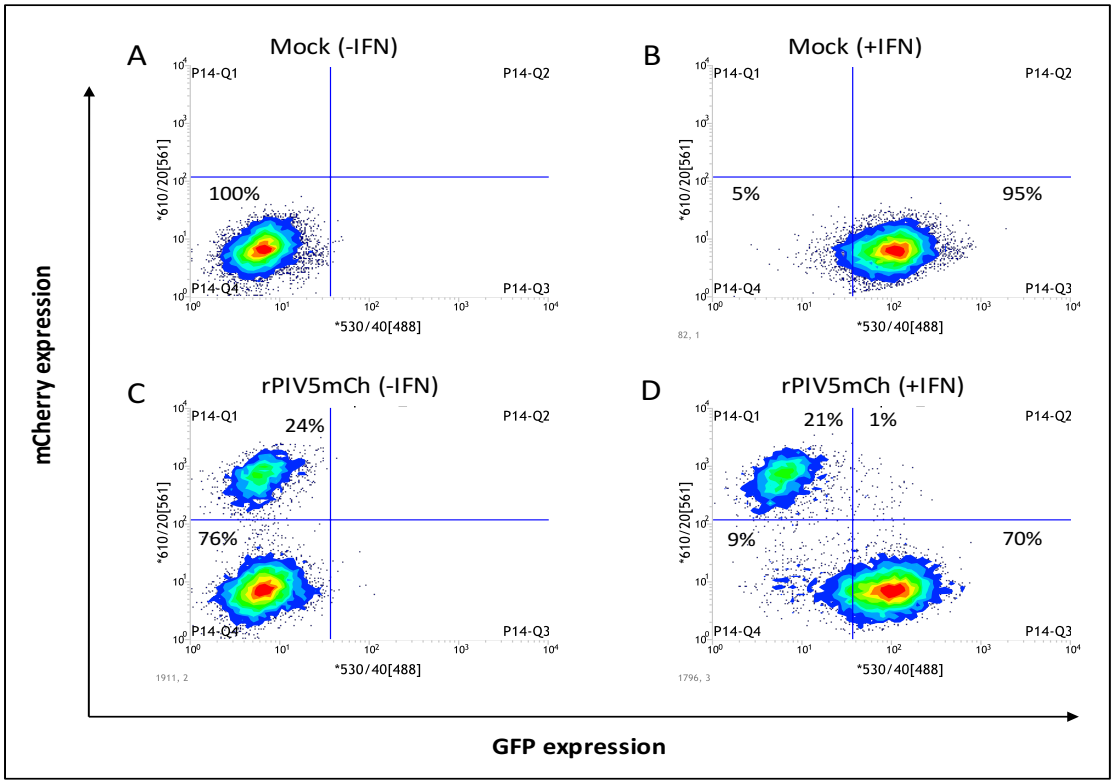

Figure 5.1: FACS analysis and selection of potentially IFN-sensitive mutant viruses from rPIV5mCh. A549/pr(ISRE).GFP/ISG56^{-}/BVDV Npro cells were mock infected or infected with rPIV5mCh virus at MOI 0.5 for 1h. Virus inoculum was then removed, cells washed with PBS and incubated in SF media. After 6 hours, a mixture of PIV5 anti-HN and anti-F neutralizing antibody was added to all samples and cells were treated with or without IFN as indicated (-/+IFN). After 24hours, single cell suspensions were made from mock infected cells (panel A, -IFN), mock infected cells incubated in the presence of IFN (panel B, +IFN), rPIV5mCh infected cells (panel C, -IFN) and rPIV5mCh infected cells incubated in the presence of IFN (panel D, +IFN). Each sample was then subjected to FACS analysis. Cells from panel D P14-Q2 were then sorted into 96 well plates containing confluent monolayers of A549/pr(ISRE).GFP/ISG56^{-}/BVDV Npro cells. (Data representative of two independent repeats).

5.1.2 Selection of potentially IFN-sensitive mutants

Having selected and sorted GFP and mCherry positive cells onto preformed monolayers of A549/pr(ISRE).GFP/ISG56-/Npro cells and incubating these plates for 3-4 days, next we needed to determine which monolayers contained potentially IFN-sensitive mutant viruses. The primary rationale for using preformed monolayers of A549/pr(ISRE).GFP/ISG56-/Npro cells was that these cells allowed a suitable environment for IFN-sensitive viruses to propagate, however, they were also essential to enable us to identify potentially IFN-sensitive mutants following their incubation. Specifically, the supernatant containing virus was harvested from each well and stored in a fresh 96 well micro-titer plate at -80°C. Subsequently, IFN was added to the remaining infected monolayers and incubated for 18 hours. Each monolayer was then examined for the presence of GFP and mCherry using fluorescent microscopy. Three distinct fluorescent outcomes then allowed us to determine differences in viral infection of the monolayer (Figure 5.2). The first outcome was that the monolayer was GFP positive only. This indicated that the cells were uninfected, potentially because the sorted cell died. The second was that the cells were positive for mCherry but negative for GFP expression indicating that the monolayer was infected with a wild-type virus or that it was infected with a mutant virus unable to block IFN signalling that had subsequently reverted to wild-type. The final outcome was that the well was mCherry and GFP positive, indicating that the monolayer was infected with a potentially IFN-sensitive mutant virus unable to block IFN-signalling. During the first experiment, 8 potentially IFN-sensitive viruses were identified from two 96 well plates. The experiment was then repeated and a further 25 potentially IFN-sensitive viruses

were identified from six 96 well plates. Thus providing us with an approximate yield of 4 % from each sort. The corresponding viruses were then selected from the 96 well micro-titer plates stored previously in -80°C and amplified using Vero cells.

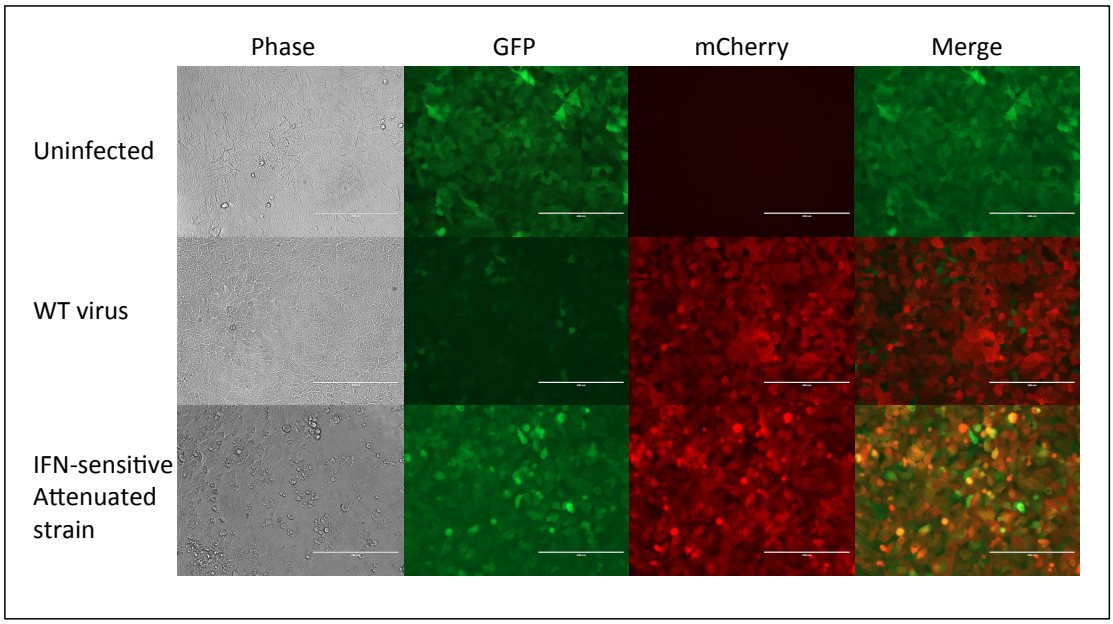

Figure 5.2: Examples of the three potential outcomes following sorting. Monolayers of A549/pr(ISRE).GFP/ ISG56^{-}/ BVDV Npro cells were seeded with single A549/pr(ISRE).GFP/ ISG56^{-}/ BVDV Npro cells that were either uninfected, infected with rPIV5mCh wild-type virus or infected with an rPIV5mCh potentially IFN-sensitive mutant virus following FACS analysis. The monolayers were then incubated for 3-4 days before the supernatant containing virus was removed and IFN treatment was added for 18hours. Cells were then analysed for GFP and mCherry expression and images taken using a fluorescent microscope (EVOS; 10x Magnification).

5.1.3 Confirmation of potentially IFN-sensitive rPIV5mCh mutants using FACS analysis

To determine if the selected viruses did in fact display an IFN-sensitive virus phenotype and ultimately select which viruses would be taken forward for sequencing, each stock of potentially IFN-sensitive virus was analysed by FACS. Specifically, A549/pr(ISRE).GFP/ISG56-/Npro cells were infected with each of the 32 newly generated virus stocks in the same manner to the original selection experiment and subjected to FACS analysis. Note to expedite the process of mutant virus identification, mutant virus stocks were not titered for this analysis. Interestingly, FACS analysis of the potential mutants demonstrated two different phenotypes (Figure 5.3, compare panels D and E). The first phenotype, attenuated mutant phenotype 1, demonstrated that all cells infected (mCherry positive) were also GFP positive, clearly indicating that the virus was unable to block IFN signalling. By contrast, the second phenotype, attenuated mutant phenotype 2, demonstrated a 'smear' of infected cells expressing various intensities of GFP. This indicated that this virus was not definitively able to block the IFN signalling response. Note that infection by two different viruses was not ruled out but deemed unlikely as simultaneous infection by a wild type virus and a virus displaying attenuated mutant phenotype 1 resulted in two distinct populations, infected GFP negative and infected GFP positive, rather than a 'smear' of infected cells expressing various intensities of GFP (Figure 5.3, panel F). Furthermore, the population could not be enriched by re-selection of the dual positive cells, which can be achieved when two differing infections are present (Data not shown), thus indicating that one population of virus exhibited the phenotype. Following this analysis, a total of 28 out of 33 potentially IFN-

sensitive mutant viruses were taken forward for sequencing, with 26 demonstrating the attenuated mutant phenotype 1, and 2 demonstrating attenuated mutant phenotype 2. The other 5 potential mutants were disregarded as each demonstrated a wild-type infection phenotype.

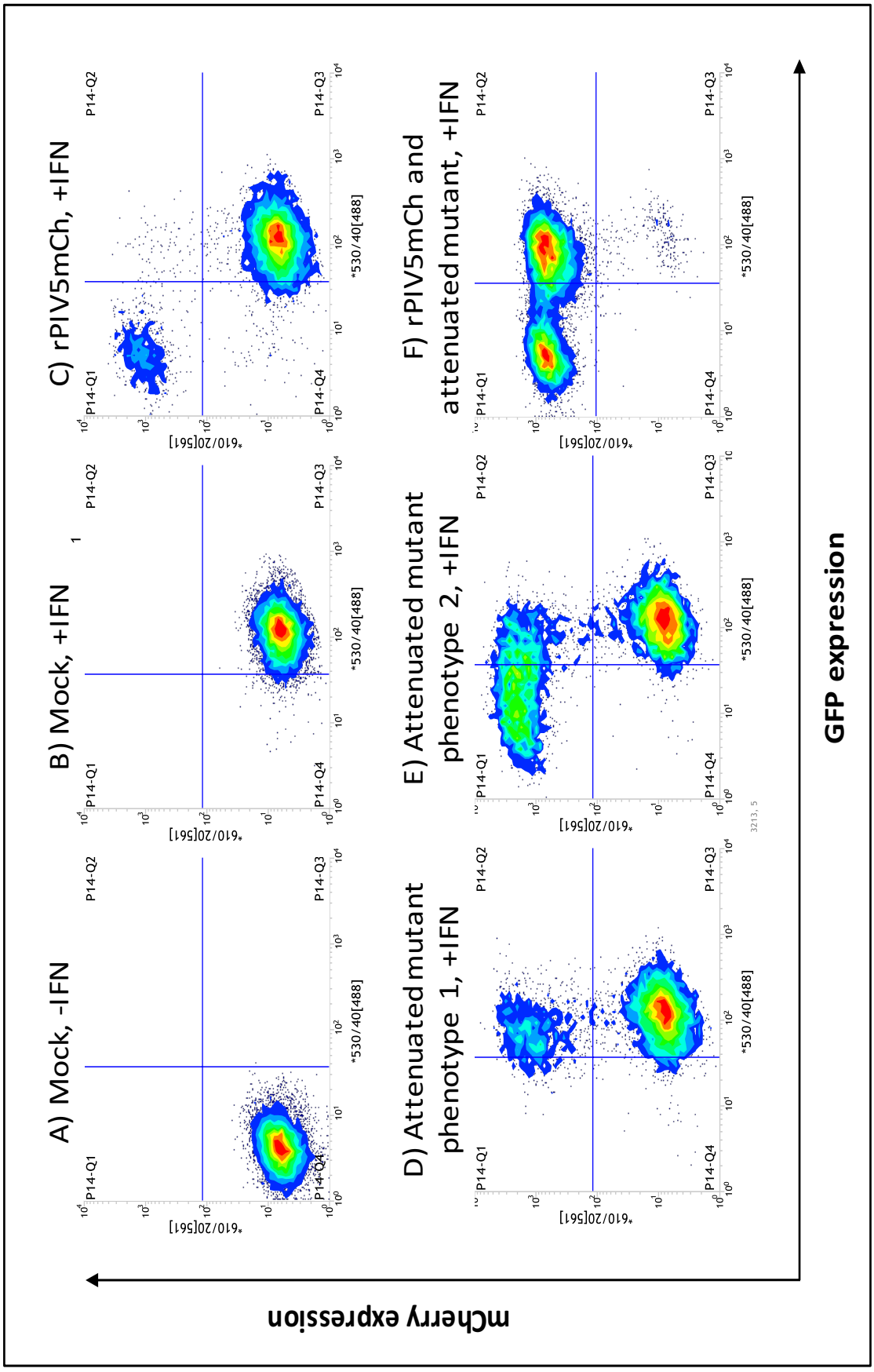
A) Mock, -IFN
B) Mock, +IFN
C) rPIV5mCh, +IFN
D) Attenuated mutant phenotype 1, +IFN
E) Attenuated mutant phenotype 2, +IFN
F) rPIV5mCh and attenuated mutant, +IFN
mCherry expression
GFP expression
P14-Q1
P14-Q2
P14-Q3
P14-Q4
*610/20[561]
*530/40[488]

Figure 5.3: FACS analysis of potentially IFN-sensitive mutant viruses. A549/pr(ISRE).GFP/ ISG56^{-}/ BVDV Npro cells were mock infected or infected with rPIV5mCh or a potentially IFN-sensitive mutant virus at an MOI 0.5 for 1h. Virus Inoculum was then removed, cells washed with PBS and incubated in SF media. After 6hours, a mixture of PIV5 anti-HN and anti-F neutralizing antibody was added to all samples and cells were treated with or without IFN as indicated (-/+IFN). After 24hours, single cell suspensions were prepared from mock infected cells (panel A, -IFN), mock infected cells incubated in the presence of IFN (panel B, +IFN), rPIV5mCh infected cells incubated in the presence of IFN (panel C, +IFN), potentially IFN-sensitive mutant virus infected cells that represent an example of attenuated mutant phenotype 1 (panel D, +IFN), potentially IFN-sensitive mutant virus infected cells that represent an example of attenuated mutant phenotype 2 (panel E, +IFN) and rPIV5mCh and potentially IFN-sensitive mutant virus infected cells (attenuated mutant phenotype 1; panel F, +IFN). Each suspension was then analysed by FACS analysis.

5.1.4 Sequencing of the V/P gene from rPIV5mCh mutants

The 28 potentially IFN-sensitive viruses selected via FACS analysis were then sequenced in an attempt to identify mutations within the rPIV5mCh genome that could contribute to their inability to block IFN signalling. As it was expected that mutations leading to this phenotype would occur in the viral IFN antagonist V protein, we first set out to sequence the V/P gene of each mutant that encodes both the V and P proteins due to a process known as 'RNA editing'. Notably, PIV5 V mRNA is a faithful transcript of the V/P gene, whereas the P mRNA contains two non-templated G residues which are added during transcription when the

viral polymerase stutters on a specific site, upstream of the insertion site (reviewed in Parks et al 2011). This results in both the V and P proteins containing a common N terminus but each having a unique C terminus.

To sequence the V/P gene of each of the potentially IFN-sensitive virus, Vero cells were infected with each of the viruses at MOI 5 and incubated for 18 hours before RNA extraction. Genomic viral RNA was then reverse transcribed to cDNA using a primer targeted against the sequence flanking the downstream sequence outside of the V/P open reading frame (ORF). This fragment was then PCR amplified, using the same primers and blunt end cloned into the vector pJET 1.2. Colony PCR using primers specific for pJET1.2 was then completed to identify colonies containing the correct insert. Sequencing of the insert was then completed from three individual positive colonies and sequences aligned to the published PIV5 W3 P (AFE48445.1) and V gene sequences (AFE48446.1). Surprisingly, 26 of the 28 viruses sequenced were found to contain the same set of 8 nucleotide mutations, subsequently named rPIV5mCh-α. Notably, each of these mutants displayed the attenuated mutant phenotype 1 during FACS analysis. The other two mutants contained a different set of 2 nucleotide mutations, subsequently named rPIV5mCh-β. Notably, each of these mutants displayed the attenuated mutant phenotype 2 during FACS analysis. Both rPIV5mCh-α and rPIV5mCh-β nucleotide and corresponding amino acid mutations are catalogued in Figure 5.4. To aid visualisation, each of these amino acid mutations was mapped relatively onto the V and P proteins also in Figure 5.4.

A) rPIV5mCh-α

Nucleotide changes in V mRNA	Amino acid changes in V protein	Nucleotide changes in P mRNA	Amino acid changes in P protein
T152C	L51P	T152C	L51P
T305C	L102P	T305C	L102P
T307C	Silent	T307C	Silent
T364C and T365C	L122P	T364C and T365C	L122P
T395C	L132P	T395C	L132P
T404C	F135S	T404C	F135S
		RNA dependent RNA polymerase GG insertion 492 and 493 to make P mRNA	
T523C	Y175H	T525C	Silent

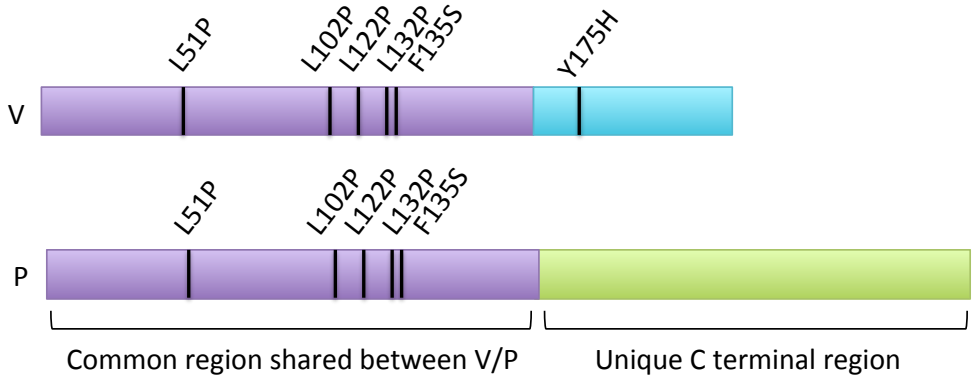

B) rPIV5mCh-β

Nucleotide changes in V mRNA	Amino acid changes in V protein	Nucleotide changes in P mRNA	Amino acid changes in P protein
T430A	F144I	T430A	F144I
		RNA polymerase GG insertion 492 and 493 to make P mRNA	
A640G	T214A	A642G	Silent

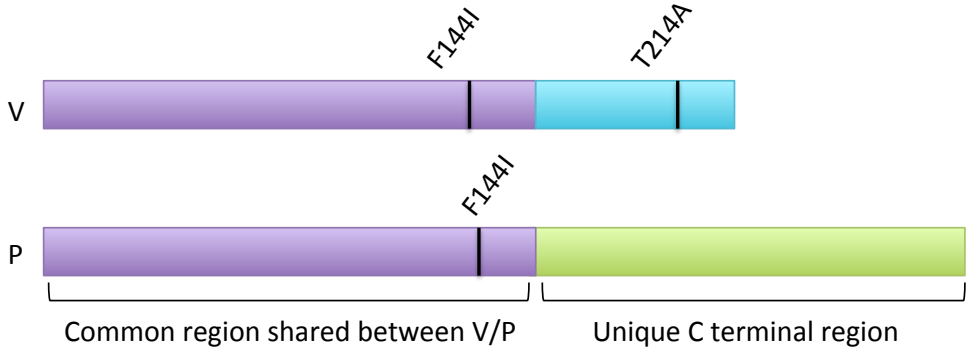

Figure 5.4: Nucleotide and amino acid mutations in V and P genes/proteins of rPIV5mCh-α and β. The nucleotide and corresponding amino acid mutations in V and P genes/proteins, followed by an illustration of the relative positions of the amino acid mutations in the V and P proteins are demonstrated for rPIV5mCh-α (panel A) and rPIV5mCh-β (panel B).

The mutant rPIV5mCh-α contains eight nucleotide changes from thymine to cytosine in the V/P gene. Specifically, 7 of these nucleotide mutations correspond to 6 amino acid changes within the V protein and 5 amino acid changes within the P protein. Interestingly, the 5 mutations found within the region common to both the V and P gene correspond to 4 amino acid changes from Leucine to Proline (L51P, L102P, L122P and L132P) and the other converts a Phenylalanine to a Serine (F135S). This was somewhat surprising, as we know that amino acid changes to Proline, which is a cyclic amino acid, can dramatically change protein structure. Furthermore we know that the P protein is essential to viral synthesis (Fuentes et al. 2010), yet despite these mutations it appears that this viral mutant can replicate efficiently. The final mutation, which is synonymous in the P protein but non-synonymous in the V protein, mutates Tyrosine to Histidine (Y175H). In contrast, the rPIV5mCh-β mutant contains only 2 nucleotide changes in the V/P gene, one thymine to adenine and one adenine to guanine. These correspond to 2 amino acid changes within the V protein and one amino acid change within the P protein. The mutation found in the common region of the V and P protein mutates Phenylalanine to Isoleucine (F144I). The other mutation, which is synonymous in the P protein but non-synonymous in the V protein,

mutates Threonine to Alanine (T214A). Once identified, each of the V protein amino acid mutations were mapped onto the V protein structure, unfortunately no structure has been solved for the PIV5 P protein (Figure 5.5). This highlighted that rPIV5mCh-α and rPIV5mCh-β mutations both appear in structured regions of the V protein such as beta sheets and alpha helices.

In summary, two different mutant viruses were isolated from a stock of rPIV5mCh multiple times and both were found to contain mutations with their V and P proteins. Before we attempted to analyse these viruses further we decided to try to increase the total number of potential mutants isolated whilst adapting this method for use with non-fluorescent viruses. This was important as not all viruses have a readily available recombinant expressing a fluorescent protein and we wanted to create an adaptable method that can be used on multiple viruses.

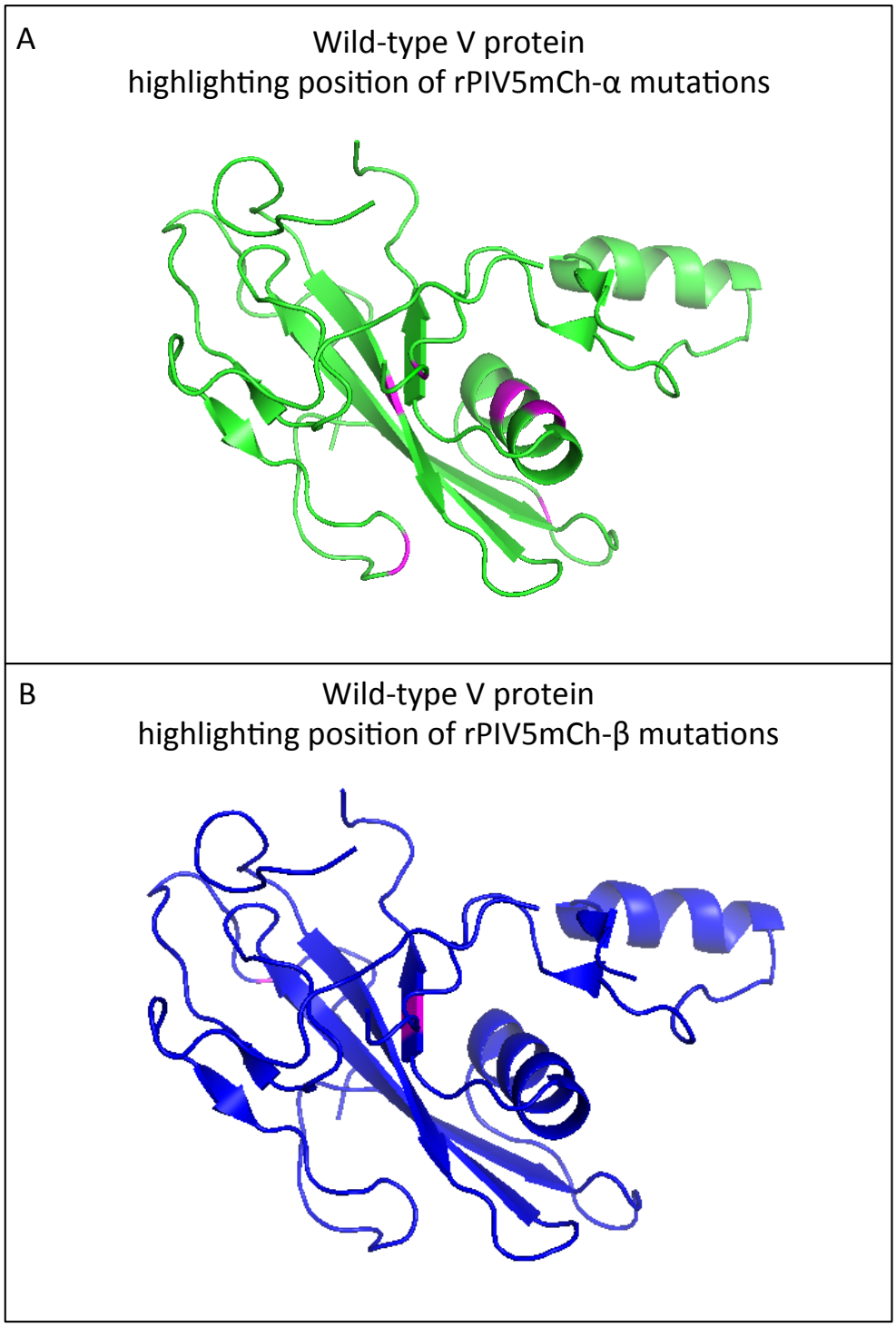

Figure 5.5: Mapping the positions of amino acid mutations rPIV5mCh-α and rPIV5mCh-β to the wild-type V protein structure (Protein Data Bank accession number 2B5L). The structure of wild-type V protein with the positions of rPIV5mCh-α (panel A) and rPIV5mCh-β (panel B) mutations highlighted (structures adapted using PyMOL (Schrodinger)).

5.1.5 Adapting the method to isolate viruses from PIV5 W3

Having successfully isolated mutants from rPIV5mCh, next we decided to adapt this method for use with the non-fluorescent virus PIV5 W3, a wild-type PIV5 virus commonly used within our laboratory. To adapt this method, we added two immunostaining steps to track for infected cells (Figure 5.6). The first step was inserted prior to collection of the cells in single cell suspensions for FACS analysis. Prior to collection, neutralising antibody targeting the HN and F proteins of PIV5 is added to inactivate progeny virus. As this neutralising antibody would also bind to HN and F viral protein on the surface of infected cells we could therefore take advantage of this to immunostain infected cells using secondary goat anti-mouse Texas Red antibody. Cells would then be prepared as single cell suspensions and analysed by FACS in the same manner as rPIV5mCh infected cells with the exception that GFP and Texas Red positive cells (instead of mCherry positive) would be selected and single cell sorted onto 96 well plates containing preformed monolayers of A549/pr(ISRE).GFP/ISG56-/Npro cells. Plates containing sorted cells would then be incubated for 3-4 days to allow virus to propagate. The second immunostaining step was then inserted here, following IFN treatment, to enable us to distinguish between cells that were uninfected (GFP positive only), infected with wild-type virus (Texas Red positive only) and infected with a virus unable to block IFN signalling (GFP and Texas Red positive). Addition of each of these steps is highlighted in a method workflow in Figure 5.6.

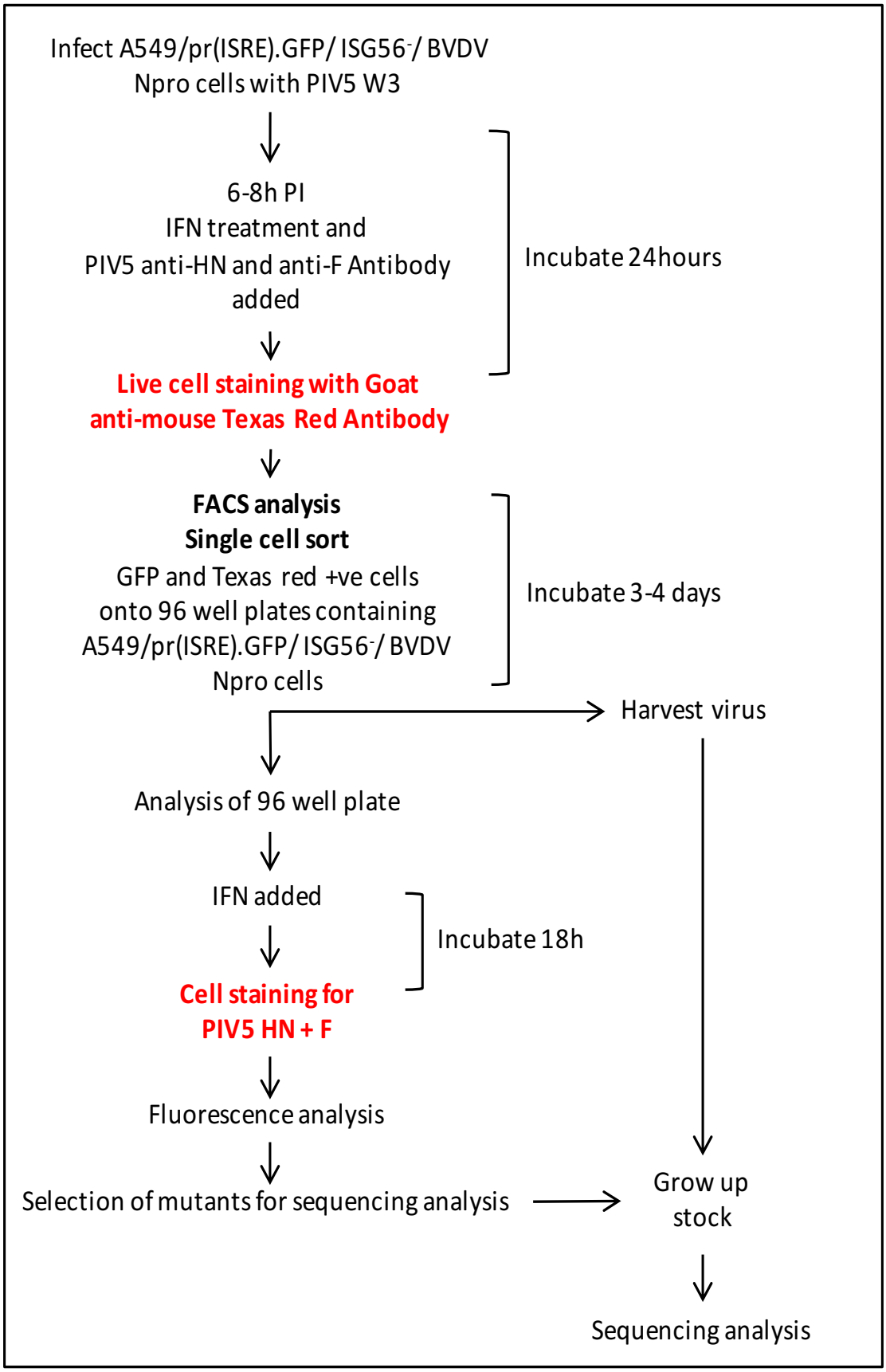
Infect A549/pr(ISRE).GFP/ ISG56-/ BVDV Npro cells with PIV5 W3
6-8h PI
IFN treatment and
PIV5 anti-HN and anti-F Antibody added
Incubate 24hours
Live cell staining with Goat anti-mouse Texas Red Antibody
FACS analysis
Single cell sort
GFP and Texas red +ve cells onto 96 well plates containing A549/pr(ISRE).GFP/ ISG56-/ BVDV Npro cells
Incubate 3-4 days
Harvest virus
Analysis of 96 well plate
IFN added
Incubate 18h
Cell staining for PIV5 HN + F
Fluorescence analysis
Selection of mutants for sequencing analysis
Grow up stock
Sequencing analysis

Figure 5.6: PIV5 W3 method workflow for the isolation of potentially IFN-sensitive mutant viruses using FACS. Initially, A549/pr(ISRE).GFP/ ISG56-/ BVDV Npro cells would be infected with PIV5 W3 at MOI 0.5. Then 6-8h PI, IFN and PIV5 anti-HN and anti-F antibody would be added to initiate GFP expression and to neutralize progeny virus, respectively. Following 24h, cells would then be immunostained with goat anti-mouse Texas Red antibody and prepared as single cell suspensions for FACS analysis. GFP and Texas Red positive cells would then be selected and single cell sort onto 96 well micro-titer plates containing A549/pr(ISRE).GFP/ISG56-/BVDV Npro cells. After 3-4 days the supernatant containing virus would be harvested to a fresh 96 well plate and stored at -80°C. The remaining monolayers containing virus-infected cells would then be incubated in the presence of IFN for 18h, fixed, immunostained with goat anti-mouse Texas Red antibody and then analysed for fluorescence. Uninfected monolayers and monolayers infected with wild-type viruses would be GFP positive only and Texas Red positive only, respectively, whereas monolayers infected with a virus unable to block IFN-signalling would be positive for both GFP expression and Texas Red staining allowing for their selection. The corresponding viruses would then be selected from the 96 well micro-titer plates stored previously in -80°C, amplified in Vero cells and then subjected to sequencing analysis.

Following addition of these two staining steps, we implemented this method to isolate potentially IFN-sensitive viruses from PIV5 W3 (Figure 5.7). Dual GFP and Texas Red positive cells (~1% of the population) were selected and single cell sorted onto preformed monolayers of A549/pr(ISRE).GFP/ISG56-/Npro cells from P13-Q2 (Figure 5.7, panel D), following examination of the control samples. However, despite several attempts (12 x 96 well plates) we identified only one potential mutant from the PIV5 W3 stock following sorting and subsequent FACS analysis. This mutant, named PIV5 W3-γ, was sequenced and found to contain only one nucleotide mutation from thymine to cytosine. This corresponds to the amino acid mutation Leucine to Proline (L132P), which is common to both the V and P protein (Figure 5.8). This amino acid mutation was then mapped to the wild type V protein structure, which highlights that this mutation occurs in the centre of an alpha helix (Figure 5.9). In summary, one potentially IFN-sensitive mutant virus was isolated from a stock of PIV5 W3 and this was shown to contain one mutation within the V and P proteins. Logically, further optimisation of the method would be required to obtain more mutants, for example, mutagenizing the original stock may increase the number of potentially IFN-sensitive mutant viruses present for isolation.

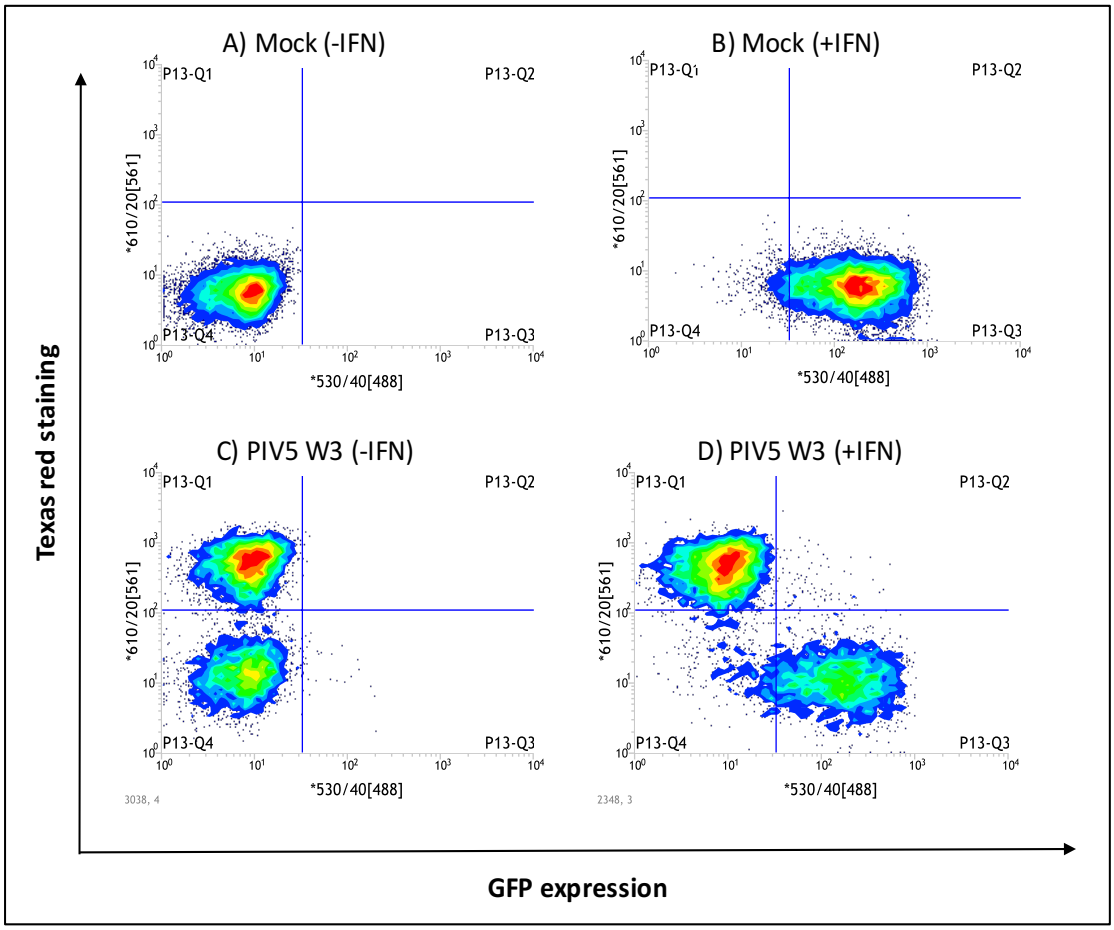

Figure 5.7: FACS analysis of PIV5 W3 virus. A549/pr(ISRE).GFP/ ISG56^{-}/ BVDV Npro cells were infected with PIV5 W3 virus at MOI 0.5 for 1h. Virus Inoculum was then removed, cells washed with PBS and incubated in SF media. After 6hours, a mixture of PIV5 anti-HN and anti-F neutralizing antibody was added to all samples and cells were treated with or without IFN as indicated (-/+IFN). After 24hours single cell suspensions were made from mock infected cells (panel A, -IFN), mock infected cells incubated in the presence of IFN (panel B, +IFN), PIV5 W3 infected cells (panel C, -IFN) and PIV5 W3 infected cells incubated in the presence of IFN (panel D, +IFN). Each sample was then subjected to FACS analysis. Cells from panel D P13-Q2 were then sorted into 96 well plates containing confluent monolayers of A549/pr(ISRE).GFP/ISG56^{-}/BVDV Npro cells. (Data representative of three independent repeats).

A

Nucleotide changes in V mRNA	Amino acid changes in V protein	Nucleotide changes in P mRNA	Amino acid changes in P protein
T395C	L132P	T395C	L132P

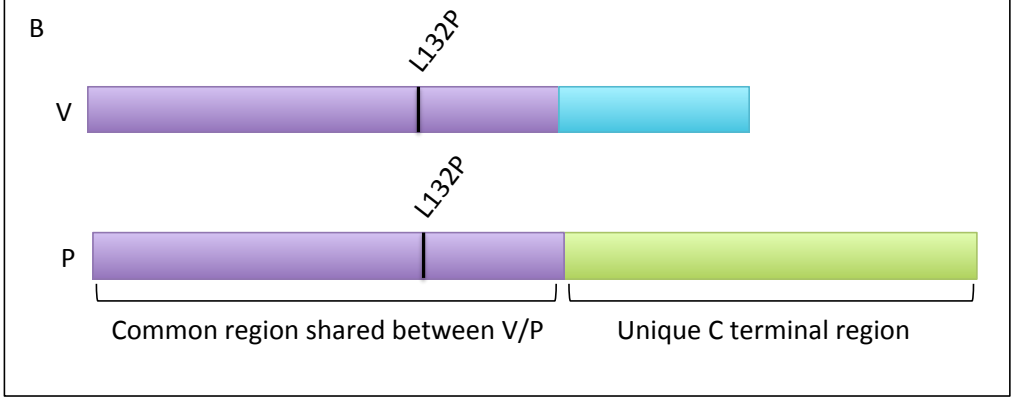

Figure 5.8: Mutations in V and P proteins of PIV5 W3-γ. A) Demonstrates the nucleotide and corresponding amino acid changes in the V and P genes/proteins of PIV5 W3-γ **B)** Illustrates the relative position of the amino acid mutation in the V and P proteins for PIV5 W3-γ

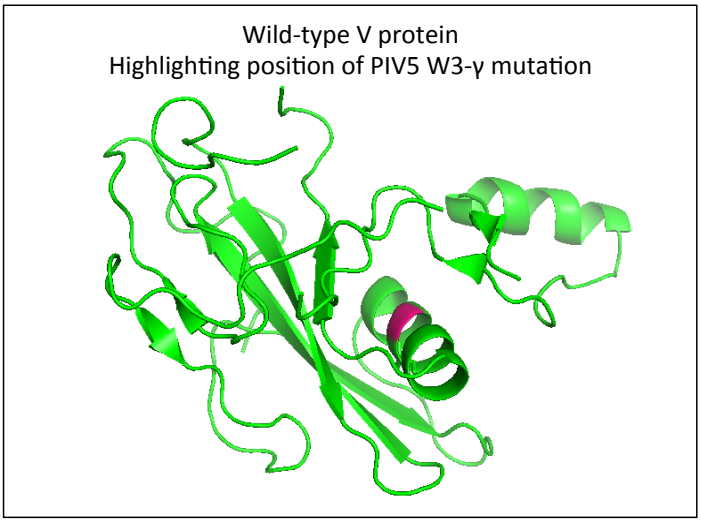

Figure 5.9: Mapping the position of amino acid mutation found in PIV5 W3-γ to wild-type V protein structure (Protein Data Bank accession number 2B5L). The structure of wild-type PIV5 W3 V protein is depicted with the positions of the PIV5 W3- γ mutation highlighted (structures adapted using PyMOL (Schrodinger)).

In conclusion, a total of three potentially IFN-sensitive mutant viruses, containing mutations within both the V and P proteins, were successfully isolated using our method, namely, rPIV5mCh-α, rPIV5mCh-β and PIV5 W3-γ. Specifically, rPIV5mCh-α and rPIV5mCh-β were isolated multiple times from rPIV5mCh and PIV5 W3-γ was isolated once from PIV5 W3. In the next chapter we further examine each of these mutant viruses to investigate a number of features including V protein function and sensitivity to IFN.

6 Chapter 6

6.1 Analysis of PIV5 mutants rPIV5mCh-α, rPIV5mCh-β and PIV5 W3-γ

6.1.1 Analysis of PIV5 mutants rPIV5mCh-α, rPIV5mCh-β and PIV5 W3-γ and ability to block IFN signalling

6.1.1.1 FACS analysis of mutant PIV5 viruses at different MOI

Following their isolation, mutant's rPIV5mCh-α, rPIV5mCh-β and PIV5 W3-γ were further analysed using several methods. Initially, we decided to investigate the interesting phenotype (attenuated mutant phenotype 2) seen during FACS analysis of the mutant rPIV5mCh-β. This mutant presented a distinctive 'smear' across the top two quadrants during FACS analysis as infected cells expressed varying intensities of GFP (Figure 5.3). As some of the infected cells were negative for GFP expression indicating that IFN signalling was blocked and some were positive for GFP indicating that IFN signalling was active it was hypothesised that the mutant V protein of rPIV5mCh-β may be partially functional. Consequently, it was predicted that this mutant might respond differently at different MOI's. Here we sought to analyse this further by comparing each of the mutants by FACS analysis following infection at different MOI.

Specifically, A549/pr(ISRE).GFP/ISG56-/BVDV Npro cells were infected with rPIV5mCh, rPIV5mCh-α, rPIV5mCh-β, PIV5 W3 and PIV5 W3-γ at MOI 0.1, 1, 5 or 10 for 1hour. Six hours post infection IFN and PIV5 anti-HN and anti-F monoclonal antibodies were added to induce GFP expression and to inactivate progeny virus, respectively. Cells were then immunostained for PIV5 HN if

required (PIV5 W3 and PIV5 W3-γ) and then prepared as single cell suspensions for FACS analysis. As before, mCherry expression or Texas red staining combined with GFP expression indicates that the infecting virus is unable to block the IFN response.

The results show that increasing the MOI of wild type rPIV5mCh or PIV5 W3 increased the number of cells that were mCherry positive only, reiterating that these wild-type viruses can block IFN signaling (Figure 6.1). In contrast, increasing the MOI of the mutants rPIV5mCh-α and PIV5 W3-γ increased the number of mCherry and GFP positive cells, reiterating that these viruses are potentially IFN-sensitive as they cannot block IFN-signalling. Conversely, rPIV5mCh-β infection presented an interesting result. At low MOI of rPIV5mCh-β infection the majority of infected cells are also GFP positive, thus indicating that at low MOI this virus cannot block IFN-signalling. However, as MOI increases it appears that the ability to block IFN-signalling also increases. At MOI 1 this creates a 'smear' of infected cells (as seen previously) each expressing varying intensities of GFP. At MOI 10 the majority of infected cells are GFP negative, thus indicating that at high MOI this virus can block IFN-signalling. One explanation for this is that rPIV5mCh-β has at least a partially functional V protein as at a higher MOI the increase in abundance of partially functional V protein may overcome the IFN signalling pathway leading to an increased block of GFP expression, however, further investigation into V protein functionality would be required to determine if this was the case. Subsequently we sought to specifically analyse the V protein activity of each mutant using a number of assays.

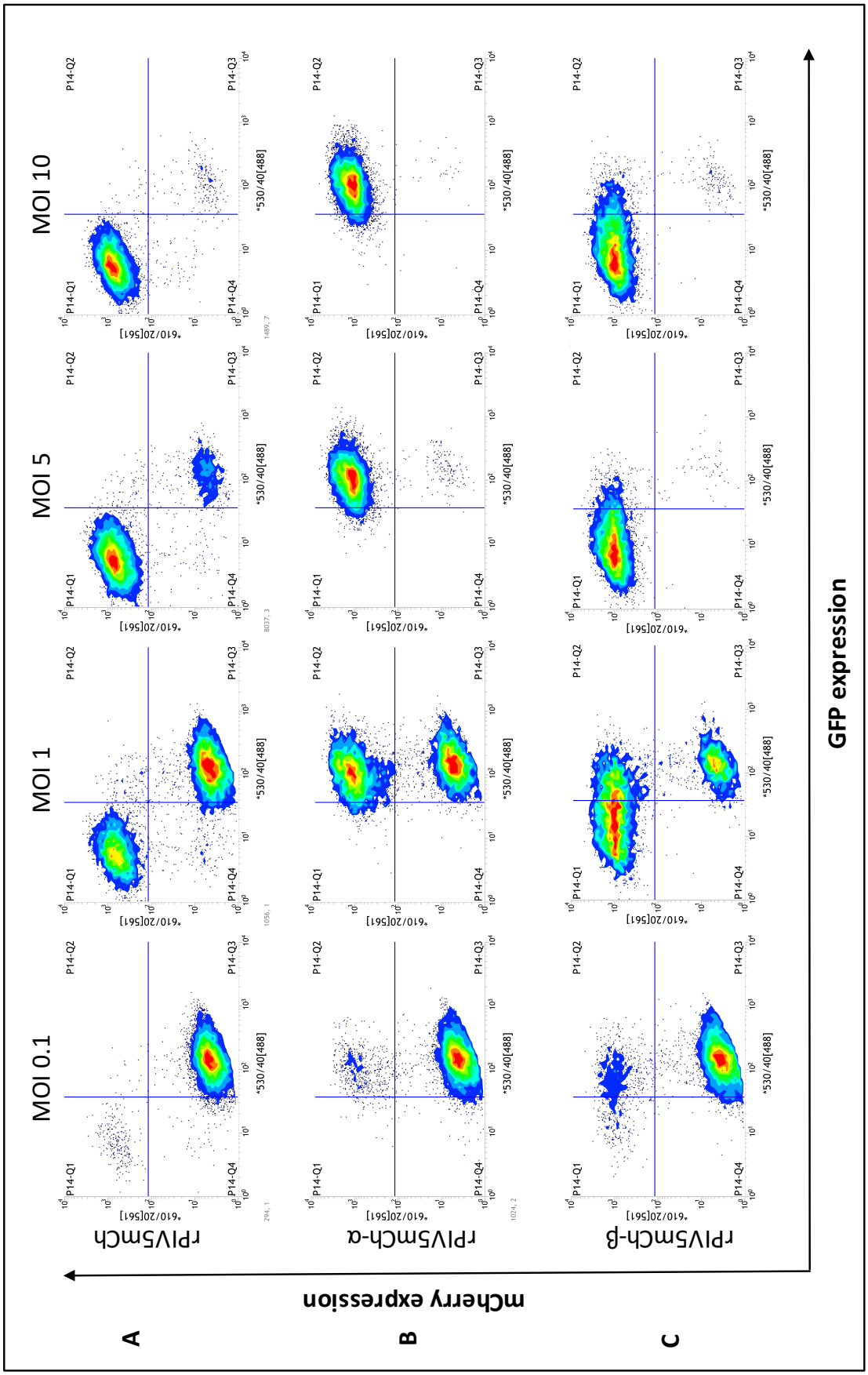
MOI 0.1
MOI 1
MOI 5
MOI 10
rPIV5mCh
rPIV5mCh-α
rPIV5mCh-β
A
B
C
mCherry expression
GFP expression
P14-Q1
P14-Q2
P14-Q3
P14-Q4
*610/20[561]
*530/40[488]

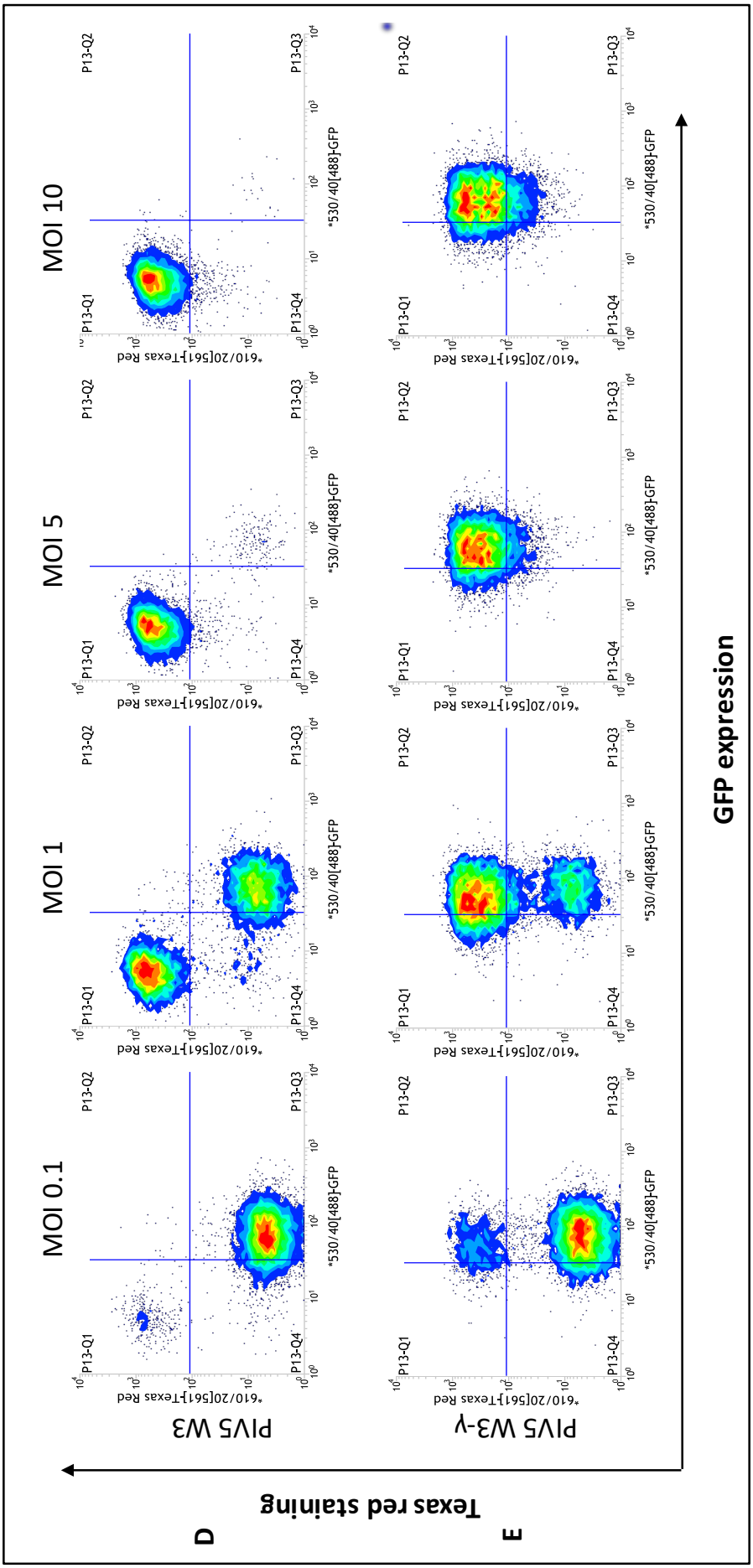
MOI 10
MOI 5
MOI 1
MOI 0.1
PIV5 W3
PIV5 W3-γ
D
E
Texas red staining
GFP expression
P13-Q1
P13-Q2
P13-Q3
P13-Q4
*610/20[561]-Texas Red
*530/40[488]-GFP

Figure 6.1: FACS analysis of isolated PIV5 mutants at different MOI. A549/pr(ISRE).GFP/ ISG56-/ BVDV Npro cells were infected at MOI 0.1, 1, 5 or 10 for 1hour with rPIV5mCh (A), rPIV5mCh-α (B), rPIV5mCh-β (C), PIV5 W3 (D) and PIV5 W3-γ (E). 6 hours post infection IFN and anti-HN antibody was added, respectively. Samples were then collected as single cell suspensions and analysed by FACS analysis.

6.1.1.2 Analysis of mutant V protein ability to cause STAT1 degradation

Initially, we set out to examine the mutant V proteins ability to target STAT1 for proteasome-mediated degradation. Previously, it has been shown that the wild-type V protein of PIV5 can hijack the DDB1-Cul4A-Roc1 E3 ligase complex to target STAT1 for proteasome-mediated degradation, thus preventing activation of the IFN signalling pathway (Didcock et al. 1999; Li et al. 2006). To determine mutant V protein function, we analysed STAT1 expression by western blot following infection by each of mutant PIV5 viruses. Specifically, A549: naïve cells were mock infected or infected with the control viruses PIV5 W3, rPIV5mCh, PIV5 CPI- and the mutant viruses rPIV5mCh-α, PIV5mCh-β and PIV5 W3-γ at MOI 10 followed by treatment with or without IFN for 16hours (to induce STAT1 expression) before collection and analysis via western blot.

Importantly, the positive control samples demonstrate that infection with the wild-type viruses rPIV5mCh and PIV5 W3, which both contain a functional V protein, both lead to the degradation of STAT1. In addition, the negative control demonstrates that infection with the IFN-sensitive virus PIV5 CPI- that does not contain a functional V protein does not lead to the degradation of STAT1.

Interestingly, the experimental results demonstrate that infection with the mutant's rPIV5mCh-α and PIV5 W3-γ did not lead to degradation of STAT1 (Figure 6.2). Furthermore, the same levels of STAT1 were expressed following infection with these mutants as was seen following infection with the IFN-sensitive virus PIV5 CPI-, thus indicating that the V protein of these mutants is non-functional. By contrast, infection with the mutant rPIV5mCh-β did lead to the degradation of STAT1 to the same extent as the wildtype viruses' rPIV5mCh and PIV5 W3, thus indicating that the V protein of this mutant is fully functional with regards to blocking the IFN signaling pathway. This disagrees with our initial hypothesis that rPIV5mCh-β V protein was partially functional. Next we decided to specifically analyse V protein function independent of virus infection.

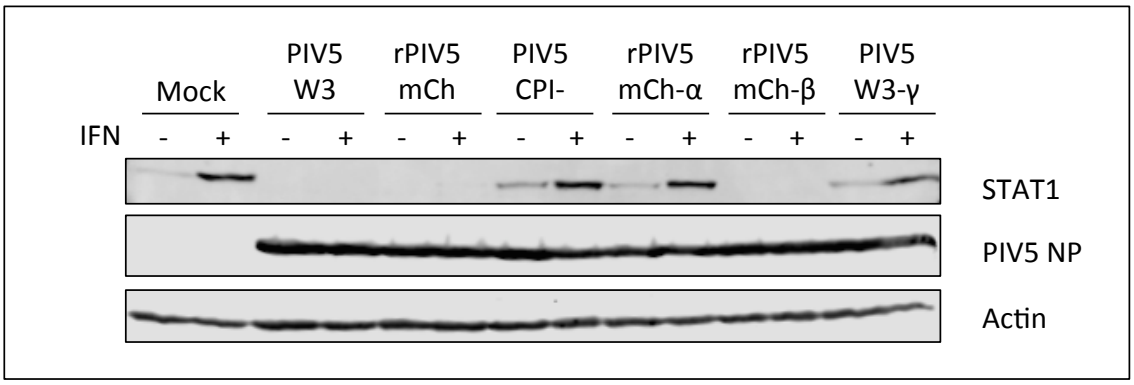

Figure 6.2: Analysis of STAT1 expression following infection by isolated PIV5 mutant viruses. A549: naïve cells were mock infected or infected with the control viruses PIV5 W3, rPIV5mCh, PIV5 CPI- and the mutant viruses rPIV5mCh-α, PIV5mCh-β and PIV5 W3-γ at MOI 10 for 12 hours, followed by a 16 hour IFN treatment to induce STAT1 expression before collection in disruption buffer and analysis via western blot for STAT1, PIV5 NP and Actin.

6.1.1.3 Analysis of mutant V protein activity independent of virus infection

To analyse V protein activity independent of virus infection, the V protein from each mutant was cloned into the expression vector pcDNA3.1(-). This expression vector could then be used in both an IFN signalling and an IFN induction luciferase reporter assay to determine V protein activity against each of these pathways.

6.1.1.3.1 IFN signalling luciferase reporter assay to analyse mutant V protein function

Initially, an IFN signalling luciferase reporter assay was used to determine if the mutant V proteins could block IFN signalling in a similar manner to the wild-type V protein. Briefly this assay required transfection of each mutant V protein alongside a reporter plasmid containing firefly luciferase under the control of an ISRE. As stated previously this element is found within the promoters of numerous ISGs and is triggered following activation of the IFN signalling pathway by addition of IFN. Hence, treatment of the cells with IFN following transfection with this plasmid would result in luciferase expression and indicates that the IFN signalling pathway is intact. Consequently, mutant V protein activity can then be analysed by its ability to block luciferase expression.

Specifically, each mutant V protein plasmid was transfected (with the exception of the control sample which was set up in the absence of a V protein expressing plasmid) into 293T cells in combination with two plasmids that expressed i) firefly luciferase under the control of four tandem repeat sequences of the ISRE from the IFN-inducible gene 9-27 and ii) β-galactosidase, which was used as a transfection control to determine transfection efficiency. At 48h post

transfection the media was then supplemented with IFN (+IFN) to activate luciferase expression or left untreated (-IFN). After 6h the cells were lysed in buffer and the luciferase activity was measured and normalised to β-galactosidase activity. Relative luciferase activity was then graphed using GraphPad Prism 6 (-/+ Standard Deviation) and is demonstrated in Figure 6.3.

Importantly, the control sample, excluding the V protein expressing plasmid, demonstrated that luciferase is produced following IFN treatment. Furthermore, the positive control, expressing wild-type V protein, demonstrated that an active V protein blocks expression of luciferase following IFN treatment. Interestingly, the experimental results showed that expression of the mutant V proteins of rPIV5mCh-α and PIV5 W3-γ did not block expression of luciferase in the presence of IFN, thus reiterating our previous analysis that the V proteins of these two mutants cannot block the IFN signalling pathway. On the other hand, expression of the mutant rPIV5mCh-β V protein blocked the expression of luciferase to a similar level as the Wild-type V protein, thus reiterating that the mutant rPIV5mCh-β V protein can block IFN signalling.

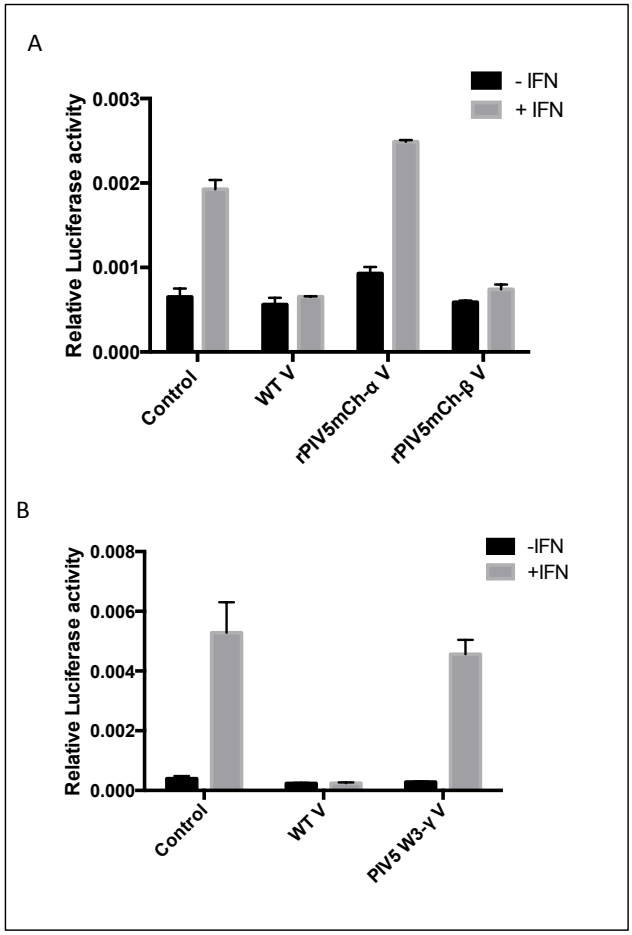

Figure 6.3: Analysis of mutant V proteins ability to block the IFN signalling pathway using an IFN signalling luciferase reporter assay. 293T cells were transfected in triplicate with (A) plasmids expressing wildtype (WT), rPIV5mCh-α and rPIV5mCh-β V protein and (B) plasmids expressing WT and PIV5 W3-γ V protein with the exception of the control sample. Each sample was also transfected with two other plasmids, one that expresses firefly luciferase under the control of an ISRE and another that expresses β-galactosidase. At 48h post transfection the media was supplemented with IFN to activate luciferase expression (+IFN) or left untreated (-IFN). After 6h the cells were lysed in buffer and the luciferase activity measured and normalised to β-galactosidase activity. Relative luciferase activity was then graphed using GraphPad Prism 6 (mean -/+ Standard Deviation; Data representative of three independent repeats)

6.1.1.3.2 IFN induction luciferase reporter assay to analyse mutant V protein function.

Next we sought to determine the mutant V proteins ability to block IFN induction using an IFNβ induction luciferase reporter assay. In addition to blocking the IFN signalling pathway, previous research has shown that the wild-type V protein also interacts with Mda5 to block the IFN induction pathway (Andrejeva et al. 2004). This second luciferase reporter assay therefore sought to determine if the mutant V proteins could inhibit the IFN induction pathway in a similar manner to the wild-type V protein. Briefly this assay required transfection of each of the mutant V proteins in combination with a plasmid expressing firefly luciferase under the control of the IFN promoter and a plasmid that expressed Mda5. Previous work has demonstrated that over expression of Mda5 and other signalling intermediates activates IFN induction (Andrejeva et al. 2004), therefore, overexpression of Mda5 was used here to trigger activation of the IFN promoter and subsequent luciferase expression, thus demonstrating an intact IFN induction pathway. Consequently, mutant V protein activity would then be analysed by its ability to block luciferase expression. Specifically, each mutant V protein plasmid was transfected into 293T cells in combination with three plasmids that expressed i) firefly luciferase under the control of the IFNβ promoter, ii) Mda5 and iii) β-galactosidase, which was used to determine transfection efficiency. Notably a negative control (excluding the V protein and Mda5 expressing plasmids) and a positive control (excluding the V protein) were also set up. At 48h post transfection the cells were then lysed in buffer and the luciferase activity measured and normalised to β-galactosidase activity. Relative

luciferase activity was then graphed using GraphPad Prism 6 (mean -/+ Standard Deviation) and is demonstrated in Figure 6.4.

Importantly, the negative and positive control demonstrated that Mda5 expression results in luciferase expression via activation of the IFN signalling pathway. Furthermore, expression of the wild-type V protein demonstrated that luciferase expression is blocked in the presence of an active V protein. Interestingly, the experimental results show that expression of each of the mutant V proteins blocked luciferase expression comparable to the wild-type V protein. Thus indicating that all mutant V proteins have retained the ability to block the IFN induction pathway irrespective of their activity against the IFN signalling pathway.

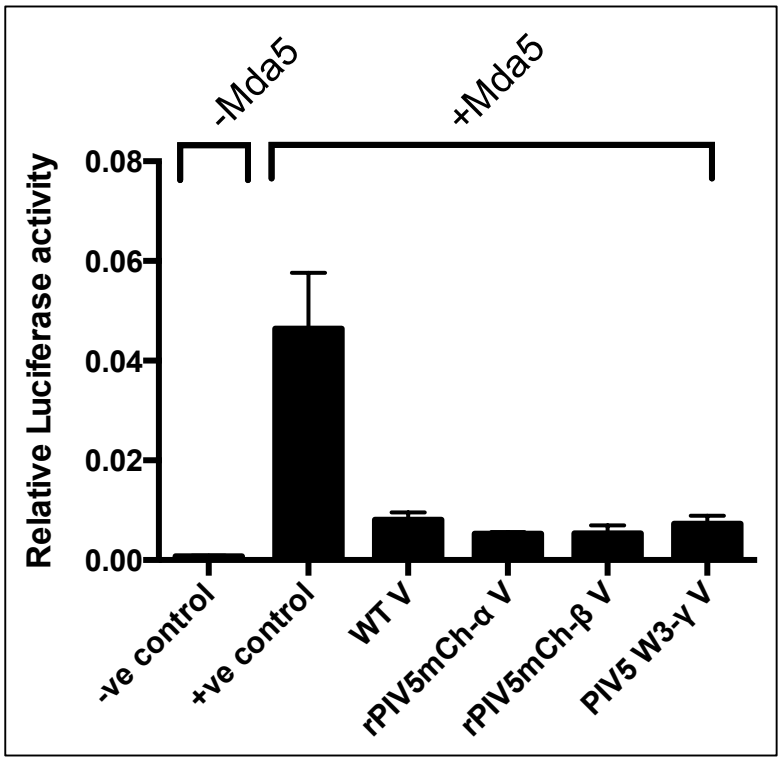

Figure 6.4: Analysis of mutant V protein ability to block IFN induction via an IFN induction luciferase reporter assay. 293T cells were transfected in triplicate with plasmids expressing wildtype (WT), rPIV5mCh-α, rPIV5mCh-β and PIV5 W3-γ V protein in combination with two other plasmids that express i) firefly luciferase under the control of the IFNβ promoter and ii) β-galactosidase (with the exception of the negative (–ve) and positive (+ve) control which were both set up in the absence of a V expressing protein). Finally, a third plasmid that expresses Mda5 was also transfected to the samples as indicated (-/+ Mda5) to activate the IFN induction pathway and subsequent luciferase expression. At 48h post transfection the cells were lysed in buffer and the luciferase activity measured and normalised to β-galactosidase activity. Relative luciferase activity was then graphed using GraphPad Prism 6 (mean -/+ Standard Deviation; Data representative of three independent repeats)

In conclusion, we set out to examine the activity of the mutant V proteins found within each mutant PIV5 virus. Interestingly, the results have determined that rPIV5mCH-α and PIV5 W3-γ mutant V proteins have lost the ability to block the IFN signalling pathway however they have retained the ability to block the IFN induction pathway. Furthermore, despite initially hypothesizing that rPIV5mCh-β contained a partially functional mutant V protein the results have shown that rPIV5mCh-β remains functional and can block both the IFN induction and signalling pathways in a similar manner to the wild-type V protein. Now that we had established V protein activity in the IFN induction and IFN signalling pathways, next we examined each mutant's sensitivity to IFN by comparing their viral growth in the presence and absence of an active IFN response.

6.1.2 Analysis of IFN sensitivity of PIV5 mutant viruses.

Now that we had established IFN antagonist activity, next we wanted to examine each mutant's sensitivity to IFN. Previously we have demonstrated that the IFN inhibitor, Rux, can block the IFN signalling pathway and subsequently increase the growth of IFN-sensitive viruses. Consequently, we used this drug to compare growth of each of the mutant viruses in the presence and absence of an active IFN response using both plaque assays and multistep viral growth curves.

6.1.2.1 Comparison of plaque development of PIV5 mutant viruses in the presence and absence of an active IFN response.

To determine the IFN sensitivity of each mutant virus we examined plaque development of each mutant in the presence and absence of an active IFN response. Specifically, we compared plaque development of each virus in A549 naïve cells -/+ Rux and in Vero cells (which do not contain an intact IFN response) (Figure 6.5).

The results demonstrate that in A549: naive cells in the absence of Rux the wild-type viruses rPIV5mCh and PIV5 W3 produced small plaques. Also note that rPIV5mCh plaques were of varied size indicating a heterogeneous population. In contrast, rPIV5mCh-α did not produce any visible plaques and PIV5 W3-γ produced plaques that are slightly smaller than the wild-type virus, PIV5 W3, thus indicating that the mutant virus is more sensitive to an active IFN response. Furthermore, rPIV5mCh-β produced plaques similar in size to the wild-type virus thus indicating that this virus is not sensitive to an active IFN response. In A549: naive cells in the presence of Rux, the plaque size of all viruses was

increased compared to that seen in the absence of Rux, with the greatest increases demonstrated by each of the mutant viruses. Interestingly, rPIV5mCh-α and rPIV5mCh-β appeared to produce larger plaques than the wild-type virus in A549 naïve cells in the presence of Rux, a similar trend although less obvious also appeared for rPIV5mCh-α in Vero cells. We therefore quantified the plaque size of rPIV5mCh-α and rPIV5mCh-β and compared this to the wild-type virus rPIV5mCh in each condition (Figure 6.6). Plaque size was measured using PixelStick and normalised to rPIV5mCh. Significance was then determined using an unpaired T test. This indicated that there was a significant increase in plaque size for both rPIV5mCh-α ($P < 0.0001$) and rPIV5mCh-β ($P = 0.0002$) viruses compared to the wild-type virus in A549 naïve cells in the presence of Rux. Furthermore, there was a small but significant increase ($P=0.0484$) in rPIV5-mCh-α plaque size compared to the wild-type virus in Vero cells**.** Interestingly, this could indicate that these mutant viruses and particularly rPIV5mCh-α had a growth advantage in IFN incompetent cells compared to the wild-type virus. In summary, this data indicates that rPIV5mCh-α and PIV5 W3-γ, which do not contain a functional V protein, are sensitive to IFN. Conversely, it appears that rPIV5mCh-β, which contains a functional V protein, is not.

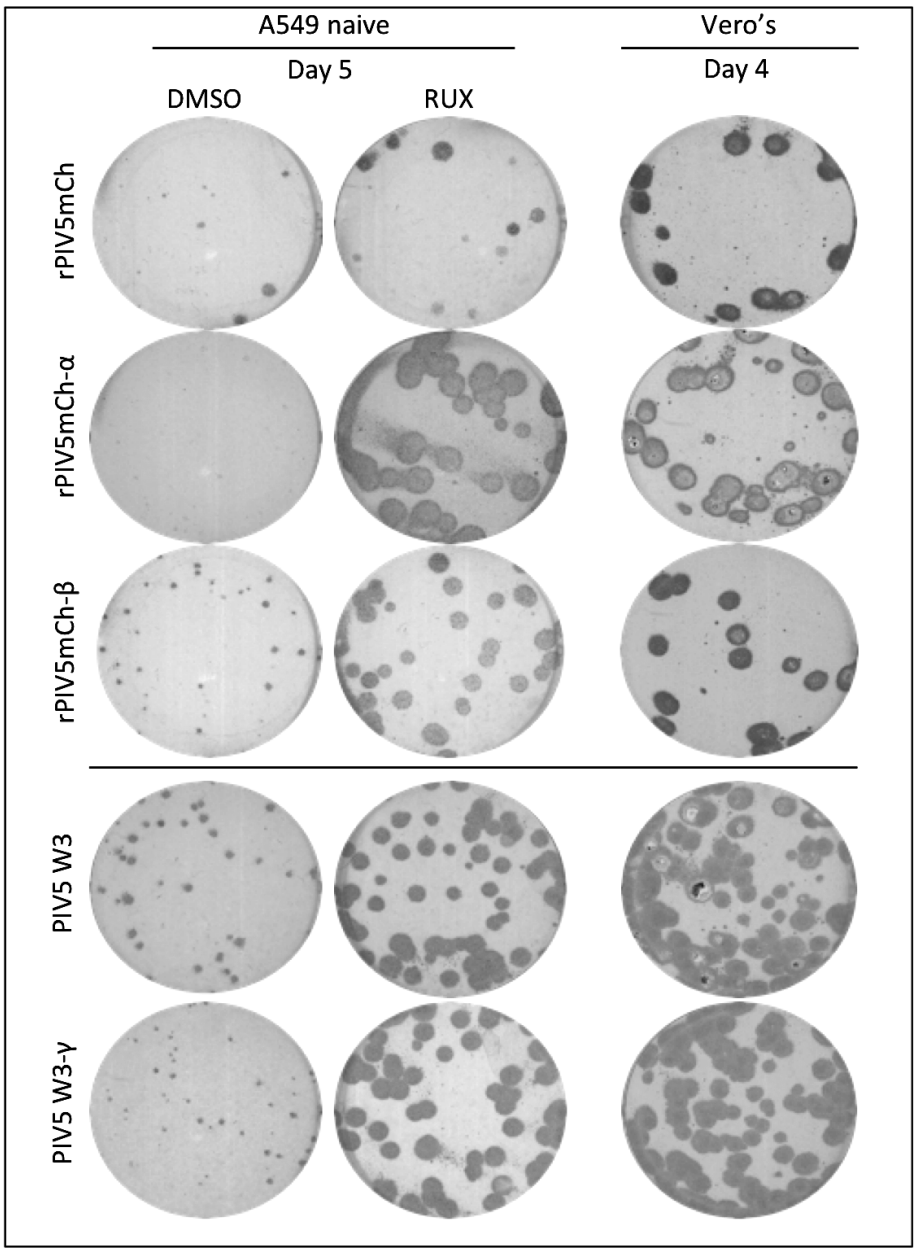

Figure 6.5: Comparison of mutant virus plaque development in A549 naïve -/+ Rux and Vero cells. Each virus (rPIV5mCh, rPIV5mCh-α, rPIV5mCh-β, PIV5 W3 and PIV5 W3-γ) was incubated in A549 naïve or Vero cells for 1hour before removal of the inoculum, PBS wash and addition of avicell plaque assay overlay with 4μM Rux treatment or equivalent volume DMSO. Plaques were fixed at the day indicated and immunostained using antibodies against PIV5 NP and HN. (Data representative of three independent repeats).

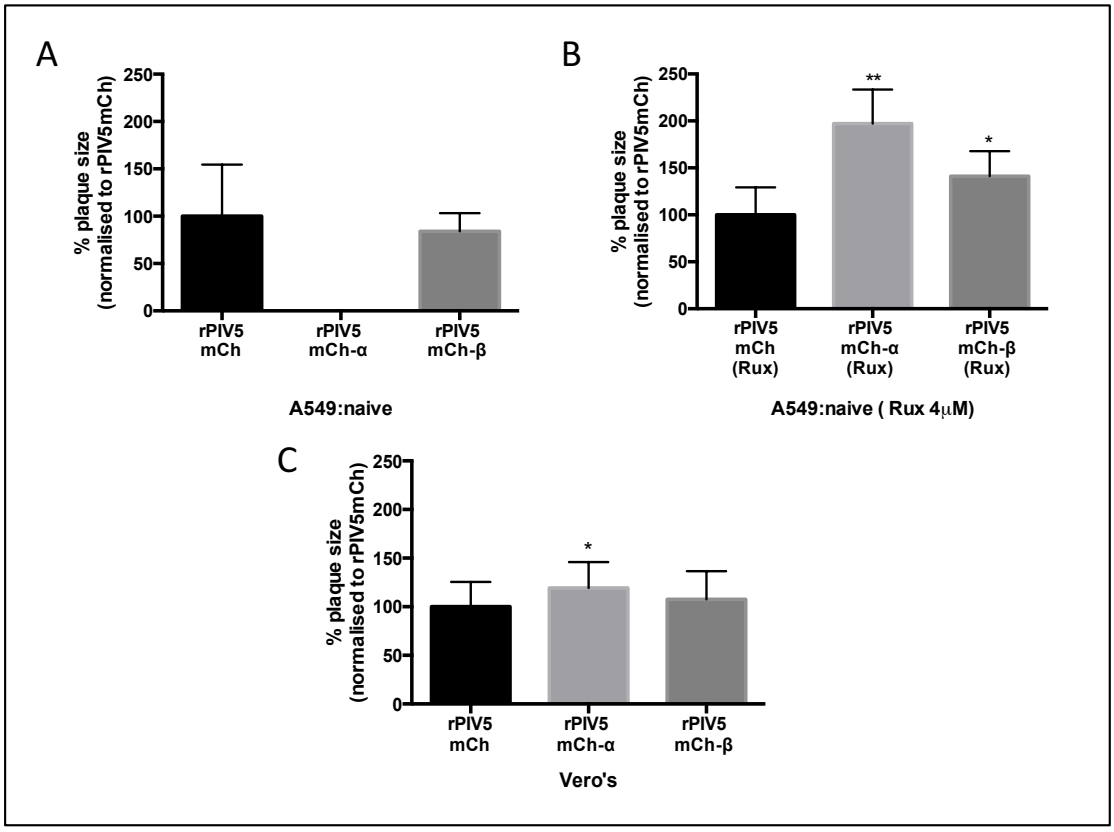

Figure 6.6: Quantification of virus plaque size. Percentage (%) plaque size of mutant virus grown in A549 naïve -/+ Rux and Vero cells is represented in A, B and C, respectively. Plaque size was measured using Pixelstick and normalised to rPIV5mCh in each case. Significance was then analysed using an unpaired T test comparing each mutant to rPIV5mCh (For A549:naïve (Rux 4μM) *P= 0.0002, ** P < 0.0001, for Vero cells *P=0.0484).

6.1.2.2 Analysis of PIV5 mutant virus growth in the presence and absence of an active IFN response using a multistep viral growth curve

In addition to plaque analysis, the IFN sensitivity of each mutant virus was also examined using a multistep viral growth curve. Specifically, we compared the growth of each mutant virus in A549 naïve cells in the presence and absence of Rux (Figure 6.7). The results demonstrate that in the absence of Rux both rPIV5mCh-α and rPIV5mCh-γ viral titers are approximately 1.5 logs lower than their respective wild-type viruses, rPIV5mCh and PIV5 W3, at 48 hours post infection. By contrast, in the presence of Rux rPIV5mCh-α and rPIV5mCh-γ viral titers increase to the same level as their respective wild-type viruses, thus reiterating that both rPIV5mCh-α and rPIV5mCh-γ are sensitive to IFN. Conversely, in the presence and absence of an intact IFN response rPIV5mCh-β reaches a high titer similar to the wildtype virus thus reiterating that this virus is not sensitive to IFN. Surprisingly the growth of the mutant viruses rPIV5mCh-α and rPIV5mCh-β was very similar to their respective wildtype viruses in A549 naïve cells in the presence of Rux. This was in contrast to the increased growth of rPIV5mCh-α and rPIV5mCh-β seen in the previous plaque assay and possible reasons for this are discussed later.

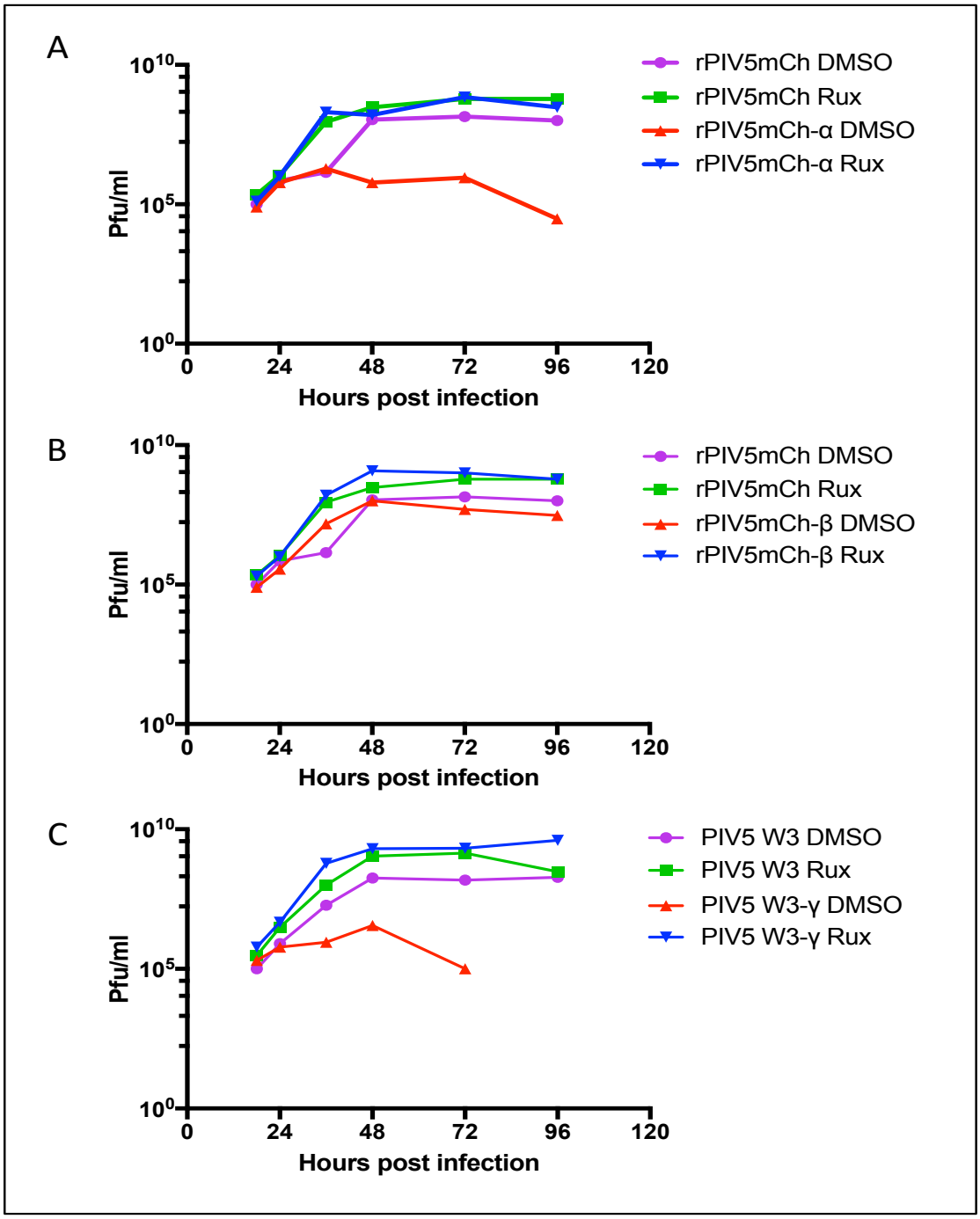

Figure 6.7: Multistep viral growth curve analysis of PIV5 mutants. A549: naïve cells were infected with **A)** rPIV5mCh and rPIV5mCh-α, **B)** rPIV5mCh and rPIV5mCh-β and **C)** PIV5 W3 and PIV5 W3-γ and incubated -/+ 4μM Rux or equivalent volume of DMSO. Samples were then taken at numerous timepoints and titered on Vero cells. (Data representative of three independent repeats with a lower limit of detection of 1x 10^3 PFU/ml).

In conclusion, we set out to analyse the IFN sensitivity of each mutant. The results demonstrate that the mutant viruses containing non-functional V proteins, rPIV5mCh-α and PIV5 W3-γ, are sensitive to IFN. This is demonstrated in both the plaque assay and viral growth curve as growth is attenuated compared to wild-type virus growth in the presence of an intact IFN response. Furthermore, there is a large increase in growth in the absence of an intact IFN response. By contrast, growth of rPIV5mCh-β, which contains a functional V protein, is not sensitive to IFN. This is demonstrated by both the plaque assay and viral growth curve, as the virus is able to grow in the presence of an intact IFN response and this growth is increased in the absence of an intact IFN response in a similar manner to the wild-type virus. Following confirmation that both rPIV5mCh-α and PIV5 W3-γ cannot block the IFN response and are therefore sensitive to IFN, we focused our studies to further examine these two IFN-sensitive mutants.

6.1.3 Further analysis of the IFN-sensitive mutant viruses rPIV5mCh-α and PIV5 W3-γ

Following confirmation that the both rPIV5mCh-α and PIV5 W3-γ cannot block the IFN response and are therefore sensitive to IFN, we set out to further examine these two IFN-sensitive mutants. Initially we set out to examine each mutant V protein by examining if the mutations within the V protein could easily revert to regain the ability to block the IFN response. Secondly, we wanted to examine two features noted during previous analysis of the viruses in the presence and absence of an intact IFN response. Firstly, that rPIV5mCh-α had increased fusogenicity compared to the wild-type virus in the absence of an intact IFN response and secondly that both rPIV5mCh-α and PIV5 W3-γ induced greater levels of apoptosis compared to the wild-type virus in the presence of an intact IFN response.

6.1.3.1 Analysis of the ability of the IFN-sensitive mutant viruses to regain V protein function

To assess the ability of the IFN-sensitive mutants to regain V protein function, we analysed rPIV5mCh-α and PIV5 W3-γ infected IFN competent A549/pr(ISRE).GFP cells. As these cells have an intact IFN response this may push the virus to select mutations that regain the ability to block IFN signalling. Following IFN treatment, each of these samples was analysed by FACS and cells infected with virus that could potentially block IFN signalling (mCherry/Texas Red positive and GFP negative cells) were selected. Selected single cells were then sorted into 1x96 well plate containing A549/pr(ISRE).GFP cells and incubated for 3-4 days to allow virus amplification for further analysis. Each of the monolayers was then analysed by fluorescent microscopy following IFN

treatment to assess the ability of the infecting virus to block IFN signalling. Specifically, 5 viruses displayed the wild-type phenotype (mCherry/Texas Red positive and GFP negative) following selection from PIV5 W3-γ infected cells however no viruses displayed the wild-type phenotype following selection from rPIV5mCh-α infected cells. The V/P gene of the 5 PIV5 W3-γ selected viruses was then sequenced to analyse for reversion to wild-type sequence or compensatory mutations that allow the V protein to regain function. This identified that all 5 selected viruses had reverted to wild-type demonstrating that the single mutation L132P contained in PIV5 W3-γ V protein could easily revert to wild-type to regain the ability to block IFN signalling.

In addition to FACS analysis and selection, we also passaged each virus in IFN competent A549:pr(ISRE).GFP cells for 60 days and then reassessed the population for regain of V protein function using FACS analysis (Figure 6.8). The results demonstrated that following 60 days there were few rPIV5mCh-α virus infected cells and those infected were still unable to block the IFN signalling pathway suggesting that the virus had been unable to regain V protein function. By contrast there was a large population of PIV5 W3-γ infected cells that were unable to block the IFN signalling pathway however there was also a new population of infected cells which could block the IFN signalling pathway. Cells from this population were sorted into 1x96 well plate containing A549/pr(ISRE).GFP cells. The monolayers were then incubated for 3-4 days to allow the virus to propagate and then analysed by fluorescent microscopy following IFN treatment for ability to block IFN signalling. Ten viruses displaying the wild-type phenotype (mCherry/Texas Red positive and GFP positive) were

then selected for sequencing of the V/P gene. As expected, the results identified that each of the viruses' had reverted to the wild-type V protein sequence. In summary, the results highlight that the numerous mutations within the V protein of rPIV5mCh-α are difficult to revert in combination however the single mutation (L132P) contained within PIV5 W3-γ is easily reverted.

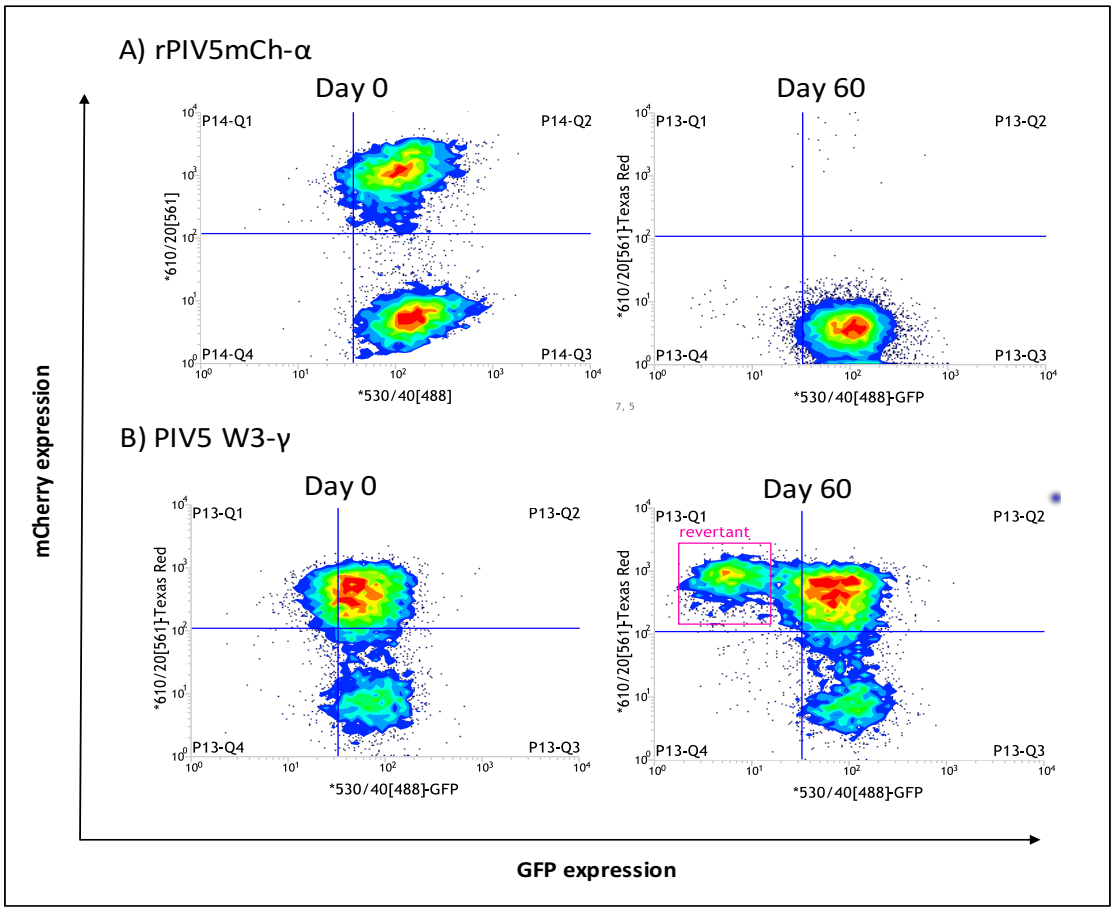

Figure 6.8: rPIV5mCh-α and PIV5 W3-γ serial passage. rPIV5mCh-α (panel A) and PIV5 W3-γ (panel B) infected cells were prepared as single cell suspensions, following IFN treatment, at Day 0 and Day 60 following passage in IFN competent A549:pr(ISRE).GFP, and examined by FACS analysis.

6.1.3.2 Analysis of IFN-sensitive mutant virus fusogenicity in Vero cells

Notably, the wild-type viruses PIV5 W3 and rPIV5mCh are characteristically non-fusogenic during infection however during previous analysis, it was noted that rPIV5mCh-α is highly fusogenic in Vero cells and A549 naïve cells in the presence of Rux but not in A549 naïve cells. To analyse this further we applied DAPI staining to Vero cells following infection with each of the IFN-sensitive mutants to examine the fusogenicity of each virus (Figure 6.9). The results demonstrate that rPIV5mCh-α was highly fusogenic in cells without an intact IFN response compared to the wild-type virus. Furthermore, PIV5 W3-γ demonstrated small patches of fusion but it could not be stated that this was significantly more fusogenic than the wildtype virus. In summary, this indicates that IFN-sensitive virus, rPIV5mCh-α is highly fusogenic compared to the wild-type virus in the absence of an intact IFN response.

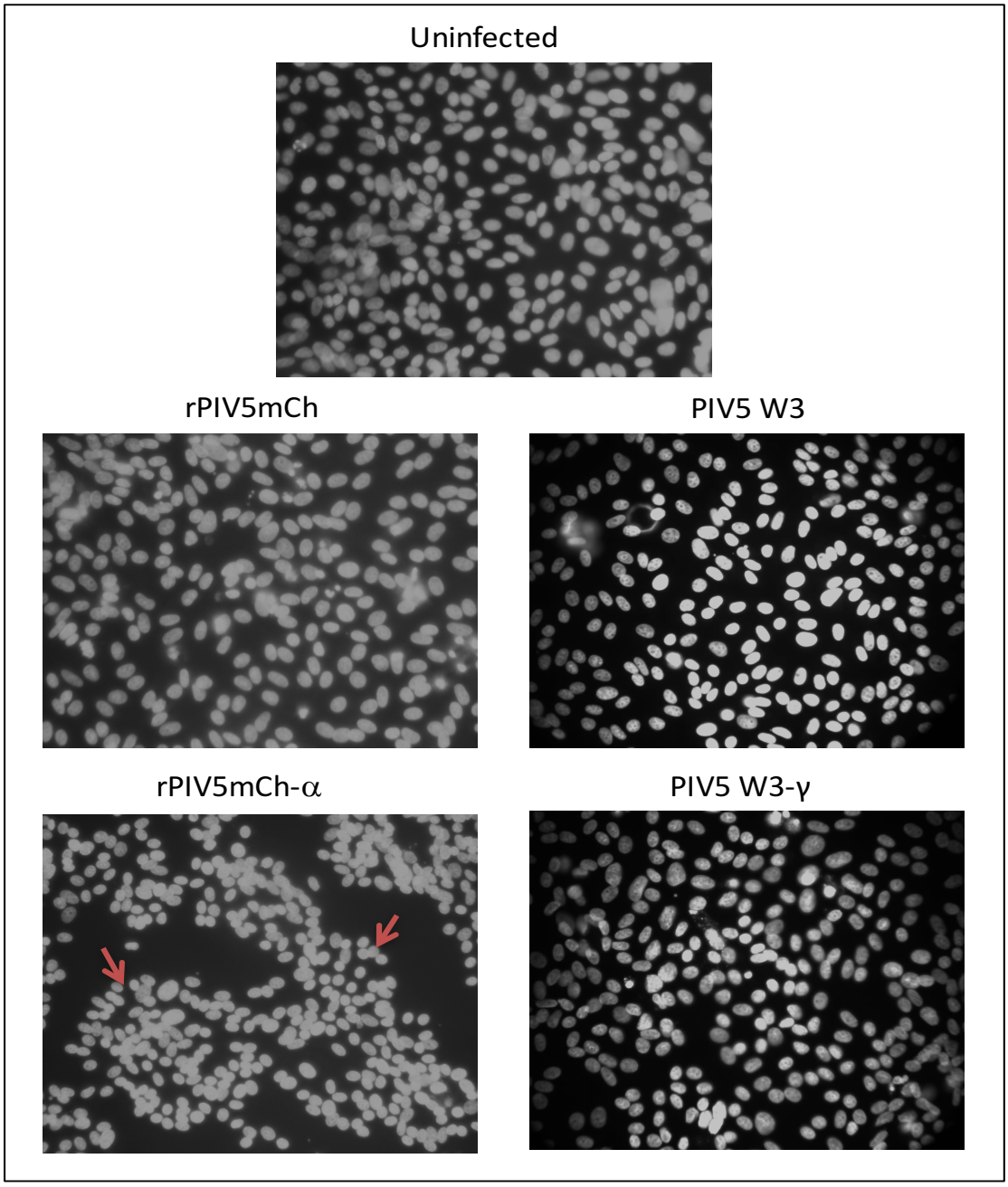

Figure 6.9: Analysis of mutant fusogenicity. Vero cells seeded onto coverslips were mock infected or infected with rPIV5mCh, PIV5 W3, PIV5mCh-α and PIV5 W3-γ at MOI 10 for 1 hour before replacement of the virus inoculum with serum-free DMEM and incubation for 48hours. Cells were then stained using DAPI and mounted onto glass slides before analysis by fluorescent microscopy (10x Magnification). (Data representative of two independent repeats).

6.1.3.3 Analysis of the induction of apoptosis by the IFN-sensitive mutants rPIV5mCh-α and rPIV5mCh-γ in A549 naïve cells -/+ Rux

Characteristically the wild-type viruses PIV5 W3 and rPIV5mCh do not trigger apoptosis following infection. However, during previous analysis it was noted that both rPIV5mCh-α and rPIV5mCh-γ induced an increased apoptotic response compared to the wild-type virus in A549 naïve cells whereas this response was abrogated in cells without an intact IFN response (A549 naïve cells in the presence of Rux and Vero cells). To investigate this further, we applied DAPI staining to IFN competent A549 naïve cells -/+ Rux following infection with each of the mutant viruses to examine for apoptotic cells (Figure 6.10). The results show that rPIV5mCh-α and rPIV5mCh-γ demonstrate an increased number of apoptotic nuclei during infection of A549 naïve cells however this is abrogated in the presence of the IFN inhibitor Rux. In summary, this indicates that there is an increase in induction of apoptosis following infection of IFN competent cells with the IFN-sensitive mutants rPIV5mCh-α and rPIV5mCh-γ infection, which is negated in the absence of an intact IFN response.

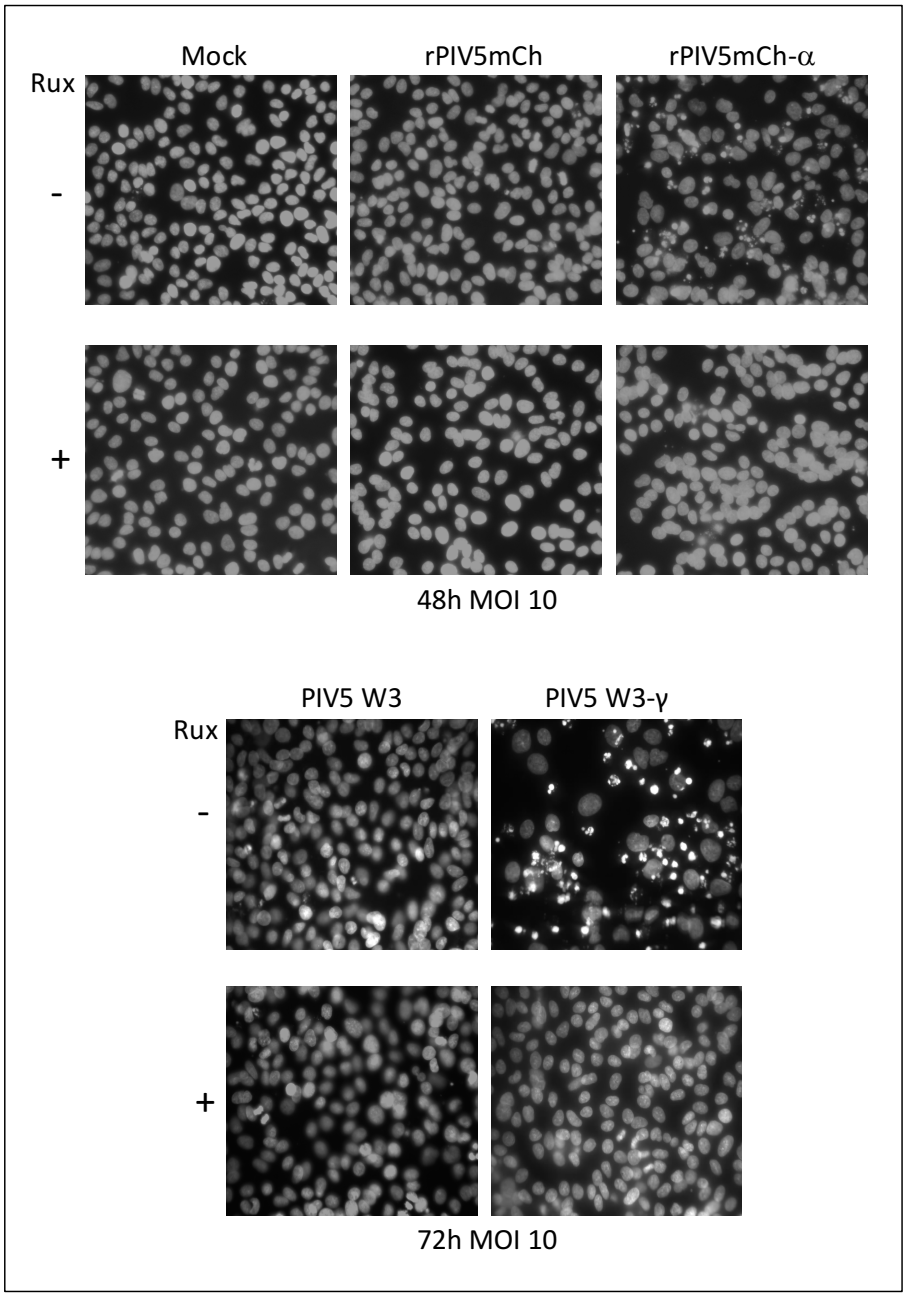

Figure 6.10: Analysis of apoptosis following mutant virus infection. A549 naïve cells seeded onto coverslips were infected with rPIV5mCh, PIV5 W3, PIV5mCh-α and PIV5 W3-γ at MOI 10 for 1 hour before replacement of the virus inoculum with serum-free DMEM -/+ 4μM Rux and incubation for 48 or 72 hours. Cells were then stained using DAPI and mounted onto glass slides before analysis using a fluorescence microscope (10x Magnification). (Data representative of two independent repeats).

In conclusion, we set out to further characterise the IFN-sensitive mutants rPIV5mCh-α and PIV5 W3-γ. The results demonstrate that the combination of mutations within the V protein of the IFN-sensitive mutant rPIV5mCh-α are unable to revert for up to 60 days. In addition, this IFN-sensitive mutant exhibits both increased fusogenicity in the absence of an intact IFN response and increased induction of apoptosis in the presence of an intact IFN response that was abrogated in the absence of an intact IFN response. By contrast, the mutation within the V protein of the IFN-sensitive virus PIV5 W3-γ is easily reverted as we can select revertants to the wild-type V protein sequence directly from one infection of the virus preparation and there is an increase in wild-type virus following passage in IFN competent cells for 60 days. In addition, this virus also induced apoptosis in the presence of an intact IFN response that was abrogated in the absence of an intact IFN response. Next we decided to sequence the entire mutant genome to determine if any mutations found within genes other than V/P, could indicate an explanation for these interesting features.

6.1.4 Full genome sequencing of PIV5 mutant viruses

Following the observation that the IFN-sensitive mutants rPIV5mCh-α and PIV5 W3-γ exhibited differences in fusogenicity and apoptosis, it was decided to fully sequence each mutant using directional sequencing (performed by Elizabeth Fleming; University of St Andrews/University of Glasgow). This would enable us to determine if any mutations found within genes other than V/P, could indicate an explanation for the phenotypes seen previously. Notably we also decided to fully sequence the rPIV5mCh-β virus to identify if any mutations could explain the interesting phenotype seen at low MOI.

Firstly, the recombinant PIV5mCh was compared to the original PIV5 W3 wild-type virus. This highlighted that there were some differences between PIV5 W3 and the recombinant virus rPIV5mCh besides the mCherry insertion (Table 6.1). Specifically, two non-synonymous mutations were found in the F protein (T24A and S217N), however, as rPIV5mCh and PIV5 W3 behave similarly with regards to fusion then it seems likely that these mutations do not affect protein function.

Table 6.1: Mutations found during full genome sequencing. The mutations found within each mutant are depicted below. The position of each nucleotide change is numbered according to the genomic sequence of PIV5 W3. The amino acid change is numbered according to the individual proteins with ATG equal to number 1 in each case. Non-synonymous mutations are indicated with a 'Y' and synonymous mutations indicated with 'Y*'.

Gene	Position	Nucleotide change	rPIV5mCh	rPIV5mCh-α	rPIV5mCh-β	PIV5 W3-γ	Amino Acid change
NP	1066	C>T	Y*	Y*	Y*		-
V/P	2001	T>C		Y			L51P
V/P	2154	T>C		Y			L102P
V/P	2156	T>C		Y*			-
V/P	2213	T>C		Y			L122P
V/P	2214	T>C		Y			L122P
V/P	2244	T>C		Y		Y	L132P
V/P	2253	T>C		Y			F135S
V/P	2279	T>A			Y		F144I
P only	2372	T>C		Y			Y175H
P only	2489	A>G			Y		T214A
F	4599	A>G	Y	Y	Y		T24A
F	4658	G>A	Y*	Y*	Y*		-
F	4661	C>T	Y*	Y*	Y*		-
F	5179	G>A	Y				S217N
SH							
HN	7171	C>T	Y*	Y*	Y*		-
mCherry (rPIV5mCh only)							
L	8517	A>C				Y	E35A
L	10641	A>G	Y*	Y*	Y*		-
L	11607	T>C		Y*			-

Next each IFN-sensitive mutant virus was compared to both the PIV5 W3 and rPIV5mCh sequences. Interestingly, the only non-synonymous mutation identified in rPIV5mCh-α (aside from the numerous mutations already identified in the V/P gene) was found in the fusion protein (T24A), however, this mutation was also found in both the wild-type virus rPIV5mCh and the mutant virus rPIV5mCh-β. Furthermore, the only other non-synonymous mutation identified in PIV5 W3-γ (aside from the single mutation already identified in the V/P gene) was found in the L protein (E35A), however, no differences are seen in viral replication of this mutant compared to the wild-type virus. Hence, there are no mutations that would immediately suggest an explanation for increased fusogenicity of rPIV5mCh-α or increased apoptosis of both rPIV5mCh-α and PIV5 W3-γ compared to rPIV5mCh and PIV5 W3.

Finally, rPIV5mCh-β was also compared to both the PIV5 W3 and rPIV5mCh sequences. Interestingly only one other non-synonymous mutation was found, T24A, however, this mutation as stated previously was also found within the wild-type virus therefore this could not provide an explanation for the unique phenotype demonstrated by this mutant when the MOI is altered.

In conclusion, this suggests that the mutations seen within the V/P gene of each virus are responsible for the different phenotypes demonstrated by each mutant virus.

6.1.5 Overall conclusions

In conclusion, we have developed a method that has successfully isolated three mutant viruses from rPIV5mCh and PIV5 W3 namely, rPIV5mCh-α, rPIV5mCh-β and PIV5 W3-γ. Further examination of these mutant viruses indicates that both rPIV5mCh-α and PIV5 W3-γ contain non-functional V proteins that cannot block the IFN signalling pathway and thus are sensitive to IFN. Surprisingly, the mutant rPIV5mCh-β was unable to block IFN signalling at low MOI but could block IFN signalling at high MOI. Subsequently, it was found to contain a functional V protein that can block the IFN signalling pathway and is therefore not sensitive to IFN. Furthermore, sequencing of the full genome did not reveal any other mutations, outwith the V/P gene, which could explain this unique phenotype. Consequently, this led us to focus our further investigation into the two IFN-sensitive mutants rPIV5mCh-α and PIV5 W3-γ. This further investigation found that rPIV5mCh-α demonstrates an IFN-sensitive mutant that cannot easily revert to regain V protein function. Furthermore, this virus also exhibits increased fusogenicity in the absence of an intact IFN response and increased induction of apoptosis in the presence of an intact IFN response. By contrast, the IFN-sensitive virus PIV5 W3-γ can easily revert to the wild-type V protein as wild-type V can be selected directly from the virus preparation at Day 0, however, this virus, like rPIV5mCh-α, also increased induction of apoptosis in the presence of an intact IFN response. Intriguingly, this then led us to fully sequence the genome of these IFN-sensitive mutants however this failed to offer any other mutations outwith the V/P gene that could explain these features. This therefore suggests that the mutations seen within the V/P gene of each virus are responsible for the different phenotypes demonstrated by each mutant virus.

7 Discussion

7.1 Analysis of the IFN inhibitor Rux and its ability to enhance viral replication *in vitro*

7.1.1 Rux and its array of potential applications

Currently the default option for growth of IFN-sensitive viruses is in Vero cells, however due to host-cell constraints not all viruses can be grown in such cells (Barrett et al. 2009). Subsequently it was demonstrated that growth of IFN-sensitive viruses can be increased in cells able to produce and respond to IFN using stable expression of viral IFN antagonists (Young et al. 2003). However, this method was relatively inflexible as new cell-lines would need to be created depending on host cell constraints and it creates regulatory problems for vaccine manufacturers. Our study has shown that supplementing the media with Rux provides a more efficient and flexible approach to increase growth of IFN-sensitive viruses in a cell-line of choice than these existing methods. In particular, we have shown that i) the addition of Rux to A549: naïve cells could provide a more rapid and hence more efficient alternative for growth of IFN-sensitive viruses than Vero cells and ii) that addition of Rux, can increase growth of the IFN-sensitive virus BUNΔNSs, BUN WT and several other viruses from the *Bunyaviridae* family in a number of cell-lines including MRC5 cells which are used widely in vaccine production and a number of cell-lines derived from different mammalian species. Ultimately, this supports the concept that Rux could aid in many practical applications such as i) vaccine production and ii) techniques to isolate newly emerging viruses. Notably, the importance of developing such techniques is highlighted by the current Zika virus outbreak

(Wahid et al. 2016), where both fundamental research and prophylactic treatment are urgently required.

7.1.2 Fundamental studies initiated during this study

7.1.2.1 BUN WT growth is suppressed in MDBK bovine cells

In addition to practical applications we have also demonstrated the ability of Rux to initiate fundamental studies of the IFN response. In our study we demonstrated that during a plaque assay BUN WT infection is suppressed in MDBK cells, and blocking the IFN response using the IFN inhibitor Rux negates this effect. However, further examination of this effect using a multistep viral growth curve conflicted with our original plaque development data and indicated that there was no difference in viral growth in the presence and absence of the inhibitor (Figure 3.7). One potential explanation for this is that a plaque assay is a more sensitive measure of the IFN response than a viral growth curve. During a plaque assay, the cell culture plates are kept stationary within the incubator meaning that the initial virus infected cell releases virus which can only infect neighbouring cells as the plaque assay is not moving and therefore the virus cannot travel far. It may therefore take multiple rounds of replication to develop a plaque giving the surrounding cells more chance to mount an IFN response. Conversely, during a multistep viral growth curve the flask is constantly moving following the initial infection as the flask is placed on a rocking platform. This would allow the virus released during the initial round of infection to spread more rapidly throughout the monolayer, potentially allowing the spread of infection to outrun the IFN response in only a few rounds of replication.

A second potential explanation for this conflicting result is offered in Barecca and Hare 2004. Previously they demonstrated that Herpes Simplex Virus 1 (HSV-1) is suppressed in MDBK cells following infection and that this effect was negated by the blockage of the IFN response by expression of the V protein from PIV5 (Barreca & Hare 2004; Barreca & O'Hare 2006). During this study they examined growth of HSV-1 in MDBK cells using different initial MOI of infection and concluded that if enough cells were infected initially then the infection progressed and the cell monolayer was destroyed. This indicates that within our experiment perhaps the initial infection during the multistep viral growth curve infected enough cells to counteract the immune system and subsequently the infection progressed. Further multistep viral growth curves investigating different MOI of initial infection may help to identify if this is the case.

If the initial plaque development experiment is to be accepted irrespective of the multistep viral growth curve two potential explanations for this unusual response are proposed i) the IFN antagonist proteins of these viruses are non-functional in this cell line or ii) the IFN system in MDBK cells is highly responsive. With regard to IFN antagonist function, the possibility exists that the IFN antagonists of both BUN WT and HPV-1 (NSs and ICP0) are non-functional in these cells. With regards to the IFN system, it seems possible due to the differences in responses at different MOI that MDBK cells have a highly responsive IFN system. Further evidence to emphasize this case was provided by our final experiment involving Rux, where we analysed a number of different viruses from the *Bunyaviridae* family (ANAV, BWAV, CVV, KIRV, MDV and SBV) in different cell-lines including MDBK cells in the absence and presence of Rux

(Figure 3.9). In this study we demonstrated that none of the viruses tested could plaque well in the absence of Rux in MDBK cells but CVV, KRIV and MDV plaque size was increased in the presence of Rux. As growth of each of these viruses (CVV, KRIV and MDV) is increased in the presence of Rux then this indicates that the IFN response limits the infection of each of these viruses in this cell line. Notably it also appeared that MDCK cells might also exhibit a similar response as none of the viruses were able to plaque well in MDCK cells and each was increased in the presence of Rux. Potentially, this provides further evidence that these cells have a particularly strong IFN response. Furthermore, as both cell-lines were derived from renal tissue this could indicate that this strong antiviral response is a common quality of such cells. Despite defining these two potential explanations individually it is also possible that a combination of these two factors exhibit this unusual response.

7.1.2.2 Other host cell constraints aside from the IFN response limit infection of the Bunyaviridae virus family

The second fundamental study initiated using Rux set out to analyse species-specific host cell constraints on the *Bunyaviridae* virus family. Other than sequencing data there is a lack of information regarding the interactions of ANAV, BWAV, CVV, KIRV, MDV with the IFN response. This study was therefore the first to analyse the species-specific host cell constraints of these different viruses of the *Bunyaviridae* family in addition to the previously studied SBV in different mammalian cell-lines (Figure 3.9). One of the first interesting features that we wanted to examine was the growth of ANAV which has been previously shown to lack an NSs IFN antagonist protein and induce IFN production upon

infection (Mohamed et al. 2009). Here we have demonstrated that this virus could produce small plaques in A549 naïve cells in the absence of Rux which are greatly increased in the presence of Rux. Furthermore, ANAV did not grow in MDCK cells in the absence of Rux but large plaques are formed in the presence of Rux. This indicates that the presence of an active IFN response restricts viral growth in A549: naïve and MDCK cells as expected due to the lack of an IFN antagonist. However, the IFN response is not the only constraint on infection as even when the IFN response is inhibited by the addition of Rux then the virus still cannot grow in many of the cell-lines tested. Interestingly, recent work has determined that many Bunyamwera viruses do not contain NSs proteins and contain another unknown mechanism by which they achieve IFN antagonism (Shchetinin et al. 2015). Further studies are required to decipher the mechanism by which these viruses lacking an NSs protein achieve IFN antagonism and aptly identification of areas that permit IFN antagonism could be investigated using the method developed in the second part of this study.

A second feature we wanted to further examine in this study was if the IFN response was the only limit to *Bunyaviridae* infections or if other host cell constraints limit the spread of infection. From this study it was evident that the IFN response was not the only constriction to virus infection of many of these viruses in numerous cell-lines. For example, ANAV, BWAV and SBV were unable to grow in many cell-lines even in the absence of the IFN response. One possible explanation for this is that there are differences in the cellular receptors used for entry of the virus to host cells and/or there is variation in the virus glycoproteins that allow entry. Currently the cellular receptors for entry of *Bunyaviridae* are

unknown (Bowden et al. 2013), and until the cellular receptors required for entry are identified it is difficult to determine if this is the limitation on host range demonstrated here. Other limitations to infection could be limited/lack of host cell factors required for the production of infectious virus, for example, it is known that host cell proteases are required to cleave the Glycoprotein precursor to form the fusion and attachment proteins that are essential for formation of infectious viral particles (Shi et al. 2016), therefore if these cellular proteins were not present then this would also limit infection.

In general, this study provides evidence that Rux can be used as a broad-spectrum aid to the production of viral stocks and in particular for newly emerging viruses where there is a lack of information regarding host cell range. Recently a study described the growth of SBV in numerous mammalian cell-lines including A549, MDBK and MDCK cells and indicated that low titers of virus were harvested following infection of these cells with a low or high MOI. This study was used to identify the most effective cell line to plaque SBV and produce viral stocks for fundamental study at the time of the SBV outbreak 2011-13 and it was found that BHK-21 (hamster) cells, which are IFN deficient, gave the most discernable plaques with a size of 3mm after 3 days (Elliott et al. 2013; Otsuki et al. 1979; Chinsangaram et al. 1999). Our study provides evidence that the addition of Rux can enable SBV to produce large plaques and hence greatly increase viral growth in MDCK cells and RK.13 cells thus indicating a potential use for Rux in the study and production of SBV stocks for use in fundamental studies. However, a direct comparison between BHK-21 and MDCK cells would be necessary to determine which cell line produces the greatest yield. Ultimately

this approach does not only apply to SBV as this study could be used to identify and expand the range of host cells suitable for production of stocks of each of these different viruses. As a result of this flexibility Rux may also prove useful in techniques to isolate newly emerging viruses or viruses from clinical samples by expanding the range of cells capable of supporting the growth of such viruses.

7.1.3 Other potential uses of Rux not explored in this study

7.1.3.1 The use of Rux in the application of oncolytic viruses

So far we have discussed that Rux has many practical applications as well as applications in fundamental research however there are other examples of the use of the IFN inhibitor Rux that we have not explored in this study such as its use in the application of oncolytic viruses. The concept of oncolytic viruses relies on the fact that cancer cells have a dysregulated tumour environment where the oncolytic virus can thrive causing lysis of tumour cells, whereas the growth of such viruses is prevented in adjacent or distant normal tissue (Ferguson et al. 2012). One such dysregulation is that cancer cells often have a defective IFN signalling pathway and are therefore highly susceptible to infection. By contrast, non-transformed cells contain an intact IFN response and respond to infection with production of IFN and subsequently inhibit viral replication and spread. Previously, it has been shown that certain tumours are highly sensitive to oncolysis following infection with the highly lytic VSV, however, others are resistant. Subsequently it has been shown that application of IFN inhibitors including the JAK1/2 inhibitor Rux can reverse this resistance. As Rux has already been approved for clinical treatment of myelofibrosis, a rare blood cancer that causes overproduction of blood cells in the bone marrow (Vaddi et al.

2012; Verstovsek et al. 2015), and has therefore been analysed in clinical trials and declared safe for use in humans then this may accelerate the use of this specific inhibitor in future virotherapy trials (Escobar-Zarate et al. 2013).

Notably, the approval of Rux for clinical treatment may also open up many potential uses for Rux in *in vivo* studies. Currently many *in vivo* studies on the IFN response rely on the ability to make IFN deficient transgenic mice. We have demonstrated the ability of Rux to block the IFN response in numerous mammalian tissues thereby indicating a role for Rux in the development of other IFN deficient animal models. Furthermore, Rux may also have applications in multi culture systems used to analyse viral infection such as human airway epithelium. For example, it could be used to analyse whether the IFN response restricts viral infection in such cells.

7.1.4 Potential Drawbacks

Despite the many benefits of the use of the IFN inhibitor Rux in many different applications there are some potential drawbacks. These include: (i) the cost of the inhibitor and (ii) the obtained stocks of virus would contain the IFN inhibitor. With regard to the cost of the inhibitor, the benefits of Rux in vaccine production such as reduced time to achieve higher titers may significantly outweigh the cost of the inhibitor therefore it is worthwhile investigating this technique. With regard to viral stocks containing Rux, again it should be noted that Rux has been approved for the treatment of myelofibrosis therefore it is declared safe for use in humans. Furthermore, purification of the virus stock would eliminate any IFN inhibitor present, and this should always be considered for fundamental studies

and for the production of vaccines using cell-lines as a variety of different cytokines are induced and secreted in response to viral infection and would also be present in unpurified stocks.

7.1.5 Concluding remarks

In conclusion, we have demonstrated that Rux could be used in the production of live attenuated vaccines as exemplified by the more efficient production of IFN-sensitive viruses in A549: naïve cells in the presence of Rux than the default Vero cell line and the ability to increase viral growth in a cell-line of choice. Furthermore, the inhibitor may also prove useful in initiation of fundamental studies of IFN antagonists and the IFN response as exemplified by our initial studies into the IFN response of MDBK cells and the host range of *Bunyaviridae*. Finally, the inhibitor may also become a general approach to aid growth and isolate newly emerging viruses as exemplified by our ability to increase viral growth of several viruses from the *Bunyaviridae* family in numerous host cells. Consequently, our further investigation of the use of IFN inhibitor Rux has established that supplementing the media with this inhibitor could become a valuable technique that could aid in numerous aspects of virological research.

7.2 Isolation of IFN-sensitive viruses using FACS

Currently, methods to isolate attenuated viruses include i) traditional methods such as serial passage of the wild type virus in a foreign host or at abnormal temperatures or ii) rational design. However, traditional methods can be lengthy and rational design relies on the notion that the IFN antagonist is already known and is complicated due to the multifunctional nature of IFN antagonists. Consequently, we developed a novel method to rapidly isolate IFN-sensitive mutant viruses using FACS. The establishment of this technique aimed to speed traditional methods of obtaining attenuating IFN-sensitive viruses and select viable viruses that can often be difficult to obtain because of the multifunctional nature of IFN antagonists. Furthermore, it does not rely on prior knowledge of the IFN antagonists. Following optimisation of this method we successfully isolated three mutant viruses from rPIV5mCh and PIV5 W3. Upon examination of these mutants two, namely rPIV5mCh-α and PIV5 W3-γ were confirmed as IFN-sensitive and the other rPIV5mCh-β exhibited an interesting phenotype in that it could not block the IFN signalling pathway at low MOI but it could at high MOI.

7.2.1 Potential drawbacks to the method

As one of the main objectives of this study was to develop a method it is important to discuss the limitations and potential drawbacks of this method as despite successfully obtaining IFN-sensitive mutant viruses, it is likely that this method would require further optimisation before it could be developed as a general method to isolate various types of viruses. One potential limitation includes the essential requirement for neutralizing antibody to prevent the infection of uninfected cells by progeny viruses following initial infection (Figure

4.5). This was an important part in the optimisation of the method as the release and infection of uninfected cells by progeny virus could lead to the selection of false positives. If this method was to be further developed as a general method to isolate IFN-sensitive viruses then this necessity could impede this process, as a good neutralizing antibody is not available for every virus. One potential method to alleviate this issue could be to find a more generalised method to inhibit virus entry following infection. For example, as sialic acid is the receptor which allows entry of viruses such as Influenza and certain paramyxoviruses including the majority of the Respiroviruses, Rubulaviruses and Avulaviruses we could investigate the possibility of inhibiting virus entry through the use of sialidase inhibitors such as Tamiflu and Relenza or cleaving sialic acid using neuraminidase following initial infection (Villar & Barroso 2006; Magesh et al. 2009; Itzstein & Thomson 2009; Shtyrya et al. 2009). This would therefore alleviate the requirement for neutralising antibody by preventing any further infection by blocking or cleaving sialic acid on host cells. Initial attempts to optimise this method proved successful in that neuraminidase treatment of cells prior to infection could prevent subsequent infection by influenza virus (Data not shown). Despite not attaining a completely general method, as viruses use different receptors for entry, this would broaden the range of viruses suitable for use in this assay to include clinically important viruses such as Influenza.

7.2.2 Cell-line development

A second step of optimisation that may be required is to further develop the cell line used for the isolation of IFN-sensitive mutants. In our study we developed the A549:(ISRE).GFP/ISG56$^-$/Npro cell line which expressed shRNA to ISG56 and

the BVDV Npro protein to knockdown the expression of ISG56 and to block the IFN induction pathway, respectively (Figure 4.3). The reason we developed this cell line is that ISG56 has been shown to specifically prevent the infection of Rubulaviruses such as PIV5 and would therefore abrogate growth of our IFN-sensitive viruses before selection (Young et al. 2016). However, this ISG is not important for abrogation of other viruses. Consequently, other cell-lines that knock down ISGs known to prevent virus growth of the particular test virus may be required for the isolation of mutants from other viruses.

7.2.2.1 Increasing the number of IFN-sensitive mutant viruses available for selection

A third step of optimisation would be to determine methods to increase the number of potential mutants. When adapting the method to the non-fluorescent virus PIV5 W3, only one potential mutant was isolated and analysed whereas we obtained two mutants multiple times from rPIV5mCh. Notably one possible explanation for this is that the passage history of rPIV5mCh differs from PIV5 W3, as we do not know the passage history of these stocks prior to our analysis. In particular, if the rPIV5mCh mutant had been passaged multiple times in IFN incompetent cells such as Vero's then perhaps this would have created more opportunity for IFN-sensitive viruses to generate. As we wanted to avoid the lengthy process of serial passage another possible method to increase the number of mutant viruses would be to mutagenize the virus stock using chemical agents such as 5' fluorouracil or sub optimal levels of the nucleoside inhibitor Ribavirin to increase the number of potential mutants available for selection (Agudo et al. 2009; Marcelin et al. 2014).

7.2.2.2 Development of an automated analysis method

A final stage of optimisation suggested to develop this method is to the advance the analysis method following sorting. The process of individually analysing 96 well plates is time consuming, however, the creation of an automated system should be possible. This system would require measurement of GFP and mCherry fluorescence or Texas red immunostaining. Initial studies identified that GFP and mCherry fluorescence could be measured using the IncuCyte zoom quantitative live cell analysis system and a ratio of GFP to mCherry fluorescence calculated. Any well found to be exhibiting a ratio of 1:1 could then be further analysed to examine if it exhibited dual fluorescent cells (Data not shown). However, this process was not possible for GFP fluorescence and Texas red immunostaining as GFP expression was significantly brighter than Texas red immunostaining therefore a more sophisticated method to measure GFP and Texas red is required to automate this system. Notably this highlighted one of the many advantages of using a fluorescently labelled virus and with the increasing number of fluorescent viruses available for viruses such as RSV and PIV3 then it is not unreasonable to recommended that a fluorescently labelled virus be used for this method if available.

7.2.3 Analysis of PIV5 mutants

Using our method we isolated three PIV5 mutant viruses namely, rPIV5mCh-β which was unable to block IFN signalling at low MOI but could block IFN signalling at high MOI and rPIV5mCh-α and PIV5 W3-γ which could not block IFN signalling and were subsequently shown to be IFN-sensitive. The results from analysis of rPIV5mCh-β represent an interesting enigma with regards to V

protein function. Specifically, this virus could not block IFN signalling at low MOI but could block IFN signalling at high MOI. Deep sequencing of the rPIV5mCh-β mutant demonstrated that this mutant only contained non-synonymous mutations within the V/P gene of the viral genome (aside from the T24A mutation found in F protein which was also found in the parental rPIV5mCh strain), leading us to suggest that this unusual phenotype is as a result of the two mutations found in the V/P gene of the virus.

During further analysis of the rPIV5mCh-β V protein we determined that the V protein was functional with regards to blocking the IFN signalling pathway as it was able to block luciferase expression (a reporter of activation of IFN signalling) during an IFN signalling luciferase assay. Upon reflection, one potential problem with this experiment exists in that we overexpressed the V protein during the luciferase assay. As one potential explanation for the ability of rPIV5mCh-β to block IFN signalling at high but not low MOI is that the V protein function is partially functional and therefore concentration dependent, then analysis of the V protein function at low and high concentrations within the luciferase assay may have provided a better assessment of V protein function.

A second potential explanation for this unusual rPIV5mCh-β V protein activity is that the mutations permit the V protein to have a slightly higher affinity for another cellular or viral protein. This effect would be evident at low concentrations (low MOI) as some of the V protein would be bound to another protein thereby impeding its interaction with DDB1 and its subsequent block of the IFN signalling pathway, however when the concentration of V protein is

increased (high MOI) this effect would be negated. To test this, again we could complete an IFN signalling luciferase assay using a concentration gradient of the rPIV5mCh-β V protein against the wild-type V protein to identify if the activity of the V protein is dependent on its concentration. We could then also assess for new binding partners using pull downs.

A final explanation is that the single mutation that affects the P protein affects the ability of the virus to replicate. For example, if the virus is subtly slowed due to the changes to RNA replication then at a low MOI the virus may be unable to block IFN induction but this affect would be negated at high MOI. As there are two mutations within this mutant, one that affects both V and P and another that affects only V, the two mutations could be looked at individually by reverse genetics to narrow down which mutation is responsible for this interesting phenotype.

7.2.4 PIV5 W3-γ

A second mutant identified, PIV5 W3-γ, was shown to be unable to block IFN signalling and was consequently IFN-sensitive, due to a single mutation in the N terminal V/P common domain (L132P). Previously it has been shown that the C terminal cysteine rich domain of the V protein is highly important for blocking the IFN response as a recombinant hPIV2 virus that expresses a truncated form of V lacking the C-terminal domain appeared to be sensitive to IFN (Kawano et al. 2001). Furthermore, a PIV5 virus lacking the cysteine rich domain of the V protein was shown to be unable to block IFN induction or IFN Signalling (He et al. 2002). Subsequently, the IFN-sensitive virus PIV5 CPI- was shown to be

unable to block IFN signalling due to the combination of Y26H, L50P and L102P mutations found in the V/P common domain (Chatziandreou et al. 2002), for the first time implicating the V/P common domain with V protein function. Interestingly, we have identified that a single mutation (L132P) found in the N-terminal V/P common domain can prevent the V proteins ability to block IFN signalling, however, this mutation is readily reverted back to the wild-type sequence. Interestingly, the PIV5 W3-γ mutant V protein lost the ability to lead to the degradation of STAT1 but retained the ability to interact with Mda-5. This taken together with the fact that mutations from Leucine to Proline are likely to dramatically affect protein structure indicates that the structure in this region of the V protein is essential for its interaction with DDB1 and the resultant degradation of STAT1. To examine this further mutagenesis of this amino acid to another residue that is less likely to affect V protein structure such as an Alanine residue could be completed. This would determine if the structure, the amino acid itself or both are essential to this particular V protein function.

7.2.5 rPIV5mCh-α

The final mutant that we isolated, rPIV5mCh-α, was found to contain 6 mutations within the V/P gene which we have later identified to disable the V proteins ability to block IFN signalling, thus rendering the virus IFN-sensitive. Interestingly the mutant was found to contain the L132P mutation as was found in PIV5 W3-γ, however, unlike the PIV5 W3-γ mutant, rPIV5mCh-α was unable to revert to wild-type either directly from one infection with the viral stock or following 60 days of passage in IFN competent cells. Following my study, the rPIV5mCh-α virus was passaged for a further 60 days and sequenced. The

results indicate that the virus had still not reverted to wild-type or regained the ability to block IFN-signalling through compensatory mutations (Dan Young and David Hughes, University of St Andrews), thus indicating that this combination of mutations is very difficult to revert.

Interestingly, five of the mutations found in the V/P gene were found to be in the common V/P region, thus both the V and P protein would be affected. Furthermore, four of these changes were leucine to proline changes that are known to dramatically affect protein structure. As stated previously the P protein is essential for RNA synthesis (Fuentes et al. 2010), therefore it is remarkable that the P protein could tolerate this number of mutations and particularly proline changes, without having any significant adverse effects on protein function. Upon deep sequencing of the virus, no other non-synonymous mutations were found apart from the mutations previously identified in the V/P gene thus indicating that these mutations are strongly selected for. Furthermore, this mutant was isolated numerous times from the same stock indicating that this mutant is present in high levels in the population. A potential reason for obtaining so many mutations in both the V and particularly the P gene may be that it actually provides a selective advantage in IFN incompetent conditions. As the virus was grown in Vero cell's, and these cells are IFN incompetent the V protein function of blocking IFN signalling would no longer be required, therefore perhaps this would allow mutations to build that provide a selective advantage based on P protein function.

Previously, it has been shown that phosphorylation at T286 within the P protein increased RNA synthesis (Sun, Luthra, et al. 2011), whereas phosphorylation at S157 and S308 can inhibit RNA synthesis (Timani et al. 2008), however these previously identified sites of phosphorylation were not affected by the mutations seen here. We have presented evidence whereby our mutant appears to have an increased speed of replication by producing larger plaques than the wild-type virus during plaque analysis (Figure 6.5). However, this could not be replicated during a multi-step viral growth curve. As stated previously this could be due to differences in sensitivity of the plaque assay compared to the multistep growth curve in assessing the IFN response. If time had allowed, we could have tested this more accurately using qPCR to determine viral RNA levels rather than only determining the production of infectious viral particles. What's more, competition assays could be completed to determine if the mutant virus could out-compete the wild-type virus in IFN incompetent conditions. Without further investigation it is difficult to say whether these sites represented further sites of interest for increased activity of the P protein however given that these mutations are being readily selected for and that this mutant is abundant within the viral stock then it seems likely that there is a significant advantage to obtaining these mutations.

7.2.5.1 Increased apoptosis and fusogenicity

In addition to inability to block IFN signalling, we have also shown that rPIV5mCh-α infection exhibits enhanced apoptosis in IFN competent cells (A549: naïve cells) however, this effect is negated in the presence of the IFN inhibitor Rux. As apoptosis is blocked in the presence of Rux then is likely that this

apoptosis has been induced in an IFN dependent manner as this virus is unable to block IFN signalling. Notably the same effect is also seen following infection with PIV5 W3-γ which is also unable to block IFN signalling.

A second interesting feature of rPIV5mCh-α is that in IFN incompetent conditions (A549: naïve cells in the presence of Rux and Vero cells) this virus exhibits increased cell-cell fusion. Prior to deep sequencing it was hypothesised that mutations elsewhere in the viral genome would explain the gain of this attribute however surprisingly no other mutations were found outside of the V/P gene. Consequently, this leads us to suggest that either the V and/or the P protein is responsible for preventing cell-cell fusion.

7.2.5.2 The development of rPIV5mCh-α as a viral vaccine vector

Excitingly, the many additional features outlined for rPIV5mCh-α above, indicate that rPIV5mCh-α may have a potential application in the development of vaccines. Currently there is increasing interest in the development of PIV5 based vaccine vectors, as PIV5 demonstrates a number of characteristics that are highly sought after in such vaccines. For example, i) PIV5 is avirulent in humans, ii) PIV5 based vaccines have been used safely for kennel cough in dogs for over 30 years and have not attributed to any human illness despite the close association of humans with dogs, iii) PIV5 can be readily produced in many cell-lines including Vero cells that are approved for vaccine manufacture, iv) PIV5 can readily infect human cell-lines as well as primary human cell-lines, and finally v) it has been shown that pre-existing immunity to PIV5 does not prevent immunity from PIV5-based vaccines and that vaccination can rapidly induce protective

immunity in a mouse model (Li et al. 2015). In light of this, the mutant rPIV5mCh-α may be of interest for the production of such vaccine vectors due to the additional beneficial features we have identified. In particular, we have shown that this virus has been unable to revert to regain the ability of the IFN antagonist V protein to block IFN signalling following 120 days of passage in IFN competent cells. This property highlights that this IFN-sensitive attenuated virus is difficult to revert which is an essential basis of a successful vaccine. In addition, we have shown that this virus enhances apoptosis in IFN competent conditions. Importantly, this feature could be preferential in the development of vaccines, as it is thought that increased apoptosis could lead to increased antigen production and immunogenicity. For example, rBRSVΔSH (bovine RSV with deleted SH protein) was shown to exhibit increased apoptosis and pro-inflammatory cytokines *in vitro* but it is attenuated and induced greater protective immunity to BRSV in calves than use of the wild-type virus (Taylor et al. 2014). In addition to this, attenuated PIV5 viruses such as PIV5ΔSH shown to enhance induction of apoptosis, were also shown to have enhanced immunogenicity and provided better protection against viral challenge in mice compared to wild type PIV5 (Li et al. 2013). Finally, we have suggested that rPIV5mCh-α may have a potential growth advantage in IFN incompetent conditions which may be useful in vaccine production however further investigation of this property is required. Ultimately these features combined with the many already identified advantages of PIV5, may make the rPIV5mCh-α mutant of great interest in the development of PIV5 based vaccines.

7.2.6 Concluding remarks

In conclusion, we have successfully developed a method to isolate IFN-sensitive mutant viruses from Paramyxoviruses. Not only have these viruses instigated further fundamental studies into the function of the V and P proteins of PIV5 but they may also aid in the design of live-attenuated vaccines and specifically PIV5 based vaccines. Ultimately, this study is the first step towards creating a general method to isolate various types of IFN-sensitive viruses that as well as aiding fundamental studies, may be further developed as live-attenuated virus vaccines for clinically important viruses lacking vaccines.

8 References

Abraham, G. & Banerjee, A.K., 1976. Sequential transcription of the genes of vesicular stomatitis virus. *Proceedings of the National Academy of Sciences of the United States of America*, 73(5), pp.1504–8.

Agudo, R., Arias, A. & Domingo, E., 2009. 5-fluorouracil in lethal mutagenesis of foot-and-mouth disease virus. *Future Medicinal Chemistry*, 1(3), pp.529–539.

Alayyoubi, M. et al., 2015. Structure of the paramyxovirus parainfluenza virus 5 nucleoprotein-RNA complex. *Proceedings of the National Academy of Sciences of the United States of America*, 112(14), pp.E1792-9.

Alexopoulou, L. et al., 2001. Recognition of double-stranded RNA and activation of NF-[kappa]B by Toll-like receptor 3. *Nature*, 413(6857), pp.732–738.

Andrejeva, J. et al., 2013. ISG56/IFIT1 is primarily responsible for interferoninduced changes to patterns of parainfluenza virus type 5 transcription and protein synthesis. *Journal of General Virology*, 94(PART11), pp.59–60.

Andrejeva, J. et al., 2004. The V proteins of paramyxoviruses bind the IFN-inducible RNA helicase, mda-5, and inhibit its activation of the IFN-beta promoter. *Proceedings of the National Academy of Sciences of the United States of America*, 101(49), pp.17264–9.

Asenjo, A. & Villanueva, N., 2016. Phosphorylation of the human respiratory syncytial virus P protein mediates M2-2 regulation of viral RNA synthesis, a process that involves two P proteins. *Virus Research*, 211, pp.117–125.

Au-Yeung, N., Mandhana, R. & Horvath, C.M., 2013. Transcriptional regulation by STAT1 and STAT2 in the interferon JAK-STAT pathway. *JAK-STAT*, 2(3),

p.e23931.

Audsley, M.D., 2013. Paramyxovirus evasion of innate immunity: Diverse strategies for common targets. *World Journal of Virology*, 2(2), p.57.

Bancerek, J. et al., 2013. CDK8 kinase phosphorylates transcription factor STAT1 to selectively regulate the interferon response. *Immunity*, 38(2), pp.250–62.

Bankamp, B. et al., 2011. Genetic characterization of measles vaccine strains. *The Journal of infectious diseases*, 204 Suppl(suppl_1), pp.S533-48.

Barreca, C. & Hare, P.O., 2004. Suppression of Herpes Simplex Virus 1 in MDBK Cells via the Interferon Pathway Suppression of Herpes Simplex Virus 1 in MDBK Cells via the Interferon Pathway. , 78(16), pp.8641–8653.

Barreca, C. & O'Hare, P., 2006. Characterization of a potent refractory state and persistence of herpes simplex virus 1 in cell culture. *Journal of virology*, 80(18), pp.9171–80.

Barrett, P.N. et al., 2009. Vero cell platform in vaccine production: moving towards cell culture-based viral vaccines. *Expert review of vaccines*, 8(5), pp.607–18.

Baxter, D., 2007. Active and passive immunity, vaccine types, excipients and licensing. *Occupational Medicine*, 57(8), pp.552–556.

Bhoj, V.G. & Chen, Z.J., 2009. Ubiquitylation in innate and adaptive immunity. *Nature*, 458(7237), pp.430–437.

Billiau, A. & Matthys, P., 2009. Interferon-g: A historical perspective.

Bird, B.H. et al., 2008. Rift valley fever virus lacking the NSs and NSm genes is highly attenuated, confers protective immunity from virulent virus challenge, and allows for differential identification of infected and vaccinated animals. *Journal of virology*, 82(6), pp.2681–91.

Blaney, J.E. et al., 2001. Chemical mutagenesis of dengue virus type 4 yields mutant viruses which are temperature sensitive in vero cells or human liver cells and attenuated in mice. *Journal of virology*, 75(20), pp.9731–40.

Bonaparte, M.I. et al., 2005. Ephrin-B2 ligand is a functional receptor for Hendra virus and Nipah virus. *Proceedings of the National Academy of Sciences of the United States of America*, 102(30), pp.10652–7.

Bose, S. et al., 2013. Mutations in the Parainfluenza Virus 5 Fusion Protein Reveal Domains Important for Fusion Triggering and Metastability. *Journal of Virology*, 87(24), pp.13520–13531.

Bose, S. et al., 2011. Structure and mutagenesis of the parainfluenza virus 5 hemagglutinin-neuraminidase stalk domain reveals a four-helix bundle and the role of the stalk in fusion promotion. *Journal of Virology*, 85(24), pp.12855–66.

Bowden, T.A. et al., 2013. Orthobunyavirus Ultrastructure and the Curious Tripodal Glycoprotein Spike T. C. Pierson, ed. *PLoS Pathogens*, 9(5), p.e1003374.

van Boxel-Dezaire, A.H., Sandhya Rani, M. & Stark, G.R., 2006. Review Complex Modulation of Cell Type-Specific Signaling in Response to Type I Interferons. *Immunity*, 25, pp.361–372.

Bridgen, A. et al., 2001. Bunyamwera bunyavirus nonstructural protein NSs is a nonessential gene product that contributes to viral pathogenesis. *Proceedings of the National Academy of Sciences of the United States of America*, 98(2), pp.664–9.

Broz, P. & Monack, D.M., 2013. Newly described pattern recognition receptors team up against intracellular pathogens. *Nature Reviews Immunology*, 13(8),

pp.551–565.

Byrappa, S., Pan, Y.-B. & Gupta, K.C., 1996. Sendai Virus P Protein Is Constitutively Phosphorylated at Serine249: High Phosphorylation Potential of the P Protein. *Virology*, 216(1), pp.228–234.

Cai, X., Chiu, Y.H. & Chen, Z.J., 2014. The cGAS-cGAMP-STING pathway of cytosolic DNA sensing and signaling. *Molecular Cell*, 54(2), pp.289–296.

Carlos, T.S. et al., 2007. Interferon-induced inhibition of parainfluenza virus type 5; the roles of MxA, PKR and oligo A synthetase/RNase L. *Virology*, 363(1), pp.166–73.

Chang, A. & Dutch, R.E., 2012. Paramyxovirus fusion and entry: Multiple Paths to a common end. *Viruses*, 4(4), pp.613–636.

Chatziandreou, N. et al., 2002. Differences in interferon sensitivity and biological properties of two related isolates of simian virus 5: a model for virus persistence. *Virology*, 293(2), pp.234–242.

Chatziandreou, N. et al., 2004. Relationships and host range of human, canine, simian and porcine isolates of simian virus 5 (parainfluenza virus 5). *Journal of General Virology*, 85(10), pp.3007–3016.

Childs, K. et al., 2007. mda-5, but not RIG-I, is a common target for paramyxovirus V proteins. *Virology*, 359(1), pp.190–200.

Childs, K., Randall, R. & Goodbourn, S., 2012. Paramyxovirus V Proteins Interact with the RNA Helicase LGP2 To Inhibit RIG-I-Dependent Interferon Induction. *Journal of Virology*, 86(7), pp.3411–3421.

Chinsangaram, J., Piccone, M.E. & Grubman, M.J., 1999. Ability of foot-and-mouth disease virus to form plaques in cell culture is associated with suppression of alpha/beta interferon. *Journal of virology*, 73(12), pp.9891–8.

Choppin, P.W., 1964. Multiplication of a Myxovirus (Sv5) With Minimal Cytopathic Effects and Without Interference. *Virology*, 23(2), pp.224–33.

Collins, D.M., 2000. New tuberculosis vaccines based on attenuated strains of the Mycobacterium tuberculosis complex. *Immunology and Cell Biology*, 78(4), pp.342–348.

Corish, P. & Tyler-Smith, C., 1999. Attenuation of green fluorescent protein half-life in mammalian cells. *Protein Engineering Design and Selection*, 12(12), pp.1035–1040.

Cui, J. et al., 2014. USP3 inhibits type I interferon signaling by deubiquitinating RIG-I-like receptors. *Cell research*, 24(4), pp.400–16.

Desmyter, J., Melnick, J.L. & Rawls, W.E., 1968. Defectiveness of interferon production and of rubella virus interference in a line of African green monkey kidney cells (Vero). *Journal of virology*, 2(10), pp.955–61.

Didcock, L. et al., 1999. The V protein of simian virus 5 inhibits interferon signalling by targeting STAT1 for proteasome-mediated degradation. *Journal of virology*, 73(12), pp.9928–33.

Elliott, J. et al., 2007. Respiratory Syncytial Virus NS1 Protein Degrades STAT2 by Using the Elongin-Cullin E3 Ligase. *Journal of Virology*, 81(7), pp.3428–3436.

Elliott, R.M. et al., 2013. Establishment of a reverse genetics system for Schmallenberg virus, a newly emerged orthobunyavirus in Europe. *Journal of General Virology*, 94(PART4), pp.851–859.

Elliott, R.M. & Blakqori, G., 2011. Molecular biology of orthobunyaviruses.

Elliott, R.M. & Weber, F., 2009. Bunyaviruses and the type I interferon system. *Viruses*, 1(3), pp.1003–21.

Elwood, J.M., 1989. Smallpox and its eradication. *Journal of epidemiology and community health*, 43(1), p.92.

Emmons, R.W. et al., 1983. Main Drain virus as a cause of equine encephalomyelitis. *Journal of the American Veterinary Medical Association*, 183(5), pp.555–8.

Escobar-Zarate, D. et al., 2013. Overcoming cancer cell resistance to VSV oncolysis with JAK1/2 inhibitors. *Cancer Gene Therapy*, 20(10), pp.582–589.

Evermann, J.F., Lincoln, J.D. & McKiernan, A.J., 1980. Isolation of a paramyxovirus from the cerebrospinal fluid of a dog with posterior paresis. *Journal of the American Veterinary Medical Association*, 177(11), pp.1132–4.

Ferguson, M.S. et al., 2012. Systemic Delivery of Oncolytic Viruses: Hopes and Hurdles. *Advances in Virology*, 2012, pp.1–14.

Fields, B.N., Knipe, D.M. (David M. & Howley, P.M., 2013. *Fields virology*, Wolters Kluwer Health/Lippincott Williams & Wilkins.

Fiore, A.E., Bridges, C.B. & Cox, N.J., 2009. Seasonal Influenza Vaccines. In Springer Berlin Heidelberg, pp. 43–82.

Fleming, S.B., 2016. Viral Inhibition of the IFN-Induced JAK/STAT Signalling Pathway: Development of Live Attenuated Vaccines by Mutation of Viral-Encoded IFN-Antagonists. *Vaccines*, 4(3).

Friedman, C.S. et al., 2008. The tumour suppressor CYLD is a negative regulator of RIG-I-mediated antiviral response. *EMBO reports*, 9(9), pp.930–6.

Fu, X.Y. et al., 1990. ISGF3, the transcriptional activator induced by interferon alpha, consists of multiple interacting polypeptide chains. *Proceedings of the National Academy of Sciences of the United States of America*, 87(21), pp.8555–9.

Fuentes, S.M. et al., 2010. Phosphorylation of paramyxovirus phosphoprotein and its role in viral gene expression. *Future microbiology*, 5(1), pp.9–13.

Gack, M.U. et al., 2007. TRIM25 RING-finger E3 ubiquitin ligase is essential for RIG-I-mediated antiviral activity. *Nature*, 446(7138), pp.916–920.

Gage, Z.O. et al., 2016. Cell-based High-Throughput Screening Assay to Identify Inhibitors of the Type I Interferon Induction. *Journal of Biomolecular Screening (submitted)*.

Gainey, M.D., Manuse, M.J. & Parks, G.D., 2008. A hyperfusogenic F protein enhances the oncolytic potency of a paramyxovirus simian virus 5 P/V mutant without compromising sensitivity to type I interferon. *Journal of virology*, 82(19), pp.9369–80.

Gan, S.-W. et al., 2012. The small hydrophobic protein of the human respiratory syncytial virus forms pentameric ion channels. *The Journal of biological chemistry*, 287(29), pp.24671–89.

Garigliany, M.-M. et al., 2012. Schmallenberg virus: A new Shamonda/Sathuperi-like virus on the rise in Europe. *Antiviral Research*, 95(2), pp.82–87.

Gauzzi, M.C. et al., 1996. Interferon- -dependent Activation of Tyk2 Requires Phosphorylation of Positive Regulatory Tyrosines by Another Kinase. *Journal of Biological Chemistry*, 271(34), pp.20494–20500.

Ghildyal, R., Ho, A. & Jans, D.A., 2006. Central role of the respiratory syncytial virus matrix protein in infection. *FEMS Microbiology Reviews*, 30(5), pp.692–705.

Goldsmith, C.S. et al., 2003. Elucidation of Nipah virus morphogenesis and replication using ultrastructural and molecular approaches. *Virus research*, 92(1), pp.89–98.

Goodbourn, S. & Randall, R.E., 2009. The regulation of type I interferon production by paramyxoviruses. *Journal of interferon & cytokine research : the official journal of the International Society for Interferon and Cytokine Research*, 29(9), pp.539–547.

Goswami, R. et al., 2013. Viral degradasome hijacks mitochondria to suppress innate immunity. *Nature Publishing Group*, 23(23).

Goubau, D. et al., 2013. Cytosolic Sensing of Viruses. *Immunity*, 38(5), pp.855–869.

Hale, B.G. et al., 2008. The multifunctional NS1 protein of influenza A viruses. *The Journal of general virology*, 89(Pt 10), pp.2359–76.

Haller, O., Kochs, G. & Weber, F., 2006. The interferon response circuit: Induction and suppression by pathogenic viruses. *Virology*, 344(1), pp.119–130.

Hamming, O.J. et al., 2013. Interferon lambda 4 signals via the IFNλ receptor to regulate antiviral activity against HCV and coronaviruses. *The EMBO journal*, 32(23), pp.3055–65.

He, B. et al., 2002. Recovery of paramyxovirus simian virus 5 with a V protein lacking the conserved cysteine-rich domain: the multifunctional V protein blocks both interferon-beta induction and interferon signaling. *Virology*, 303(1), pp.15–32.

He, B. et al., 2001. The SH integral membrane protein of the paramyxovirus simian virus 5 is required to block apoptosis in MDBK cells. *Journal of virology*, 75(9), pp.4068–79.

Heaton, S.M., Borg, N.A. & Dixit, V.M., 2016. Ubiquitin in the activation and attenuation of innate antiviral immunity. *The Journal of experimental medicine*, 213(1), pp.1–13.

Heil, F. et al., 2004. Species-specific recognition of single-stranded RNA via toll-like receptor 7 and 8. *Science (New York, N.Y.)*, 303(5663), pp.1526–9.

Heinen, E., Herbst, W. & Schmeer, N., 1998. Isolation of a cytopathogenic virus from a case of porcine reproductive and respiratory syndrome (PRRS) and its characterization as parainfluenza virus type 2. *Archives of virology*, 143(11), pp.2233–9.

Hilton, L. et al., 2006. The NPro product of bovine viral diarrhea virus inhibits DNA binding by interferon regulatory factor 3 and targets it for proteasomal degradation. *Journal of virology*, 80(23), pp.11723–11732.

Honda, K. et al., 2004. Role of a transductional-transcriptional processor complex involving MyD88 and IRF-7 in Toll-like receptor signaling. *Proceedings of the National Academy of Sciences of the United States of America*, 101(43), pp.15416–21.

Horikami, S.M. et al., 1992. Complexes of Sendai virus NP-P and P-L proteins are required for defective interfering particle genome replication in vitro. *Journal of virology*, 66(8), pp.4901–8.

Hornung, V. et al., 2006. 5'-Triphosphate RNA is the ligand for RIG-I. *Science (New York, N.Y.)*, 314(5801), pp.994–997.

Hou, F. et al., 2011. MAVS forms functional prion-like aggregates to activate and propagate antiviral innate immune response. *Cell*, 146(3), pp.448–61.

House, C. & House, J.A., 1989. Evaluation of techniques to demonstrate foot-and-mouth disease virus in bovine tongue epithelium: Comparison of the sensitivity of cattle, mice, primary cell cultures, cryopreserved cell cultures and established cell lines. *Veterinary Microbiology*, 20(2), pp.99–109.

Hu, C. et al., 1999. Role of Primary Constitutive Phosphorylation of Sendai Virus P

and V Proteins in Viral Replication and Pathogenesis. *Virology*, 263(1), pp.195–208.

Hu, C. & Gupta, K.C., 2000. Functional Significance of Alternate Phosphorylation in Sendai Virus P Protein. *Virology*, 268(2), pp.517–532.

Hull, R.N. & Minner, J.R., 1957. NEW VIRAL AGENTS RECOVERED FROM TISSUE CULTURES OF MONKEY KIDNEY CELLS. II. PROBLEMS OF ISOLATION AND IDENTIFICATION. *Annals of the New York Academy of Sciences*, 67(8), pp.413–423.

Hull, R.N., Minner, J.R. & Smith, J.W., 1956. New viral agents recovered from tissue cultures of monkey cells. I. Origin and properties of cytopathogenic agents SV1, SV2, SV4, SV5, SV6, SV11, SV12 and SV15. *Am J Hyg*, 63, pp.204–215.

Irie, T. et al., 2008. Paramyxovirus Sendai virus C proteins are essential for maintenance of negative-sense RNA genome in virus particles. *Virology*, 374(2), pp.495–505.

Itzstein, M. von & Thomson, R., 2009. Anti-Influenza Drugs: The Development of Sialidase Inhibitors. In *Antiviral Strategies*. Berlin, Heidelberg: Springer Berlin Heidelberg, pp. 111–154.

Ivashkiv, L.B. & Donlin, L.T., 2014. Regulation of type I interferon responses. *Nature reviews. Immunology*, 14(1), pp.36–49.

Iwasaki, A., 2012. A virological view of innate immune recognition. *Annual review of microbiology*, 66, pp.177–96.

Jang, Y.H. & Seong, B.-L., 2012. Principles underlying rational design of live attenuated influenza vaccines. *Clinical and experimental vaccine research*, 1(1), pp.35–49.

Jenner, E., 1798. The Three Original Publications on Vaccination Against Smallpox. *The Harvard Classics*, 38(4). Available at: www.bartleby.com [Accessed April 15, 2016].

Jiang, X. & Chen, Z.J., 2012. The role of ubiquitylation in immune defence and pathogen evasion. *Nature reviews. Immunology*, 12(1), pp.35–48.

Jiang, Z. et al., 2004. Toll-like receptor 3-mediated activation of NF-kappaB and IRF3 diverges at Toll-IL-1 receptor domain-containing adapter inducing IFN-beta. *Proceedings of the National Academy of Sciences of the United States of America*, 101(10), pp.3533–8.

Kalica, A.R. et al., 1973. Electron microscopic studies of respiratory syncytial temperature-sensitive mutants. *Archiv für die gesamte Virusforschung*, 41(3), pp.248–58.

Kawagoe, T. et al., 2008. Sequential control of Toll-like receptor–dependent responses by IRAK1 and IRAK2. *Nature Immunology*, 9(6), pp.684–691.

Kawai, T. et al., 2004. Interferon-alpha induction through Toll-like receptors involves a direct interaction of IRF7 with MyD88 and TRAF6. *Nature immunology*, 5(10), pp.1061–1068.

Kawai, T. et al., 2005. IPS-1, an adaptor triggering RIG-I- and Mda5-mediated type I interferon induction. *Nature Immunology*, 6(10), pp.981–988.

Kawano, M. et al., 2001. Recovery of Infectious Human Parainfluenza Type 2 Virus from cDNA Clones and Properties of the Defective Virus without V-Specific Cysteine-Rich Domain. *Virology*, 284(1), pp.99–112.

Kim, S.H. et al., 1997. Mammalian type I interferon receptors consists of two subunits: IFNaR1 and IFNaR2. *Gene*, 196(1), pp.279–286.

Kim, T.W. et al., 2007. A critical role for IRAK4 kinase activity in Toll-like

receptor-mediated innate immunity. *The Journal of experimental medicine*, 204(5), pp.1025–36.

King, A.M.Q., Adams, M.J., Carstens, E.B., Lefkowitz, E.J., 2012. *Virus taxonomy: classification and nomemclature of viruses*,

Kolakofsky, D. et al., 2004. Viral RNA polymerase scanning and the gymnastics of Sendai virus RNA synthesis. *Virology*, 318(2), pp.463–473.

Konno, H. et al., 2009. TRAF6 Establishes Innate Immune Responses by Activating NF-κB and IRF7 upon Sensing Cytosolic Viral RNA and DNA D. Unutmaz, ed. *PLoS ONE*, 4(5), p.e5674.

Lazear, H.M. et al., 2015. Interferon-λ: Immune Functions at Barrier Surfaces and Beyond. *Immunity*, 43(1), pp.15–28.

Leonard, V.H.J. et al., 2006. Interaction of Bunyamwera Orthobunyavirus NSs Protein with Mediator Protein MED8: a Mechanism for Inhibiting the Interferon Response. *Journal of Virology*, 80(19), pp.9667–9675.

Li, T. et al., 2006. Structure of DDB1 in complex with a paramyxovirus V protein: viral hijack of a propeller cluster in ubiquitin ligase. *Cell*, 124(1), pp.105–117.

Li, Z. et al., 2015. Efficacy of a Parainfluenza Virus 5 (PIV5)-Based H7N9 Vaccine in Mice and Guinea Pigs: Antibody Titer towards HA Was Not a Good Indicator for Protection M. Tsuji, ed. *PLOS ONE*, 10(3), p.e0120355.

Li, Z. et al., 2013. Efficacy of parainfluenza virus 5 mutants expressing hemagglutinin from H5N1 influenza A virus in mice. *Journal of virology*, 87(17), pp.9604–9.

Lin, G.Y. & Lamb, R.A., 2000. The paramyxovirus simian virus 5 V protein slows progression of the cell cycle. *Journal of virology*, 74(19), pp.9152–9166.

Lin, Y. et al., 2003. Induction of apoptosis by paramyxovirus simian virus 5 lacking a small hydrophobic gene. *Journal of virology*, 77(6), pp.3371–83.

Lin, Y. et al., 2005. The role of simian virus 5 V protein on viral RNA synthesis. *Virology*, 338(2), pp.270–80.

Lo, M.S., Brazas, R.M. & Holtzman, M.J., 2005. Respiratory syncytial virus nonstructural proteins NS1 and NS2 mediate inhibition of Stat2 expression and alpha/beta interferon responsiveness. *Journal of virology*, 79(14), pp.9315–9.

Loo, L. et al., 2013. Evidence for the interaction of the human metapneumovirus G and F proteins during virus-like particle formation. *Virology Journal*, 10(1), p.294.

Loo, Y.-M. et al., 2008. Distinct RIG-I and MDA5 signaling by RNA viruses in innate immunity. *Journal of virology*, 82(1), pp.335–345.

Lu, B. et al., 2002. The major phosphorylation sites of the respiratory syncytial virus phosphoprotein are dispensable for virus replication in vitro. *Journal of virology*, 76(21), pp.10776–84.

Luthra, P. et al., 2008. AKT1-dependent activation of NF-kappaB by the L protein of parainfluenza virus 5. *Journal of virology*, 82(21), pp.10887–95.

Macadam, A.J. et al., 1991. The 5' noncoding region of the type 2 poliovirus vaccine strain contains determinants of attenuation and temperature sensitivity. *Virology*, 181(2), pp.451–8.

Magesh, S. et al., 2009. Human sialidase inhibitors: Design, synthesis, and biological evaluation of 4-acetamido-5-acylamido-2-fluoro benzoic acids. *Bioorganic & Medicinal Chemistry*, 17(13), pp.4595–4603.

Marcelin, J.R., Wilson, J.W. & Razonable, R.R., 2014. Oral ribavirin therapy for

respiratory syncytial virus infections in moderately to severely immunocompromised patients. *Transplant Infectious Disease*, 16(2), pp.242–250.

McCandlish, I.A. et al., 1978. A study of dogs with kennel cough. *The Veterinary record*, 102(14), pp.293–301.

Meng, J. et al., 2014. Refining the balance of attenuation and immunogenicity of respiratory syncytial virus by targeted codon deoptimization of virulence genes. *mBio*, 5(5), pp.e01704-14.

Merz, D.C. et al., 1981. Inhibition of the neuraminidase of paramyxoviruses by halide ions: A possible means of modulating the two activities of the HN protein. *Virology*, 112(1), pp.296–305.

Meyers, G. et al., 2007. Bovine viral diarrhea virus: prevention of persistent fetal infection by a combination of two mutations affecting Erns RNase and Npro protease. *Journal of virology*, 81(7), pp.3327–38.

Meylan, E. et al., 2005. Cardif is an adaptor protein in the RIG-I antiviral pathway and is targeted by hepatitis C virus. *Nature*, 437(7062), pp.1167–1172.

Meylan, E. et al., 2004. RIP1 is an essential mediator of Toll-like receptor 3-induced NF-kappa B activation. *Nature immunology*, 5(5), pp.503–507.

Minor, P.D., 2015. Live attenuated vaccines: Historical successes and current challenges. *Virology*, 479–480, pp.379–92.

Mohamed, M., McLees, A. & Elliott, R.M., 2009. Viruses in the Anopheles A, Anopheles B, and Tete serogroups in the Orthobunyavirus genus (family Bunyaviridae) do not encode an NSs protein. *Journal of virology*, 83(15), pp.7612–8.

Mosca, J.D. & Pitha, P.M., 1986. Transcriptional and posttranscriptional

regulation of exogenous human beta interferon gene in simian cells defective in interferon synthesis. *Molecular and cellular biology*, 6(6), pp.2279–83.

Mueller, S. et al., 2006. Reduction of the rate of poliovirus protein synthesis through large-scale codon deoptimization causes attenuation of viral virulence by lowering specific infectivity. *Journal of virology*, 80(19), pp.9687–96.

Müller, M. et al., 1993. The protein tyrosine kinase JAK1 complements defects in interferon-α/β and -γ signal transduction. *Nature*, 366(6451), pp.129–135.

El Najjar, F., Schmitt, A.P. & Dutch, R.E., 2014. Paramyxovirus glycoprotein incorporation, assembly and budding: A three way dance for infectious particle production. *Viruses*, 6(8), pp.3019–3054.

Naldini, L. et al., 1996. Efficient transfer, integration, and sustained long-term expression of the transgene in adult rat brains injected with a lentiviral vector. *Proceedings of the National Academy of Sciences of the United States of America*, 93(21), pp.11382–8.

Negrete, O.A. et al., 2006. Two key residues in ephrinB3 are critical for its use as an alternative receptor for Nipah virus. *PLoS pathogens*, 2(2), p.e7.

Noton, S.L. & Fearns, R., 2015. Initiation and regulation of paramyxovirus transcription and replication. *Virology*, 479, pp.545–554.

Ono, N. et al., 2001. Induction of the measles virus receptor SLAM (CD150) on monocytes. *Journal of General Virology*, 82(12), pp.2913–2917.

Onoguchi, K. et al., 2007. Viral infections activate types I and III interferon genes through a common mechanism. *Journal of Biological Chemistry*, 282(10), pp.7576–7581.

Otsuki, K. et al., 1979. Studies on avian infectious bronchitis virus (IBV). III. Interferon induction by and sensitivity to interferon of IBV. *Archives of virology*, 60(3–4), pp.249–55.

Parks, G.D. & Alexander-Miller, M.A., 2013. Paramyxovirus activation and inhibition of innate immune responses. *Journal of Molecular Biology*, 425(24), pp.4872–4892.

Parks, G.D., Manuse, M.J. & Johnson, J.B., 2011. The Parainfluenza Virus Simian Virus 5. In S. K. Samal, ed. *The Biology of Paramyxoviruses*. Caister Academic Press, pp. 37–68.

Paterson, R.G. et al., 1995. The paramyxovirus SV5 V protein binds two atoms of zinc and is a structural component of virions. *Virology*, 208(1), pp.121–31.

Paz, S. et al., 2011. A functional C-terminal TRAF3-binding site in MAVS participates in positive and negative regulation of the IFN antiviral response. *Cell research*, 21(6), pp.895–910.

Pei, Z., Harrison, M.S. & Schmitt, A.P., 2011. Parainfluenza virus 5 m protein interaction with host protein 14-3-3 negatively affects virus particle formation. *Journal of virology*, 85(5), pp.2050–2059.

Petersen, B.W. et al., 2016. Use of Vaccinia Virus Smallpox Vaccine in Laboratory and Health Care Personnel at Risk for Occupational Exposure to Orthopoxviruses — Recommendations of the Advisory Committee on Immunization Practices (ACIP), 2015. *MMWR. Morbidity and Mortality Weekly Report*, 65(10), pp.257–262.

Piehler, J., Roisman, L.C. & Schreiber, G., 2000. New structural and functional aspects of the type I interferon-receptor interaction revealed by comprehensive mutational analysis of the binding interface. *Journal of*

Biological Chemistry, 275(51), pp.40425–40433.

Poeck, H. et al., 2010. Recognition of RNA virus by RIG-I results in activation of CARD9 and inflammasome signaling for interleukin 1 beta production. *Nature immunology*, 11(1), pp.63–9.

Poole, E. et al., 2002. The V Proteins of Simian Virus 5 and Other Paramyxoviruses Inhibit Induction of Interferon-β. *Virology*, 303(1), pp.33–46.

Precious, B. et al., 1995. Inducible expression of the P, V, and NP genes of the paramyxovirus simian virus 5 in cell lines and an examination of NP-P and NP-V interactions. *Journal of virology*, 69(12), pp.8001–10.

Precious, B. et al., 2005. Simian virus 5 V protein acts as an adaptor, linking DDB1 to STAT2, to facilitate the ubiquitination of STAT1. *Journal of virology*, 79(21), pp.13434–13441.

Precious, B.L. et al., 2007. Catalytic turnover of STAT1 allows PIV5 to dismantle the interferon-induced anti-viral state of cells. *Virology*, 368(1), pp.114–121.

Randall, R.E. et al., 1987. Isolation and characterization of monoclonal antibodies to simian virus 5 and their use in revealing antigenic differences between human, canine and simian isolates. *The Journal of general virology*, 68 (Pt 11(11), pp.2769–80.

Randall, R.E. & Bermingham, A., 1996. NP:P and NP:V Interactions of the Paramyxovirus Simian Virus 5 Examined Using a Novel Protein:Protein Capture Assay. *Virology*, 224(1), pp.121–129.

Randall, R.E. & Goodbourn, S., 2008. Interferons and viruses: an interplay between induction, signalling, antiviral responses and virus countermeasures. *The Journal of general virology*, 89(Pt 1), pp.1–47.

Rima, B.K. et al., 2014. Stability of the Parainfluenza Virus 5 Genome Revealed by Deep Sequencing of Strains Isolated from Different Hosts and following Passage in Cell Culture. *Journal of virology*, 88(7), pp.3826–36.

Rubin, S.A. et al., 2008. Antibody Induced by Immunization with the Jeryl Lynn Mumps Vaccine Strain Effectively Neutralizes a Heterologous Wild-Type Mumps Virus Associated with a Large Outbreak. *The Journal of Infectious Diseases*, 198(4), pp.508–515.

Rueckert, C. et al., 2012. Vaccines: From Empirical Development to Rational Design T. C. Hobman, ed. *PLoS Pathogens*, 8(11), p.e1003001.

Sabin, A.B. & Boulger, L.R., 1973. History of Sabin attenuated poliovirus oral live vaccine strains. *Journal of Biological Standardization*, 1(2), pp.115–118.

Sabin, A.B. & Ward, R., 1941. THE NATURAL HISTORY OF HUMAN POLIOMYELITIS I. DISTRIBUTION OF VIRUS IN NERVOUS AND NON-NERVOUS TISSUES*.

Sato, S. et al., 2003. Toll/IL-1 receptor domain-containing adaptor inducing IFN-beta (TRIF) associates with TNF receptor-associated factor 6 and TANK-binding kinase 1, and activates two distinct transcription factors, NF-kappa B and IFN-regulatory factor-3, in the Toll-like re. *J Immunol*, 171(8), pp.4304–10.

Schneider, W.M., Chevillotte, M.D. & Rice, C.M., 2014. Interferon-stimulated genes: a complex web of host defenses. *Annual review of immunology*, 32, pp.513–45.

Schoggins, J.W. & Rice, C.M., 2011. Interferon-stimulated genes and their antiviral effector functions. *Current opinion in virology*, 1(6), pp.519–25.

Schroder, K. et al., 2004. Interferon-gamma: an overview of signals, mechanisms

and functions. *Journal of leukocyte biology*, 75(2), pp.163–189.

Shchetinin, A.M. et al., 2015. Genetic and Phylogenetic Characterization of Tataguine and Witwatersrand Viruses and Other Orthobunyaviruses of the Anopheles A, Capim, Guamá, Koongol, Mapputta, Tete, and Turlock Serogroups. *Viruses*, 7(11), pp.5987–6008.

Shi, X. et al., 2016. Bunyamwera orthobunyavirus glycoprotein precursor is processed by cellular signal peptidase and signal peptide peptidase. *Proceedings of the National Academy of Sciences of the United States of America*, 113(31), pp.8825–30.

Shtyrya, Y.A., Mochalova, L. V & Bovin, N. V, 2009. Influenza virus neuraminidase: structure and function. *Acta naturae*, 1(2), pp.26–32.

Southern, J.A. et al., 1991. Identification of an epitope on the P and V proteins of simian virus 5 that distinguishes between two isolates with different biological characteristics. *The Journal of general virology*, 72 (Pt 7), pp.1551–7.

Stark, G.R. et al., 1998. HOW CELLS RESPOND TO INTERFERONS. *Annual Review of Biochemistry*, 67(1), pp.227–264.

Stark, G.R. & Darnell, J.E., 2012. The JAK-STAT pathway at twenty. *Immunity*, 36(4), pp.503–14.

Stewart, C.E., Randall, R.E. & Adamson, C.S., 2014. Inhibitors of the interferon response enhance virus replication in vitro. *PloS one*, 9(11), p.e112014.

Suguitan, A.L. et al., 2006. Live, Attenuated Influenza A H5N1 Candidate Vaccines Provide Broad Cross-Protection in Mice and Ferrets J. S. M. Peiris, ed. *PLoS Medicine*, 3(9), p.e360.

Sun, D., Luthra, P., et al., 2011. Identification of a phosphorylation site within the

P protein important for mRNA transcription and growth of parainfluenza virus 5. *Journal of virology*, 85(16), pp.8376–85.

Sun, D. et al., 2009. PLK1 Down-Regulates Parainfluenza Virus 5 Gene Expression C. F. Basler, ed. *PLoS Pathogens*, 5(7), p.e1000525.

Sun, D., Xu, P. & He, B., 2011. Sumoylation of the P protein at K254 plays an important role in growth of parainfluenza virus 5. *Journal of virology*, 85(19), pp.10261–8.

Sun, L. et al., 2013. Cyclic GMP-AMP synthase is a cytosolic DNA sensor that activates the type I interferon pathway. *Science (New York, N.Y.)*, 339(6121), pp.786–91.

Sun, M. et al., 2004. Conserved Cysteine-Rich Domain of Paramyxovirus Simian Virus 5 V Protein Plays an Important Role in Blocking Apoptosis. *Journal of Virology*, 78(10), pp.5068–5078.

Tabeta, K. et al., 2004. Toll-like receptors 9 and 3 as essential components of innate immune defense against mouse cytomegalovirus infection. *Proceedings of the National Academy of Sciences of the United States of America*, 101(10), pp.3516–21.

Takeuchi, O. et al., 2010. Pattern Recognition Receptors and Inflammation. *Cell*, 140(6), pp.805–820.

Tartey, S. & Takeuchi, O., 2015. Chromatin Remodeling and Transcriptional Control in Innate Immunity: Emergence of Akirin2 as a Novel Player. *Biomolecules*, 5(3), pp.1618–33.

Taylor, G. et al., 2014. Recombinant bovine respiratory syncytial virus with deletion of the SH gene induces increased apoptosis and pro-inflammatory cytokines in vitro, and is attenuated and induces protective immunity in

calves. *The Journal of general virology*, 95(Pt 6), pp.1244–54.

Tayyari, F. et al., 2011. Identification of nucleolin as a cellular receptor for human respiratory syncytial virus. *Nature medicine*, 17(9), pp.1132–5.

Thomas, D. et al., 2004. Inhibition of RNA Polymerase II Phosphorylation by a Viral Interferon Antagonist. *Journal of Biological Chemistry*, 279(30), pp.31471–31477.

Thomas, S.M. et al., 1988. Two mRNAs that differ by two nontemplated nucleotides encode the amino coterminal proteins P and V of the paramyxovirus SV5. *Cell*, 54(6), pp.891–902.

Timani, K. a et al., 2008. A single amino acid residue change in the P protein of parainfluenza virus 5 elevates viral gene expression. *Journal of virology*, 82(18), pp.9123–9133.

Tong, S. et al., 2002. Regulation of Fusion Activity by the Cytoplasmic Domain of a Paramyxovirus F Protein.

Trinchieri, G., 2010. Type I interferon: friend or foe? *The Journal of experimental medicine*, 207(10), pp.2053–63.

Uddin, S. et al., 2002. Protein Kinase C-δ (PKC-δ) Is Activated by Type I Interferons and Mediates Phosphorylation of Stat1 on Serine 727. *Journal of Biological Chemistry*, 277(17), pp.14408–14416.

Uematsu, S. et al., 2005. Interleukin-1 receptor-associated kinase-1 plays an essential role for Toll-like receptor (TLR)7- and TLR9-mediated interferon-{alpha} induction. *The Journal of experimental medicine*, 201(6), pp.915–23.

Vaddi, K., Sarlis, N.J. & Gupta, V., 2012. Ruxolitinib, an oral JAK1 and JAK2 inhibitor, in myelofibrosis. *Expert opinion on pharmacotherapy*, 13(16), pp.2397–407.

Velazquez, L. et al., 1994. Activation of the protein tyrosine kinase tyk2 by interferon alpha/beta. *European Journal of Biochemistry*, 223(2), pp.427–435.

Versteeg, G.A., García-Sastre, A. & Garc??a-Sastre, A., 2010. Viral tricks to grid-lock the type I interferon system. *Current Opinion in Microbiology*, 13(4), pp.508–516.

Verstovsek, S. et al., 2015. Efficacy, safety, and survival with ruxolitinib in patients with myelofibrosis: results of a median 3-year follow-up of COMFORT-I. *Haematologica*, 100(4), pp.479–88.

Villar, E. & Barroso, I.M., 2006. Role of sialic acid-containing molecules in paramyxovirus entry into the host cell: A minireview. *Glycoconjugate Journal*, 23(1–2), pp.5–17.

Wahid, B. et al., 2016. Zika: As an emergent epidemic. *Asian Pacific Journal of Tropical Medicine*, 9(8), pp.723–729.

Weber, F. et al., 2002. Bunyamwera bunyavirus nonstructural protein NSs counteracts the induction of alpha/beta interferon. *Journal of virology*, 76(16), pp.7949–55.

de Weerd, N.A., Samarajiwa, S.A. & Hertzog, P.J., 2007. Type I Interferon Receptors: Biochemistry and Biological Functions. *Journal of Biological Chemistry*, 282(28), pp.20053–20057.

Welch, B.D. et al., 2012. Structure of the cleavage-activated prefusion form of the parainfluenza virus 5 fusion protein. *Proceedings of the National Academy of Sciences of the United States of America*, 109(41), pp.16672–7.

Welch, B.D. et al., 2013. Structure of the Parainfluenza Virus 5 (PIV5) Hemagglutinin-Neuraminidase (HN) Ectodomain F. A. Rey, ed. *PLoS*

Pathogens, 9(8), p.e1003534.

Wen, Z., Zhong, Z. & Darnell, J.E., 1995. Maximal activation of transcription by statl and stat3 requires both tyrosine and serine phosphorylation. *Cell*, 82(2), pp.241–250.

Westrop, G.D. et al., 1989. Genetic basis of attenuation of the Sabin type 3 oral poliovirus vaccine. *Journal of virology*, 63(3), pp.1338–44.

WHO, 1959. *Requirements for Smallpox Vaccine*,

Wilson, R.L. et al., 2006. Function of small hydrophobic proteins of paramyxovirus. *Journal of virology*, 80(4), pp.1700–9.

Yan, J. et al., 2014. TRIM4 modulates type I interferon induction and cellular antiviral response by targeting RIG-I for K63-linked ubiquitination. *Journal of molecular cell biology*, 6(2), pp.154–63.

Yang, Y. et al., 2015. Regulation of Viral RNA Synthesis by the V Protein of Parainfluenza Virus 5. *Journal of virology*, 89(23), pp.11845–57.

Young, D.F. et al., 2016. Human IFIT1 inhibits mRNA translation of rubulaviruses but not other members of the Paramyxoviridae family. *Journal of Virology*, (August), p.JVI.01056-16.

Young, D.F. et al., 2003. Virus replication in engineered human cells that do not respond to interferons. *Journal of virology*, 77(3), pp.2174–81.

Zandi, E. et al., 1997. The IκB Kinase Complex (IKK) Contains Two Kinase Subunits, IKKα and IKKβ, Necessary for IκB Phosphorylation and NF-κB Activation. *Cell*, 91(2), pp.243–252.

Zeng, W. et al., 2010. Reconstitution of the RIG-I pathway reveals a signaling role of unanchored polyubiquitin chains in innate immunity. *Cell*, 141(2), pp.315–30.

Zufferey, R. et al., 1997. Multiply attenuated lentiviral vector achieves efficient gene delivery in vivo. *Nature biotechnology*, 15(9), pp.871–5.